| 1. Report No. | 2. Government Accession No. | 3. Recipient's Catalog No. |
|---|---|---|
| TX-97/2965-1F | | |

| 4. Title and Subtitle | 5. Report Date |
|---|---|
| INVESTIGATION OF SWELLING CLAY SOILS IN SUBGRADES OF SH 6 AND SH 21 | November 1996 |
| | 6. Performing Organization Code |
| 7. Author(s) | 8. Performing Organization Report No. |
| Seong-wan Park, Robert L. Lytton and Joe W. Button | Research Report 2965-1F |
| 9. Performing Organization Name and Address | 10. Work Unit No. (TRAIS) |
| Texas Transportation Institute<br>The Texas A&M University System<br>College Station, Texas 77843-3135 | 11. Contract or Grant No.<br>Study No. 7-2965 |
| 12. Sponsoring Agency Name and Address | 13. Type of Report and Period Covered |
| Texas Department of Transportation<br>Research and Technology Transfer Office<br>P. O. Box 5080<br>Austin, Texas 78763-5080 | Final:<br>September 1995-August 1996 |
| | 14. Sponsoring Agency Code |

15. Supplementary Notes

Research performed in cooperation with the Texas Department of Transportation.
Research Study Title: Find an Innovative Way to Investigate the Reduction of Possible Sulfate Swells in Expansive Clays Subgrades in Spot Locations Along State Highways

16. Abstract

In the Bryan District, SH 6 and SH 21 are experiencing severe pavement distortion in several locations causing an exceptionally rough ride. Routine site investigation prior to construction did not reveal underlying soil conditions that could produce the kinds of pavement distresses that appeared relatively soon after pavement construction was completed. These 2 areas were investigated using innovative, state-of-the-art field and laboratory testing techniques to determine the origin(s) of the pavement distresses manifested at the surface and to determine what could be done to alleviate the existing pavement surface problems or what site investigation techniques should be employed in the future to circumvent the recurrence of these types of problems.

Specific objectives of the research study were to conduct detailed site investigations using state-of-the-art techniques, analyze data to isolate cause(s) of the pavement distress, suggest alternatives to stabilize the swelling soils, recommend site investigation techniques to identify similar problem soil profiles in future construction sites, and develop treatments to stabilize such soils and, thus, minimize pavement distress.

Findings indicated the swells were not caused by lime stabilization of sulfate bearing soils but were the result of surface water flowing through deep cracks or permeable soil layers to highly plastic expansive clays. Recommended remedial actions to reduce subsequent swelling and site investigation procedures to detect potential problems during the construction process are given.

| 17. Key Words | 18. Distribution Statement |
|---|---|
| Expansive Clay, Swelling Soils, Sulfate, Gypsum Pavements, Moisture Barrier, Lime | No restrictions. This document is available to the public through NTIS:<br>National Technical Information Service<br>5285 Port Royal Road<br>Springfield, Virginia 22161 |

| 19. Security Classif.(of this report) | 20. Security Classif.(of this page) | 21. No. of Pages | 22. Price |
|---|---|---|---|
| Unclassified | Unclassified | 178 | |

# INVESTIGATION OF SWELLING CLAY SOILS IN SUBGRADES OF SH 6 AND SH 21

by

Seong-wan Park
Graduate Assistant Research
Texas Transportation Institute

Robert L. Lytton
Research Engineer
Texas Transportation Institute

and

Joe W. Button
Research Engineer
Texas Transportation Institute

Research Report 2965-1F
Research Study Number 7-2965
Research Study Title: Find an Innovative Way to Investigate the Reduction of Possible Sulfate Swells in Expansive Clays Subgrades in Spot Locations Along State Highways

Sponsored by the
Texas Department of Transportation

November 1996

TEXAS TRANSPORTATION INSTITUTE
The Texas A&M University System
College Station, Texas 77843-3135

# IMPLEMENTATION RECOMMENDATIONS

Based on the findings in this study, the authors recommend the following for implementation.

## 1. REMEDIAL ACTION FOR SH 6 SITE

At the SH 6 site, the soil has a large amount of soluble sulfate, a high suction level, and a high osmotic suction level. Water is entering the soil profile from the surface due to water in the drainage ditches and median. The greatest heaves occur in the soil mass at those locations where the soil is most highly cracked, where water has more rapid access to greater depths, and where suction has changed more than elsewhere.

The moisture active zone at the SH 6 site varies between depths of 2.4 and 3.0 m, and the heaving takes place to a depth of 1.8 to 2.2 m. The heaving and the pavement roughness will continue to appear for many years to come because the suction values in the soil profile are, in no instance except boring SB 2-1, as wet as the soil can become (p 2.5). The only way to arrest the heave is by identifying the source of the water and cutting it off. Because the water is entering beneath the pavements from the side ditches and medians, sealing these is the most practical way to stabilize these pavements against uncontrolled further movements. Because of the depth to which moisture penetrates below the ground surface, it is not considered possible to shut off all of the flow of moisture with a vertical moisture barrier.

Instead, sealing the entire median and the side ditches to a distance of 4.0 meters beyond the flow line of the ditch will provide the necessary protection of the pavement. Because of the high levels of soluble sulfate in the soil, it would be unwise to use lime stabilization in any remedy used along the SH 6 site. As a less preferred alternative, a vertical moisture barrier can be installed at the edge of the paved shoulder to a depth of 2.4 m, both on the inside and outside of the pavement surface. As a hybrid alternative that is also less preferred, the median can be sealed and vertical barriers can be placed along the outside edge of the shoulders in each direction.

## 2. REMEDIAL ACTION FOR SH 21 SITE

The SH 21 site is composed of highly variable stratified expansive soil about 2.0 m deep over a hard clay pan. All of the heave occurs in the top 2.0 m and none occurs in the cemented clay pan beneath it. Water that is carried in the roadside ditches and medians enters the soil profile and percolates downward until it reaches the clay pan. At that point, it stops and runs laterally on top of the clay pan and beneath the pavement where it causes highly variable heaves, reflecting the variability of the soil along the road. There is much less soluble sulfate in the soils along this road. The suction profiles along this road indicate that the water is being carried beneath the pavement along the slope of the clay pan and in the occasional granular layers that are interbedded with the clay.

Shutting off this flow of water is most conveniently done with a vertical barrier that is carried down to and tied into the intact clay pan at depths of 1.5 to 2.0 m. The barriers should be placed on the edge of the paved shoulders on both sides of each paved surface. Paving or sealing the medians and roadside drainage ditches will probably be a more costly solution at this site and less successful because of the horizontal flow on the surface of the hard clay pan.

## 3. SITE INVESTIGATION PROCEDURE

For identifying soil profiles with the potential of causing pavement distortion, site investigation is a crucial step toward the selection of correct construction and rehabilitation techniques. Before pavement construction on or stabilization of expansive soils, detailed information on potential causes of roughness might provide feasible solutions at specific sites.

To begin the site investigation, existing information on the project areas should be reviewed. Geological survey maps and United States Department of Agriculture (USDA) county soil survey reports are valuable sources of information. Soil survey reports are rich in pedological data and provide basic geology of the particular area, detailed descriptions of the soil profiles, chemical and physical properties of soils, engineering classifications, and index properties for the major layers of soils. Soil survey reports are an excellent source to estimate the applicability of ground penetrating radar (GPR). After reviewing the soil information, a site reconnaissance should be planned and conducted. Based on this field trip, the drainage and slope condition of the area, along with any cracking or undulating patterns of pavements,

should be observed and reported. If a planned site is suspected of having high salt concentrations, the soil should be tested using the electrical conductivity tool kit. If high electrical conductivity values are encountered and the soil is to be stabilized with lime or cement, the soluble sulfate content of the soil should be measured. A level of sulfate greater than 0.2% may induce a pavement heaving problem with lime or cement stabilization.

Before planning soil sampling, GPR can be very revealing. GPR shows where and how deep various soil layers are located. Successful GPR surveys can locate discontinuities such as lenses or seams in soils. A preliminary step for a GPR survey is to determine whether site conditions are suitable. Under certain conditions, interpretation of a GPR survey can be limited due to problems such as high clay content and high salt concentration of soils.

Soil boring and sampling should be strategically planned and based on the information obtained from the GPR survey or field trip. The location and depth of each boring should be strategically selected to identify the potential problem areas. To obtain undisturbed samples, shelby thin-walled tube or equivalent sampler should be used. Undisturbed samples can be used for determination of soil suctions, water contents, and in situ density in soils. During boring, the following details should be reported in a boring log in the field:

- Location and boring number,
- Date of boring,
- Elevation of the ground surface,
- A detailed description of each stratum,
- The level at which boring was terminated, and
- Any unusual condition noted.

The soil suction test using filter paper or the transistor psychrometer is very helpful for identifying the moisture activity in soils A soil suction profile shows which direction soil water is migrating. A transistor psychrometer is capable of measuring the total suction, in 1 hour. The filter paper method can measure both the total and the matric suction but it takes 7 days to 10 days. Equilibrium suction can also be estimated from Figure 11 using Thornthwaite moisture index (Russam et al. 1961) The equilibrium suction line reveals whether the soil

condition is dry or wet when compared to measured suction at a specific site. If high osmotic suction is found in the suction profile, sulfate contents should be measured.

To estimate the flow properties of the soil, the following laboratory tests are required:

- Atterberg limits (liquid limit and plastic limit),
- Water content,
- % finer than 75 μm, and
- % finer than 2 μm.

To determine the fine clay content, a particle size analyzer is recommended. It can more accurately determine the particle size distribution of fine-grained soils than the conventional hydrometer test, as described in Chapter 2. Using the relationship between the activity and cation exchange activity of soils, the suction compression index can be obtained. The diffusion coefficient and unsaturated permeability of soils should also be estimated. This is important to determine how deep and how wide to place a vertical moisture barrier or other drainage system.

Using the previously described site investigation information, determine the proper remedial actions.

## 4. STABILIZATION OF SULFATE BEARING SOILS

Currently, several approaches are available for reducing or controlling sulfate-induced swell of soils during lime or cement stabilization.

1. Double applications of lime - Soil with low sulfate contents may be stabilized by double applications of lime along with high water contents. The ettringite is formed after the first application of lime, and then the second application of lime provides strength and decreased swell potential of the soils. A total lime content of about 6% is suitable using two applications of 3% each with at least 21 days between. Sufficient water is required to solubilize the sulfate to permit reaction with the soluble aluminate from the clay and with the calcium from the lime to form ettringite during the delay period.
2. Prewetting and mellowing - A mixing water content about 3% to 5% above optimum and mellowing for a period of 7 days before compaction will reduce subsequent swell.
3. Low calcium stabilizers - Low calcium fly ash and other commercial products will minimize the amount of expansion of clay soils with relatively high sulfate contents.
4. Pretreatment with barium compounds - Pretreating soils with barium hydroxide and barium chloride reduces the amount of soluble sulfates by chemically changing them to insoluble minerals. Therefore, the formation of ettringite is diminished. Swells have been reduced over 20% using this pretreatment method.
5. Pretreatment with potassium-based chemicals - Pretreatment of sulfate bearing soils with potassium-based chemicals (potassium salt compounds) involves saturating the soil mass with potassium ions which form a permanent, irreversible chemical bond with the clay minerals. This chemical change in the clay mineral prevents water ions from migrating between the silica sheets and limits the expansion of clay soils.

# DISCLAIMER

The contents of this report reflect the views of the authors who are responsible for the facts and the accuracy of the data presented herein. The contents do not necessarily reflect the official view or policies of the Texas Department of Transportation. This report does not constitute a standard, specification, or regulation, nor is it intended for construction, bidding, or permit purposes.

# TABLE OF CONTENTS

## TABLE OF CONTENTS (Continued)

# LIST OF FIGURES

## LIST OF FIGURES (Continued)

## LIST OF FIGURES (Continued)

# LIST OF TABLES

## LIST OF TABLES (Continued)

# SUMMARY

In the Bryan District, SH 6 and SH 21 are experiencing severe pavement distortion in several locations causing an exceptionally rough ride. Routine site investigation prior to construction did not reveal underlying soil conditions that could produce the kinds of pavement distresses that appeared relatively soon after pavement construction was completed. These 2 areas were investigated using innovative, state-of-the-art field and laboratory testing techniques to determine the origin(s) of the pavement distresses manifested at the surface and to determine what could be done to alleviate the existing pavement surface problems or what site investigation techniques should be employed in the future to circumvent the recurrence of these types of problems.

Specific objectives of the research study were to conduct detailed site investigations using state-of-the-art techniques, analyze data to isolate cause(s) of the pavement distress, suggest alternatives to stabilize the swelling soils, recommend site investigation techniques to identify similar problem soil profiles in future construction sites, and develop treatments to stabilize such soils and, thus, minimize pavement distress.

Findings indicated the swells were not caused by lime stabilization of sulfate bearing soils but were the result of surface water flowing through deep cracks or permeable soil layers to highly plastic expansive clays. Recommended remedial actions to reduce subsequent swelling and site investigation procedures to detect potential problems during the construction process are given.

## FIELD INVESTIGATION

From a geological standpoint, all the test sections along SH 6 and SH 21 are located under the Cook Mountain formation described as Ecm soils. The segments of highways are partly in the alluvium of the Brazos River and partly in the geological clay-forming strata of the Texas coastal plains. The soils are mostly weathering brownish gray to brown clays and brownish gray to yellowish gray clays. The soils in the SH 6 and SH 21 sites are fine montmorillonitic clays.

Ground penetrating radar (GPR) was used in an attempt to characterize the soil layers and to detect the presence of any water filled lenses in the pavement subgrade. The clay soils with inherently high water contents significantly attenuated the GPR signals. The high water contents make it difficult for GPR signals to penetrate deeply into the soil and, thus, prevented the observation of any pertinent soils structures.

Soil boring and sampling was conducted to obtain "undisturbed" samples. The locations of the boreholes were selected at the peak and foot of the pavement heaves. Shelby tube samples were taken at depth intervals of 40 cm, and the boring was continued until the sampler could not be pushed any deeper. A total of 17 borings were performed at both sites. After sampling, each soil sample was wrapped and stored in a temperature controlled room until time for the designated tests.

## LABORATORY TESTS

Electrical conductivity measurements were performed in an attempt to estimate the salt (sulfate) content in the soils. Results suggested a large amount of soluble sulfate in the soil at the SH 6 site but not at the SH 21 site.

Soluble sulfate contents of the soils were measured using 2 different soil-to-water ratios. Measurements confirmed the results from the electrical conductivity tests.

Particle size analysis of soils finer than 75 μm was conducted using TxDOT's Horiba laser diffraction particle size distribution analyzer.

Atterberg limits (liquid and plastic limits) and the plasticity index were determined for soils passing the 425 μm sieve size. Most of the soils are highly plastic and active swelling clays.

Soil suction profiles were used in an attempt to determine the sources of heaves in pavement. A profile of soil suction with depth provides information on which direction soil water is flowing. The source of the water causing pavement distortion can be identified using interpretation of matric and total suction in profiles. In particular, the measurements of total and matric suction determine how much of the suction is related to dissolved salts known as osmotic suction. High osmotic suction readings indicate the presence of large amounts of soluble salts in the soil.

Both total and matric suction were determined using filter papers. In addition, a transistor psychrometer was used to measure total suction. Results show the transistor psychrometer consistently measured total suctions 0.172 pF smaller than the filter paper method. All the soils in the project areas are classified as medium cracked or moderately permeable soils which have unsaturated permeabilities greater than 0.00005 $cm^2$/sec and smaller than 0.001$cm^2$/sec. Suction tests revealed a classic pattern showing that the water is entering this profile from the surface.

## SUMMARY OF FINDINGS AND CONCLUSIONS

### SH 6 Site

At the SH 6 site, the soil has a large amount of soluble sulfate, high suction level, and high osmotic suction level. Water is entering the soil profile from the surface due to deep cracks and water in the drainage ditches and median. The greatest heaves occur in the soil mass at those locations where the soil is most highly cracked, where water has more rapid access to greater depths, and where suction has changed more than the surrounding area.

The moisture active zone at the SH 6 site varies between 2.4 and 3.0 m, and the heaving takes place down to a depth of 1.8 to 2.2 m. The heaving and the pavement roughness will continue to appear for many years to come because the suction values in the soil profile are not as wet as the soil can become. The only way to arrest the heave is to identify and eliminate the source of the water. Because the water is entering beneath the pavements from the side ditches and medians, sealing these is the most practical way to stabilize the pavements against further uncontrolled movements. Because of the depth to which moisture penetrates below the ground surface, it is not considered possible to shut off all of the flow of moisture with a vertical moisture barrier. Instead, sealing the entire median and the side ditches to a distance of 4.0 m beyond the flow line of the ditch will provide the necessary protection of the pavement. Because of the high levels of soluble sulfate in the soil, it would be unwise to use lime stabilization in any remedy used along the SH 6 site. As a less preferred alternative, a vertical moisture barrier can be installed at the edge of the paved shoulder to a depth of 2.4 m, both on the inside and outside of the pavement surface. As a hybrid alternative that is also less preferred, the median can be sealed and vertical barriers can be placed along the outside edge of the shoulders in each direction.

**SH 21 Site**

The SH 21 site is a highly variable stratified expansive soil about 2.0 m deep over a hard clay pan. All of the heave occurs in the top 2.0 m, and none occurs in the cemented clay pan beneath it. Water that is carried in the roadside ditches and medians enters the soil profile and percolates downward until it reaches the clay pan. At that point, it stops and runs laterally on top of the clay pan and beneath the pavement where it causes highly variable heaves, reflecting the variability of the soil along the road. The suction profiles along SH 21 indicate that the water is being carried beneath the pavement along the slope of the clay pan and in the occasional granular layer that is interbedded with the clay.

Shutting off this flow of water is most conveniently done with a vertical barrier that is carried down to and tied into the intact clay pan at depths of 1.5 to 2.0 m. The barriers should be placed on the edge of the paved shoulders on both sides of each paved surface. Paving or sealing the medians and roadside drainage ditches will probably be a more costly solution at this site and less successful because of the horizontal flow on the surface of the hard clay pan.

**Site Investigation**

Site investigation is a crucial step toward the selection of correct construction and rehabilitation of pavements in expansive soils. A field site investigation should use tools such as geological survey maps, USDA county soil survey reports, electrical conductivity kit, GPR, soil boring and sampling, and basic laboratory testing including soil suction profiles.

**Stabilization of Sulfate Bearing Soils**

Currently, several approaches are available for reducing or controlling sulfate-induced swell of soils during lime or cement stabilization.

1. Double applications of lime,
2. Prewetting and mellowing,
3. Low calcium stabilizers,
4. Pretreatment with barium compounds, and
5. Pretreatment with potassium-based chemicals.

# CHAPTER 1
# INTRODUCTION

## BACKGROUND

State Highway 6 (SH 6) in Brazos County and State Highway 21 (SH 21) in Burleson County are experiencing severe pavement distortion (bumps and cracking) in several locations causing an exceptionally rough ride, especially for trucks with trailers. Routine site investigation prior to construction did not reveal underlying soil conditions that could produce the kinds of pavement distresses that appeared relatively soon after pavement construction was completed. An investigation is needed to determine what, if anything, can be done to ameliorate the existing pavement surface problems or what site investigation techniques should be employed in the future to circumvent the recurrence of these types of problems.

These 2 areas in the Bryan District need to be investigated in detail using innovative, state-of-the-art field and laboratory testing techniques to determine the origin(s) of the pavement distresses manifested at the surface. A pavement construction site investigation procedure that can be used to identify soil conditions that have the potential to cause these types of pavement distresses needs to be formulated. Once identified, a method of protecting or treating the subgrade soil to avoid or minimize these types of pavement distresses in future construction or rehabilitation of these pavements needs to be devised. If possible, a remedial method of treating the existing pavements to minimize the differential swelling of the underlying soils needs to be formulated.

Some of the worst pavement distortion problems on SH 6 occurred where a fairly deep cut was made. Interviews with cognizant personnel in the Bryan District revealed that, during construction, when the cut was being made, white crystals were noticed. Although no analysis was made at the time, it was later determined that these crystals were selenite or gypsum ($CaSO_4$) and, thus, a major contributor of soluble sulfate.

The roughness that needs to be controlled is due to 1 or more of the 3 principal causes listed below:

- Poor drainage (water from the surface),
- Perched or permanent water tables in the sand and gravel lenses (water from below), and
- Swelling due to the hydration of anhydride gypsum or to a lime-sulfate-clay reaction.

The solution to each of these problems will be different. Thus, it is important to determine at the outset which of these three items is the actual cause of the roughness. Armed with this information, it is important to propose a solution that is not only feasible from cost, construction, and performance points of view but also one that addresses the actual cause of the roughness. This will require the use of field and laboratory testing and some analysis to determine both the cause and the likely effectiveness of different feasible solutions.

The distortion and cracking of the pavement surface may be due to poor drainage in the median strip and in the roadside ditches or due to expansion of the subgrade soils in cuts which are fed water from lenses of sand and gravel in the alluvium of the Brazos River. A contributor may be sulfate-induced swell. It will be necessary to determine which one(s) of these problems are to be solved. Two investigative tools, ground penetrating radar (GPR) and soil suction profiles, were used to determine which of these circumstances most likely caused the swelling and where they are located.

Knowing the level of suction in the soil profile and its components, it will be possible to tell not only which direction the water is traveling, but whether the swelling or shrinking has an "osmotic" component, and how much. The solution to soil mass distortion will be different if the cause of the swelling is osmotic or matric suction.

The third step in a site investigation is the laboratory testing to estimate the volume change and water conductivity properties of the soil. Tests include Atterberg limits, water content, dry density, soil particles finer than 75 microns and finer than 2 microns. The sulfate content in the soil can be estimated using electrical conductivity.

## OBJECTIVES

The ultimate goal of this study is to provide the Bryan District with answers to the following questions:

- Why are the pavements deforming?
- What alternatives are available to rehabilitate the pavements?

Specific objectives of the research study include:

- Complete, detailed site investigations using state-of-the-art techniques,
- Analyze data to isolate cause(s) of the pavement distress,
- Suggest alternatives to stabilize the swelling soils,
- Suggest site investigation techniques to identify similar problem soil profiles in future construction sites, and
- Develop treatments to stabilize such soils and, thus, minimize pavement distress.

# CHAPTER 2
# LITERATURE REVIEW

## SULFATE SWELLING SOILS

### Background

Sulfate induced swelling in clay soils has drawn attention since James Mitchell's paper (1986) referenced this phenomena in Las Vegas. Generally, swelling in soils is a result of changes in the soil water system that disturb the internal stress state, and the soil water chemistry changed by the amount of water or the chemical composition of minerals (Nelson et al. 1992). The mechanism of heave in soils has been found to be a complex function of available water, the percentage of clay, and cation exchange capacity (Hunter 1988). Several researchers have reported that sulfate swelling in highly active clay soils containing at least 10% clay can occur when sufficient soil water is available to feed the minerals (Mitchell 1986, Hunter 1988, Petry et al. 1992).

Sulfate induced swelling has been observed when lime is added to clay soil for stabilization. Reactive environments under high pH conditions caused by lime and clay minerals could cause clay minerals to become unstable and begin to deteriorate, particularly above a pH of 10.5 (Hunter 1988). The aluminum and siliceous pozzolans are released to form calcium silicate hydrate (CSH) and calcium aluminum hydrate (CAH). The presence of sulfate can lead to the formation of ettringite, as shown in Figure 1, which can be transformed into thaumasite when a sufficient amount of carbonate and dissolved silica are present in the soil at a temperature between 4.5°C and 15°C (Metha et al. 1966). The formation of ettringite is favored in low alumina conditions. The formation of monosulfate hydrate is favored in 1:1 type clay minerals like Kaolinite, while the trisulfate hydrates would be favored in 2:1 type clay minerals like smectite or montmorillite (Petry et al. 1992).

As stated earlier, lime creates a high pH condition which accelerates flocculation of clay minerals and reduces the amount of expansion upon wetting of the stabilized soil. However, the formation of ettringite during the stabilization process could occur and induce sulfate heave when less soluble sulfates present in the soil are treated with a calcium-based stabilizer.

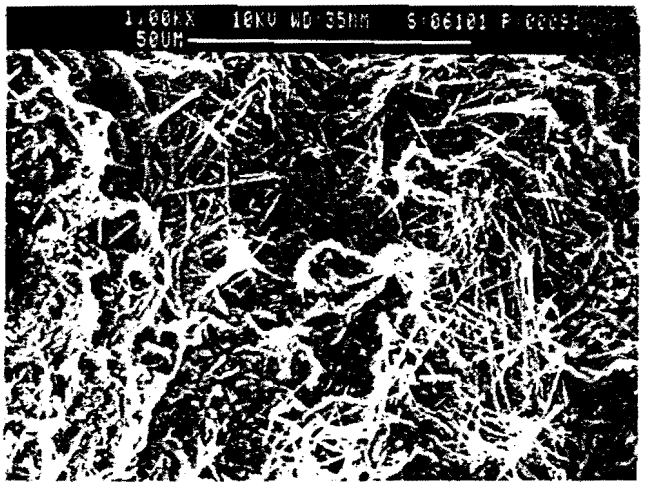


Figure 1. Magnified View of Ettringite (after Petry et al., 1992).

Therefore, reduction of ettringite formation would diminish the heave in soils due to this sulfate-induced swelling phenomena.

**Current Testing Methodology and Treatment for Sulfate Swelling Soils**

In order to reduce the sulfate induced heave of soils, three steps are recommended as follows:

1. Identification of the sulfate bearing soils,
2. Classification of the clay soils, and
3. Evaluation of treatment methods for remedial measures.

Sulfate content is the most important property indicating the extent to which ettringite will form in sulfate bearing soils. The greater the soluble sulfates, the greater the potential for its formation (Ferris et al. 1991). Unfortunately, there is no standard procedure to directly measure the level of sulfate in the field. Sulfate content of soils, however, is related to electrical conductivity. Thus, electrical conductivity could indicate the presence and level of sulfates. Electrical conductivity is influenced by the amount and size of the water pores, the water content, and the concentration of electrolytes in the soil (Rhoades et al. 1977). Jayatilaka et al. (1993) have developed an electrical conductivity test to identify soluble salt contents in soils which are candidates for soil stabilization. This approach provides the advantage that, with this simple field test, one can cover a large area effectively. Bredenkamp and Lytton (1994) give a more detailed description of testing using electrical conductivity measures in the field. Using electrical conductivity and sulfate content of soils, this method can predict the expansion.

In the laboratory, various methods are available to quantify the amount of soluble sulfate. The method in which soluble sulfates are measured is an important issue. The differences between these methods are the method of sulfate extraction and the ratio of soil to water. The soluble sulfate content and electrical conductivity of soils are highly dependent on the soil-water ratio. As a result of these differences, various criteria for potential heaving problems due to sulfate content are reported in the literature (Petry et al. 1992). A paper by Little and Petry (1992) suggested that the possible level of sulfate required to induce the heaving problem is above 2000 ppm (0.2%). The authors recommended recovering the soluble sulfates from the soil using 10 parts distilled water to 1 part soil.

Relatively low levels of sulfates can lead to heaving problems. In Las Vegas, Hunter (1988) found heaving problems where the levels of sulfates were as low as 700 ppm (0.07%), while no heave occurred where the sulfate levels were over 20,000 ppm (2%). Therefore, to quantify the problem, it is necessary to perform a laboratory test to measure swell potential. The swelling test has been used to predict the volume changes caused by hydration of ettringite (Ferris et al. 1991). A series of swell tests is the most accurate method to determine the range of possible heave problems. The test should be performed at least 30 days to 45 days before compaction (Petry et al. 1992).

Currently, several approaches are possible to reduce or control sulfate-induced swell:

- Prewetting and mellowing,
- Double applications of lime,
- Low calcium stabilizers,
- Immobilization by barium compounds, and
- Potassium-based chemicals.

Dr. Petry at the University of Texas at Arlington and C.T.L. Thompson of Denver, Colorado, demonstrated that a mixing water content about 3% to 5% above optimum and mellowing for a period of 7 days before compaction could successfully reduce subsequent swell. Double applications of lime with high water contents maintained during mixing and mellowing proved to be the most successful approach. Soil with low sulfate contents may be stabilized by double applications of lime. The ettringite is formed after the first application of lime, and then the second application of lime provides strength and decreased swell potential of the soils (Ferris et al. 1991). A total lime content of about 6% is suitable using two applications of 3% each with at least 21 days between. Sufficient water is required to solubilize the sulfate to permit reaction with the soluble aluminate from the clay and with the calcium from the lime to form ettringite during the delay period (Little et al. 1992). Laboratory testing by Bredenkamp and Lytton (1994) showed that low calcium fly ash minimized the amount of expansion of clay soils with relatively high sulfate contents.

Pretreating of soils with barium hydroxide and barium chloride could reduce the soluble sulfates before lime stabilization. Swells have been reduced over 20% by using this pretreatment method (Ferris et al. 1991, Little 1987). Therefore, the formation of ettringite can be diminished by reducing the calcium sulfates. Treatment of soils with potassium based chemicals (potassium salt compounds) was originally developed by Hayward Baker, Inc. (1996). The process involves saturating the soil mass with potassium ions which form a permanent, irreversible chemical bond with the clay minerals. Montmorillinite is a clay mineral that is very expandable and is composed of two silica sheets and one alumina sheet. The bonds between the silica sheets are very weak, and water or other exchangeable ions will

enter between the silica sheets due to a negative charge deficiency, and force their expansion. Illite has a very similar structure to montmorillinite except for a potassium atom in the interlayers and, as a result, does not have much potential for swelling. If the potassium atom fills the hexagonal hole in the silica sheet, a strong bond in the layers is created as shown in Figure 2 (Holtz and Kovac, 1981). This bond prevents water ions from migration between the silica sheets and limits the expansion of clay soils.

## SUCTION OF SOILS

### Definitions of Suction

Soil suction is an energy quantity used to evaluate the capability of a soil to attract and hold water, and is the key in situ measurement for characterizing soil water storage and movement (Lee et al. 1995). When free water enters into unsaturated soils, the water can be stored or absorbed by the soil. The applied energy per unit volume of water is called soil suction or total suction. In the field, total suction is dependent upon precipitation, evapotranspiration, groundwater table, and the level of osmotic suction.

Total suction is composed of two components, matric suction and osmotic suction. Matric suction is the difference in pressure across the air-water interface and is associated with the capillary phenomenon from the surface tension of water, while osmotic suction is that part of the retention energy due to dissolved salts in the soil water (Lee et al. 1995). Total suction is expressed by the Kelvin equation, a thermodynamic equation, as:

$$h_T = \frac{RT}{mg} \ln\left(\frac{p}{p_o}\right)$$

where,

$h_T$ = total soil suction (gm-cm/gm, or simply cm), which is a negative number, indicating that the water in the soil is in tension,

R = universal molar gas constant ($8.31432 \times 10^7$ erg / mole· K),

T = absolute temperature (°C + 273.16, K),

m = molecular mass of water vapor (18.016 g / mole),

p = partial pressure of pore water vapor (kPa),

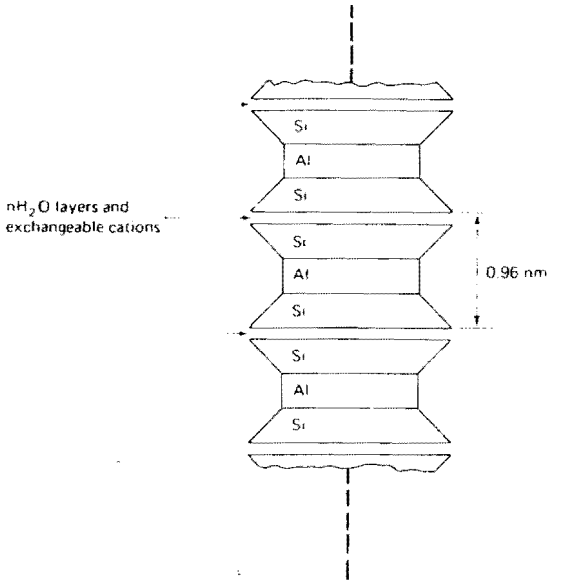


(a)

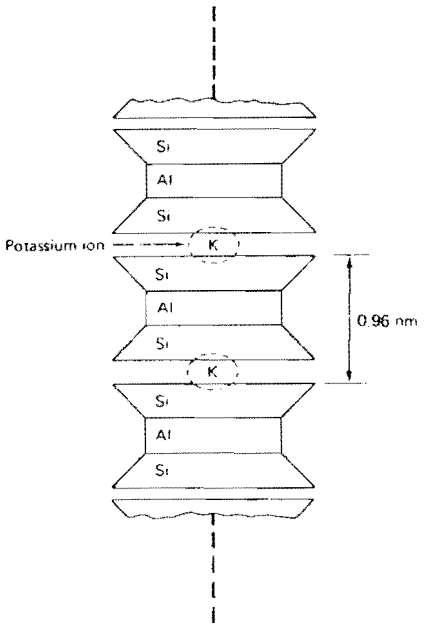


(b)

Figure 2. Schematic Diagram of the Structure of Montmorillonite (a) and Illite (b) (after Lambe, 1953).

$p_o$ = saturation pressure of water vapor over a flat surface of pure water at the same temperature (kPa), and

$p / p_o$ = relative humidity of the soil water (dimensionless).

Osmotic suction can be expressed by using Van't Hoffs' equation (Ayhan 1996):

$$\pi = \frac{RTC}{g}$$

where,

$\pi$ = osmotic suction, (gm-cm/gm or simply cm)

R = universal molar gas constant ($8.31432 \times 10^7$ erg / mole · K),

T = absolute temperature (K),

C = molar concentration (moles / liter), and

g = gravitational constant (981 cm / $sec^2$).

The matric suction is the difference between the total and the osmotic suction given by the following equation:

$$h_m = h_t - \pi$$

Among the 2 components, matric suction is very important when considering the movement of moisture. Matric suction plays the same role in moving moisture in unsaturated soils as does the hydraulic head in saturated soils.

The correct units for soil suction are in units of hydraulic head or specific energy such as kg-mm/kg in the new SI units, gm-cm/gm in the centimeter-gram-second system and pF. As a convenience to engineers, it is commonly expressed in pressure units such as kPa or atmospheres by multiplying the height of the column of water by its density. In this report, the pF scale is used to express suction. PF is the logarithm of the specific energy in gm-cm/gm or, simply, the height of the water column in centimeters

$$pF = \log_{10} |h_T|$$

where,

$h_T$ = total suction in cm of water.

In the future, when the conversion to the SI units is complete, the most consistent conversion will be to redefine pF where

$h_T$ = the total suction in kg - mm / kg or simply mm

The new pF will then be the "old pF", as is used in this report, with 1 unit added to it.

**Measurement of Soil Suction**

Soil suction can be measured using various methods based upon the determination of the soil vapor pressure or the water content (Fredlund et al. 1993). Commonly used methods are listed in Table 1.

Table 1. List of Instruments for Measuring Suction and Their Output (after Lee and Wray 1995).

| INSTRUMENT | OUTPUT |
|---|---|
| Pressure plate apparatus | Water content, air pressure |
| Heat dissipation sensor | Rate of heat dissipation |
| Electrical resistance sensor | Electrical resistance |
| Psychrometer<br>( Thermocouple & Transistor ) | Relative humidity |
| Filter paper | Water content |

The pressure plate apparatus measures only the matric suction using an axis translation technique. This laboratory apparatus is composed of a pressure chamber, a porous ceramic plate, and an air compressor. If suction values are greater than about 850 cm, the pressure

plate must be used.

The thermocouple psychrometer measures the total suction in a soil mass by determining the relative humidity in the air phase of the soil pores by using a peltier cooling technique (Fredlund et al. 1993). This device can measure suction values in the range of pF 2.0 to 4.5. However, results below pF 3.0 are not reliable. The principle involved in operating the thermocouple psychrometer is related to using a thermocouple with a sensing junction consisting of 0.025 mm diameter chromel and constantan wires. The voltage developed is proportional to suction (Lee et al. 1995).

A transistor psychrometer is used to measure the total suction in the range of pF 3.0 to 5.5 with an accuracy of ± pF 0.01. This apparatus consists of a wet and dry bulb in a probe. The temperature difference between the two transistors is converted into voltage. The test required for one set of soil samples is about 50 minutes to 1 hour, and 12 to 15 samples can be tested simultaneously (Woodburn et al. 1993).

The filter paper method can be used to measure both matric and total suction. The value of suction is inferred from water content of filter papers placed inside a sealed container along with an undistured soil specimen. When a soil sample is measured by the contact method, water can be transported in the form of liquid or gas into filter papers. Measured water content is correlated with matric suction. When suction of a soil sample is measured by the non-contact method, the measured water content is correlated with total suction. The time required to reach equilibrium is at least 7 to 10 days. Suction values in the range of pF 2.0 to 6.0 can be measured by the filter paper method in the laboratory or in the field (Lee et al. 1995, Fredlund et al. 1993).

Heat dissipation sensors or electrical resistance sensors are similar methods for measuring the matric suction. The principle of these methods is to measure the change in temperature and electrical resistance of a sensing tip made of porous ceramic with variations in water content. Lee and Wray (1995) provide more detailed information on the two methods.

## CONDUCTIVITY IN UNSATURATED SOILS

Pavement subgrades are categorized as unsaturated soils, and they exhibit no constant values of hydraulic conductivity as do saturated soils. Since hydraulic conductivity is a

function of in situ density, soils at a specific site may have different volumetric water content even though they have the same gravimetric water contents. Conductivity in unsaturated soils is dependent upon matric suction which represents the soil water movement and storage in soils. Matric suction is related to the stress state in the soil and can be used to determine the in situ hydraulic gradient (O'Kane 1996). However, the flow of water in an unsaturated soil does not fundamentally depend upon matric suction and is controlled by the hydraulic gradient as a driving potential (Fredlund et al. 1993).

Soil water moves through a soil mass from a state of low suction (wet) toward a state of high suction (dry). Therefore, soil water can be transported due to a suction gradient similar to a pressure gradient in saturated soils. Unfortunately, unsaturated conductivity or permeability is very complex to predict because laboratory measurements of conductivity are, at best, only indications of the actual field conductivity of soils. Various empirical equations have been proposed and, among these, Gardner's equation ( 1958 ) is widely accepted:

$$k = \frac{k_o}{\left( 1+b|h|^n \right)}$$

where,

$k_o$ = the permeability at zero suction (cm / sec),

$|h|$ = the absolute value of matric suction (cm), and

b, n = experimental constants ($10^{-9}$ , 3 typically).

More information on the empirical equations for permeabilities is provided by Ayhan (1996) and Fredlund et al. (1993).

In expansive clays, the flow properties are greatly influenced by the cracking pattern and block structure of the clay. From a practical standpoint, backcalculation of conductivity from field measurements of soil water flow is recommended (Lytton 1977). Unsaturated permeability is defined in terms of soil suction:

$$p = \frac{k_o \ |h_o|}{0.4343}$$

where,

$k_o$ = saturated permeability (cm / sec), and

$|h_o|$ = the absolute value of the total suction at which the soil becomes saturated (approximately -100 cm for clay).

Based on the finite element model for flow developed by Gay (Jayatilaka, et al. 1993), the unsaturated permeability or diffusion coefficient can be estimated by the following equation:

$$p = \frac{\alpha \ \gamma_d}{|S| \ \gamma_w}$$

where,

p = the unsaturated permeability ($cm^2/sec$),

$\gamma_w$ = the unit weight of water ($g/cm^3$),

$\gamma_d$ = the dry unit weight of the soil ($g/cm^3$),

$\alpha$ = the diffusion coefficient ($cm^2/sec$), and

$|S|$ = the absolute value of slope of the log suction to gravimetric water content line.

The diffusion coefficient, $\alpha$, is estimated as follows.

$\alpha$ = 0.0029 - 0.000162 (S) - 0.0122 (SCI)

where,

SCI = suction compression index, and

S = suction - water content slope (a negative number).

The suction compression index can be estimated from the plasticity index, cation exchange capacity, and the fine clay content. The slope (S) is estimated by the following parameters:

$$S = -20.29 + 0.1555\,(LL) - 0.117\,(PI) + 0.0684\,(\#\,200)$$

where,

LL = the liquid limit (%),

PI = the plasticity index (%), and

# 200 = soil passing 75 μm sieve (%).

Bulk flow of water occurs in unsaturated soils in response to a matric suction gradient. However, higher levels of osmotic suction provide a driving potential for osmotic diffusion. Osmotic diffusion is due to ionic or molecular movement in response to a concentration gradient (Fredlund et al. 1993). Most of the measurements of permeability in the laboratory and field use only distilled water and, therefore, do not consider the soluble salt concentrations that actually exist in the field. As a result, osmotic diffusion in higher osmotic suction zones may be a major factor in fine-grained soils in the field.

## VERTICAL MOISTURE BARRIERS

Moisture barriers can be used to minimize the roughness development on highway pavements due to expansive subgrade soils. A typical cross section of a vertical moisture barrier is shown in Figure 3. The basic principle of moisture barriers is that, if the soil is in a drying condition, the barrier will prevent access to free water which may flow in through shrinkage cracks. While the soil was initially wet, the soil fabric is closed, and the barrier does not allow the migration of water into subsoils beneath the pavement (Picornell 1985). Typically, vertical moisture barriers are more effective at retarding lateral water migration than horizontal barriers. They not only move the edge effect away from the pavement but they also minimize fluctuations of water content below the pavement and minimize lateral water migration near the surface. Moisture barriers can be installed as a preconstruction method or a remedial measure.

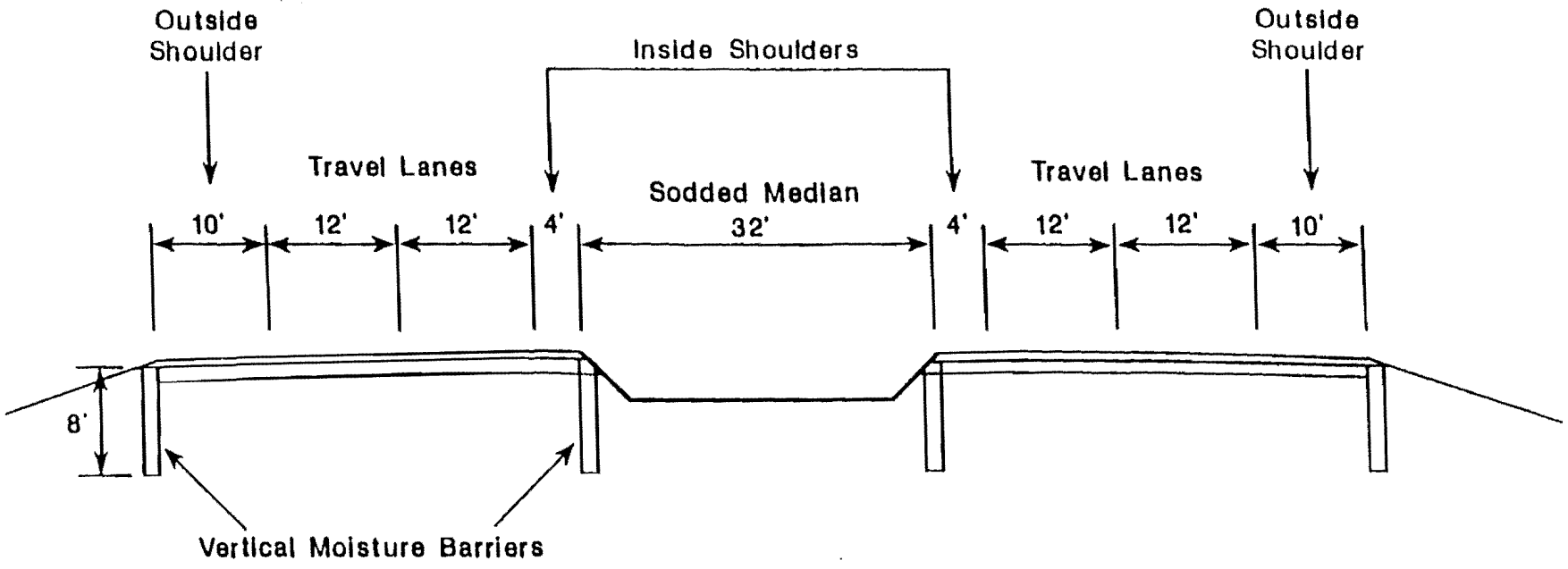


Figure 3. A Typical Cross Section of a Pavement with Vertical Moisture Barriers (Jayatilaka et al. 1993).

The main factors that affect the effectiveness of moisture barriers are annual rate of rainfall and evapotranspiration (Russam and Coleman 1961). Drainage conditions, cracking patterns at the surface, and soil properties also play important roles in determining the amount of moisture in the subgrade (Jayatilaka et al. 1993). Vertical barriers should be employed at least as deep as the zone affected by seasonal moisture change. From a practical standpoint, a depth of one half to two thirds of the moisture-active zone is recommended. The depth of the active zone is typically 2.4 to 4.5 m. Picornell (1985) developed a design procedure for determining the required depth of a barrier for a site based upon its climatic and soil conditions. He suggested that the barrier be installed to the maximum depth of vegetation roots to prevent longitudinal cracking and about 25% deeper than the root depth to stop the development of roughness.

Based on the results of a study by Jayatilaka et al. (1993), vertical moisture barriers have proved to be very effective in reducing the development of roughness in pavements built on expansive soils when medium cracked soils and uncracked soils with shallow roots are present on the site. The soil type is determined using estimated unsaturated permeability as shown in Table 2.

Table 2. Unsaturated Permeability in Different Soil Types ( after Jayatilaka et al. 1993 ).

| **Soil type** | **Unsaturated permeability ( $cm^2$ / sec )** |
|---|---|
| Cracked or highly permeable | $k > 0.001$ |
| Medium cracked or moderately permeable | $0.00005 < k < 0.001$ |
| Tightly closed cracks or minimally permeable | $k < 0.00005$ |

In medium cracked soils, vertical barriers are effective in all climates under any drainage conditions but are not effective in cracked soils even under any of the drainage conditions as shown in Figure 4. Therefore, before installing vertical moisture barriers beside pavements, an estimation of the unsaturated permeability, which depends on the crack pattern in the

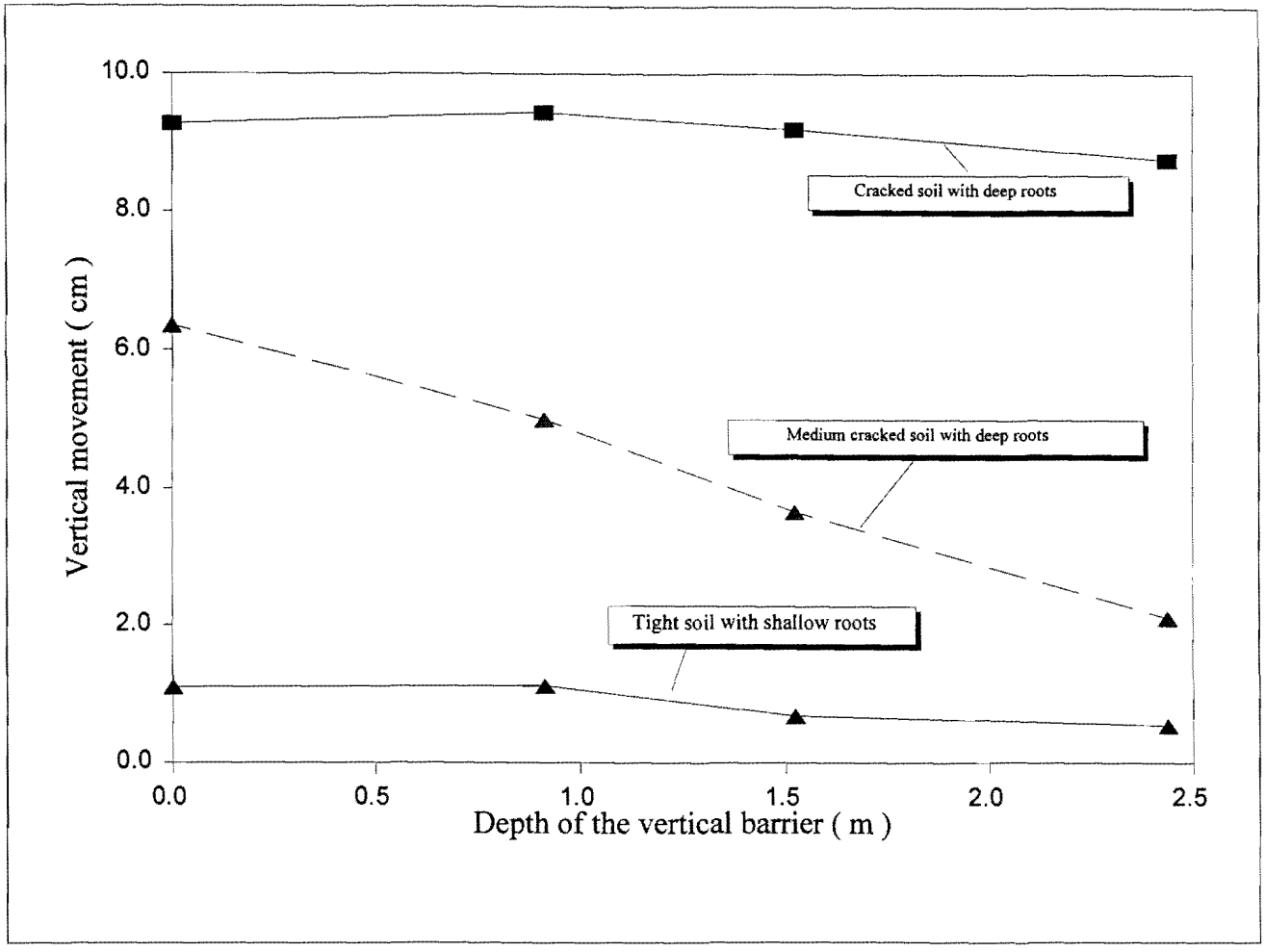


Figure 4. Vertical Barrier Effectiveness (Sodded Median and Slope Drainage) (after Jayatilaka et al. 1993).

subgrade soils, and the depth of vegetation roots should be obtained (Picornell 1985).

## GROUND PENETRATING RADAR APPLICATION ON SOILS

Ground penetrating radar (GPR) is an active remote-sensing method developed in the 1960s that uses a reflection technique wherein non-ionizing radio waves penetrate into solid materials and require relatively low power. The high frequency and short time duration electromagnetic signals from 100 to 1000 MHz are transmitted through an antenna system into the subsurface. GPR has become an effective method for non-destructive investigations to measure the thickness of ice in permafrost regions, evaluate pavement conditions, and examine subsurface soils. The GPR method produces continuous, high resolution profiles of the subsurface in a way similar to seismic reflection methods. Recent developments of the GPR have increased the depth of penetration to which the technique can distinguish soil profiles (Davis and Annan 1989).

The basic scheme for using GPR involves generating an electromagnetic (EM) pulse that penetrates the ground and is reflected from the interfaces between different types of soil layers as shown in Figure 5. The GPR system radiates short pulses of high frequency EM energy into the subsurface from a transmitting antenna. When the radiated energy encounters an interface between different layers or other inhomogeneities or anomalies in electrical properties of the subsurface, some energy is reflected back to the radar antenna (Annan 1992). Electrical properties are determined primarily by water contents, dissolved minerals, and other subsurface materials. Changes in electrical properties, which are related to changes in volumetric water content, induce reflections of the transmitted signal. The propagation of the radar signal depends on the high frequency electrical properties of the soil. The reflected signal is amplified and then transformed to the audio frequency range. Finally, the signal is recorded, processed, and displayed (Beres and Haeni 1991).

The variation of electrical properties is the dominant factor controlling GPR responses. GPR makes use of an EM field, consisting of coupled electric and magnetic fields which propagate into the ground. Conduction current and displacement current describe the mechanism of electrical charge. In the relationship between the conduction current, an energy dissipating mechanism, and the applied electric field, the conductivity is very dependent on the

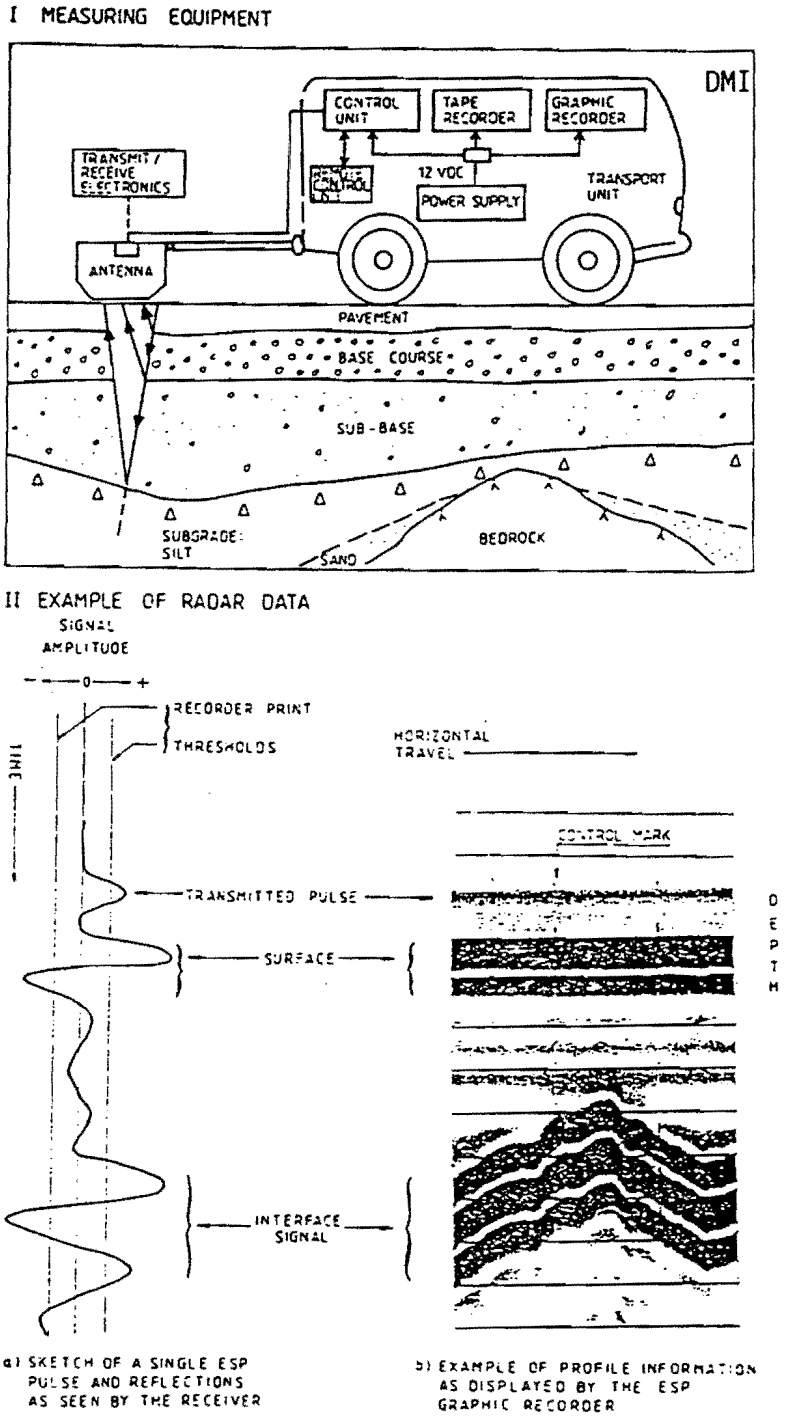


Figure 5. Principle of the Ground Penetrating Radar System (The Finnish Geotechnical Society 1992).

charge density. It can be described in the linear equation (Annan 1992):

$$J_c = \sigma E$$

where,

$J_c$ = the charge density or conduction current density (amperes/$m^2$),

E = electric field strength in (units), and

$\sigma$ = electrical conductivity (siemens/m).

Displacement (polarization) current, which is an energy storage mechanism, is associated with a dipole moment density.

$$J_D = \frac{dD}{dt} = e\frac{dE}{dt}$$

$$D = eE$$

where,

$J_D$ = displacement current or charge density (coulombs/$m^2$),

D = dipole moment density (coulombs/$m^2$),

E = electric field, and

e = permittivity (Farads/m).

Therefore, the current which flows in response to the application of an electric field is a combination of 2 currents (conduction and displacement). But the displacement properties dominate the conductivity properties for many geological materials. The presence of water is a major influence on the electric properties of soils since water molecules have a natural dipole moment. Additionally, the conductivity is approximately proportional to the total dissolved solids content. Dielectric constant and electrical conductivity values for

several materials are given in Table 3 (Beres and Haeni 1991, Saarenketo and Scullion 1992, Ulriksen 1982, The Finnish Geotechnical Society 1992).

Table 3. Typical Electrical Properties on Geologic Materials.

| Material | Dielectric constant | Conductivity (mS/m) |
|---|---|---|
| Air | 1 | 0 |
| Frozen soil | 3 - 6 | $10^{-4}$ to $10^{-2}$ |
| Quartz | 4 - 5 | $10^{-6}$ to $10^{-4}$ |
| Sandstone | 5 - 12 | $10^{-8}$ to $10^{-3}$ |
| Dry sand | 3 - 6 | $10^{-2}$ |
| Saturated sand | 20 - 30 | 0.1 - 1 |
| Dry clay | 5 | 2 |
| Saturated clay | 25 - 40 | 500 - 1000 |
| Peat | 50 - 78 | $10^{-3}$ to 2 x $10^{3}$ |
| Silts | 5 - 30 | 1 - 100 |
| Shale | 5 - 15 | 1 - 100 |
| Limestone | 7 - 9 | $10^{-9}$ to $10^{-2}$ |
| Micaceous clay | 80 - 85 | 5 x $10^{-4}$ to 5 x $10^{2}$ |
| Distilled water | 81 | 0.5 |
| Salt water | 81 | 3000 |

The performance of GPR depends on the characteristics of the radar itself and the nature of the subsurface. The major factors affecting the GPR response are the relative dielectric constant and the attenuation of the ground. The resolution of GPR depends strongly on the penetrated depth and range of the radar. When an electromagnetic pulse propagates through the ground, it is subjected to several loss mechanisms. Any type of surface attenuates the transmitted pulse through reflection and absorption losses. The

attenuation of wet clay soil is greater than that of dry sands or gravels. Wet soils cause more than twice the reflection loss than dry soils.

The dielectric constant of a soil is primarily a function of water content, soil type, and soil bulk density. Dry soil is relatively independent of wave frequency or soil type. When the soil retains water, the dielectric parameters are greatly influenced by soil type and EM wave frequency (Kutrubes 1986). In sand, the real part of the dielectric constant is influenced more by water content while the imaginary part is influenced more by frequency. Bulk soil density can significantly affect the dielectric properties of wet soil. The attenuation by the soil media increases with increasing temperature. Therefore, seasonal variations in dielectric properties affect the depth of penetration (Michelson 1985).

Several factors significantly affect the GPR responses. Conductivity of the material affects the penetration depth of the GPR and is reduced by higher water content and salts in solution. Hence, the range and resolution of GPR performance decreases with the presence of conductive materials such as clays, silts, or soil with conductive pore water (Barr 1993). The conductivity of a dielectric material causes the EM pulse to lose energy in the form of heat (Daniel 1989). Thus, a dry soil allows radar penetration to greater depths than a wet soil. The greater the difference of dielectric constants between two layers of materials, the stronger the radar reflection obtained. Attenuation increases with wave frequency (Micheson 1985). A 10% clay content can cause a reduction of depth of penetration by an order of magnitude (Olhoeft 1987) and increasing the clay content by 5% reduces the depth of penetration by a factor of 20 (Kutrubes 1986, Doolittle and Repertus 1988). The various factors affecting GPR performance are summarized in Table 4. More detailed information of GPR applications on soils and basic principles are available in papers by Black and Kopac 1992, Ulriksen 1982, Doolittle and Repertus 1988, The Finnish Geotechnical Society 1992, Saarenketo and Scullion 1994, and Sutinen 1992.

Table 4. List of Factors Affecting Ground Penetrating Radar Survey.

| Factor | How GPR is affected | Level of importance |
|---|---|---|
| **1. Dielectric permittivity ( K )** | The propagation speed of the wave and its reflection decreased with higher permittivity. | High |
| **2. Electrical conductivity of the medium (σ)** | The contrast of the conductivity control the depth capacity and resolution of GPR. | High |
| **3. Water content** | Higher water content increases electrical conductivity of soil which increases attenuation. | High, Frequency dependent |
| **4. Soil type: soil texture and structure** | Clay content affects attenuation. Dry soil is independent of frequency and soil type. Chemical composition is important | Medium |
| **5. Soil density or Porosity** | The dielectric properties of soil increase with density or water content. | High |
| **6. Soil temperature** | Dielectric constant and conductivity strongly temperature dependent. | High, The dielectric constant of water is temperature dependent. |
| **7. Excitation frequency** | As the frequency decreases, an increase in the signal levels occurs. | Low |
| **8. Ionic concentration in the ground water** | Cause attenuation and high surface reflection. | High |
| **9. Particle size of soil** | Higher surface interface increases attenuation. | Medium |
| **10. Wave length** | Long wavelength prevents discrimination of thin layers. | The wavelength of the certain frequency is changed by soil type. |
| **11. Water table** | EM contrast between dry and wet layers decreases. | Low |
| **12. Soil stratification: layer thickness** | Leads to reflection losses. | Low |
| **13. Diurnal variation** | Change of water content in soils. | Environmental effect |

| Factor | How GPR is affected | Level of importance |
|---|---|---|
| **14. Dissolved minerals** | More dissolved minerals increase water conductivity and thus increase attenuation. | Medium |
| **15. Thin layers in ground** | Scatter the EM wave energy into random directions. | Medium |

## PARTICLE SIZE MEASUREMENT FOR FINE-GRAINED SOILS

The characterization of particle size and distribution is an important step in almost every laboratory test on soils and aggregates. The parameters for characterizing subgrade soils are dependent upon the content of fine clay which is finer than 2 μm. In order to estimate the properties of expansive soils, the percentage of clay should be quantified. However, the accuracy of distribution curves for fine-grained soils is often questionable because the behavior of fine-grained soils is much more dependent upon clay minerals than on particle size (TRB 1996).

The size of silt and clay particles is commonly measured using the hydrometer test. These procedures depend on Stokes' equation for the terminal velocity of a falling sphere and require a minimum of 24 hours to test. There are a number of assumptions in Stokes' equation which result in intrinsic errors. Lambe (1991) discussed the problems related to Stokes' equation. Most fine-grained soil particles smaller than 5 μm have a plate-like shape. When such particles fall through water, the equivalent diameter of the sphere calculated by hydrometer test would be smaller than the actual diameter of the particle. Therefore, the hydrometer test likely underestimates particle size for flat shaped particles under 5 μm.

Advances in power technology have introduced a new laser diffraction technique to analyze particles. Laser diffraction methods can be used to measure the size of fine-grained soils under 75 μm. The basics of the laser diffraction particle size analyzer is to measure the particles while suspended in the liquid using the Fraunholer diffraction and Mie scattering theories. Compared with other methods used for particle size measurement, laser diffraction has some advantages as follows (Allen 1981):

- The measurement can be made accurately,
- Samples are not disturbed by the insertion of a device such as a hydrometer,
- The sample required is relatively small,
- Tests can be done rapidly,
- Test has good repeatability, and
- Results can provide the particle size distribution and discrete percentage of particles passing or retained.

This new measurement method not only provides detailed information on particle size distribution but is also an efficient tool for characterizing the fine clay and silt sized materials from pavement subgrades.

# CHAPTER 3
# SITE CHARACTERIZATION

## SITE DESCRIPTION

Two sites were selected for this study. The SH 6 site is located approximately 2.1 km north of FM 2818 in Brazos County. The northbound and southbound lanes are separated by a sodded median (Figure 6). The facility is a four-lane divided highway with paved shoulder which has a 3.3 m wide outside shoulder, a 1.2 m wide inside shoulder, and two 3.7 m wide traffic lanes. Two test sections were selected on the northbound side and 2 on the southbound side and were labeled NB1, NB2, SB1, and SB2, respectively, as shown in Figure 7. On the SH 6 site, the high points of the heaves are where borings NB1-1, NB2-1, SBA-2, and SB2-2 are located.

The SH 21 sites are located 1.6 km and 10.4 km west of FM 1362 in Burleson County. The westbound and eastbound lanes are separated by grassy medians (Figure 8). Three test sections were selected and labeled WB1, WB2, and EB1 (Figure 9). The high points of the heaves on SH 21 are where borings WB1-1, WB2-1, and EB1-3 were performed. More details of the locations are shown in Appendix A.

According to the U.S. geological surveys (USGS), all the test sections along SH 6 and SH 21 are located under the Cook Mountain formation described as Ecm in Figure 10. The segments of highway are partly in the alluvium of the Brazos River and partly in the geological clay-forming strata of the Texas coastal plains. The soils are mostly weathering brownish gray to brown clays and brownish gray to yellowish gray clays.

The soils in the SH 6 sites are fine montmorillonitic clays (U.S.D.A. Soil Conservation Service 1981). Sites NB1 and SB2 are classified as Crockett soils which have very low permeability and moderate water holding capacity. The clay subsoil has a high shrink-swell potential and has 2% gypsum at a depth of 1.2 m. Sites NB2 and SB1 are classified as Luling soils. The soil has very low permeability and high water holding capacity. The clay subsoil has a very high shrink-swell potential and has 2% to 5% gypsum at a depth from 0.9 to 1.8 m.

Figure 6. Site View of SH 6.

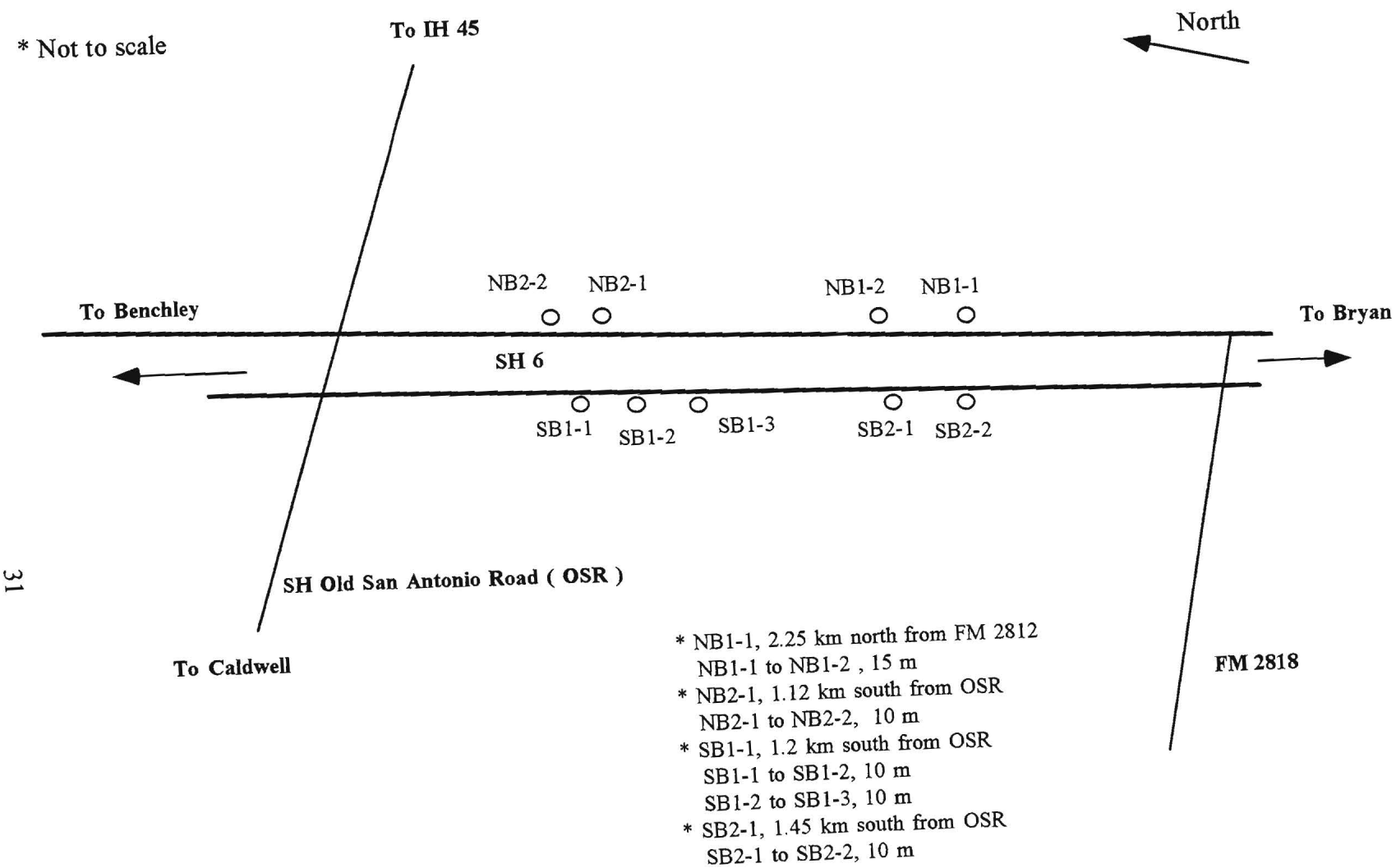


Figure 7. Site Description of SH 6 and the Location of Boreholes.

Figure 8. Site View of SH 21.

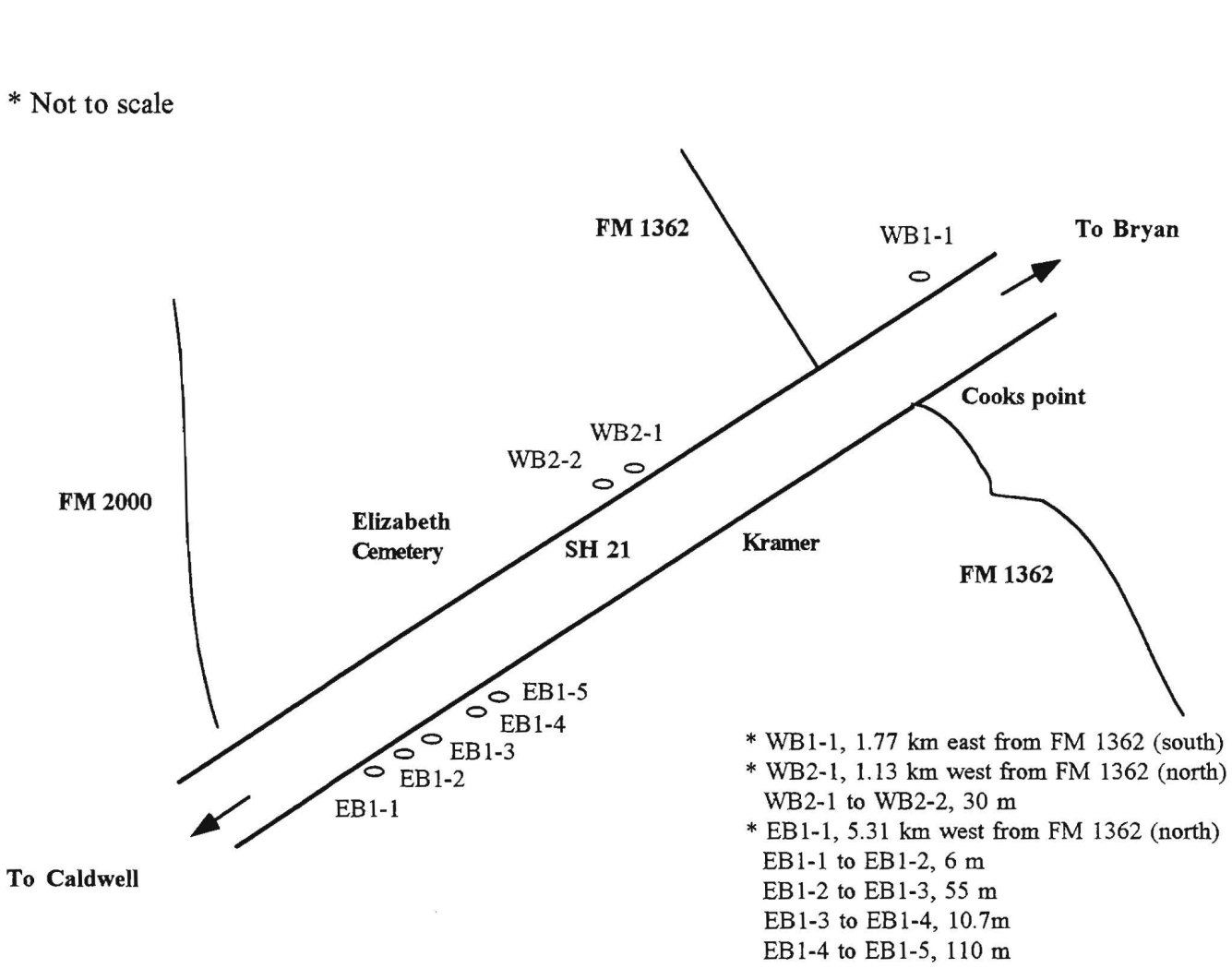


Figure 9. Site Description of SH 21 and the Location of Boreholes.

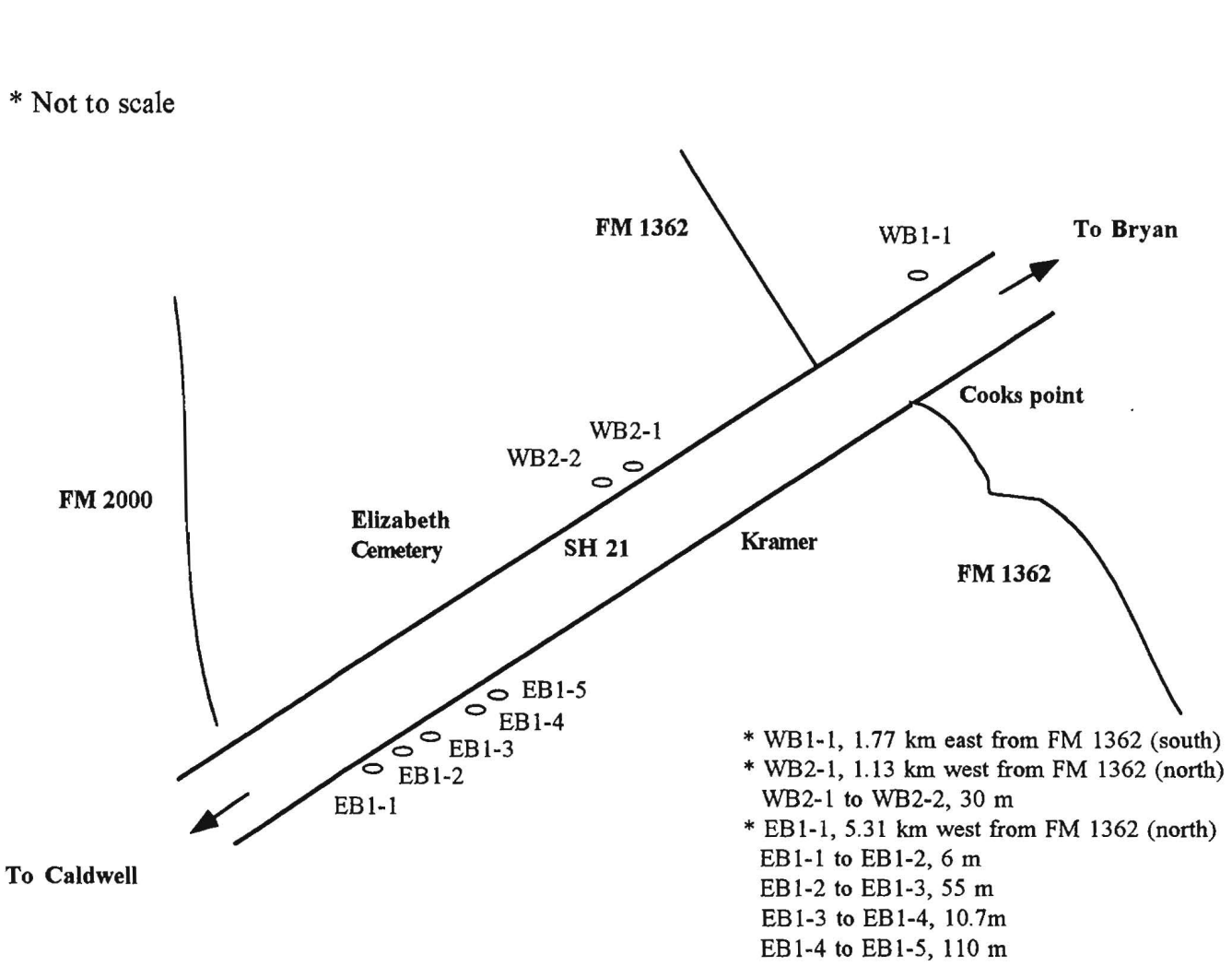


Figure 9. Site Description of SH 21 and the Location of Boreholes.

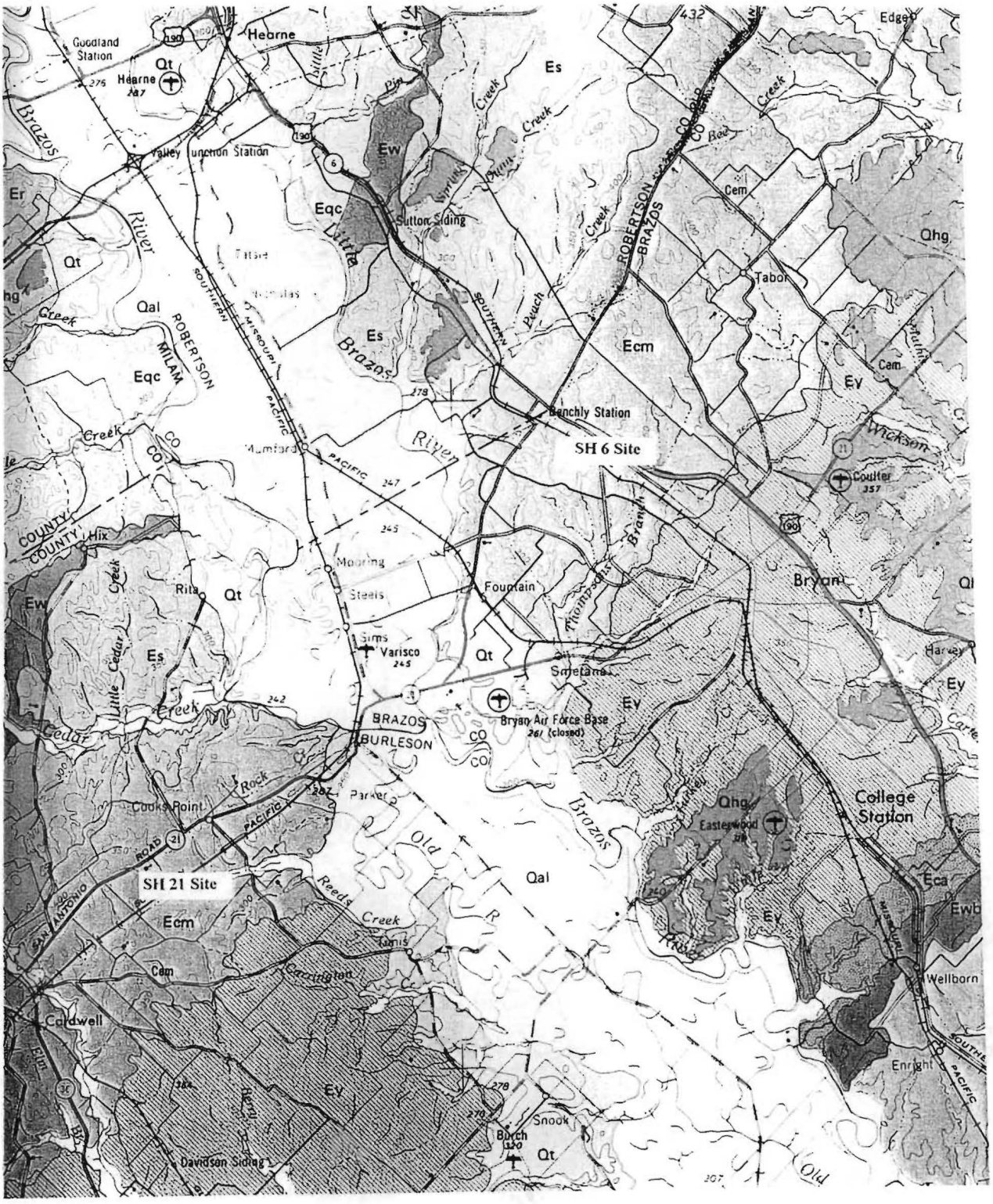


Figure 10. Geological Formation of SH 6 and SH 21 Sites.

The soils in SH 21 are also fine montmorillonitic clays. Sites WB1 and WB2 are classified as Benchley soils. The soil has low permeability and moderate water holding capacity. The clay subsoil has a moderate to high shrink-swell potential. Site EB1 is the same as Luling soils in SH 6.

The Thornthwaite Moisture Index (TMI) is + 4 in Brazos and Burleson Counties from Figure 11 (Russam and Coleman, 1961). The TMI is a number that indicates the moisture balance in soils at a particular location. Based on regional climatological data, the TMI is dependent upon rainfall, potential evapotranspiration, and the depth of available moisture in the rooting zone of vegetation. The mean monthly rainfall and temperature in Brazos and Burleson Counties are shown in Figure 12.

## FIELD INVESTIGATION

Soil boring and sampling was conducted using a continuous flight auger. A Shelby thin-walled tube sampler was used to obtain "undisturbed" samples. Figure 13 shows the soil boring operation at SH 21. The location of the boreholes described in Figures 8 and 9 were selected carefully at the peak and the foot of heaves by visual observation of pavement undulations. Samples were taken at intervals of 40 cm, and the boring was continued until the sampler could not be pushed any deeper. A total of 17 borings were performed at both sites. After sampling, each soil sample was wrapped and stored in a temperature-controlled room until time for the designated tests. During sampling of soils near NB2 and SB1, on SH 6, pieces of gypsum were found alongside the roadway. A summary of each borehole log from SH 6 and SH 21 is presented in Appendix B.

Ground penetrating radar (GPR) surveys were used in an attempt to characterize the soil layers and to detect the presence of water-saturated lenses in the pavement subgrade. All GPR surveys were performed using a ground-coupled antenna at a central frequency of 100 MHz. The GPR equipment used was a SIR 10 A system manufactured by GSSI, Inc. Traffic control was provided by TxDOT. Data from the field survey were analyzed using the software program RADAN for Windows. Figures 14 and 15 show views of the GPR survey and control units.

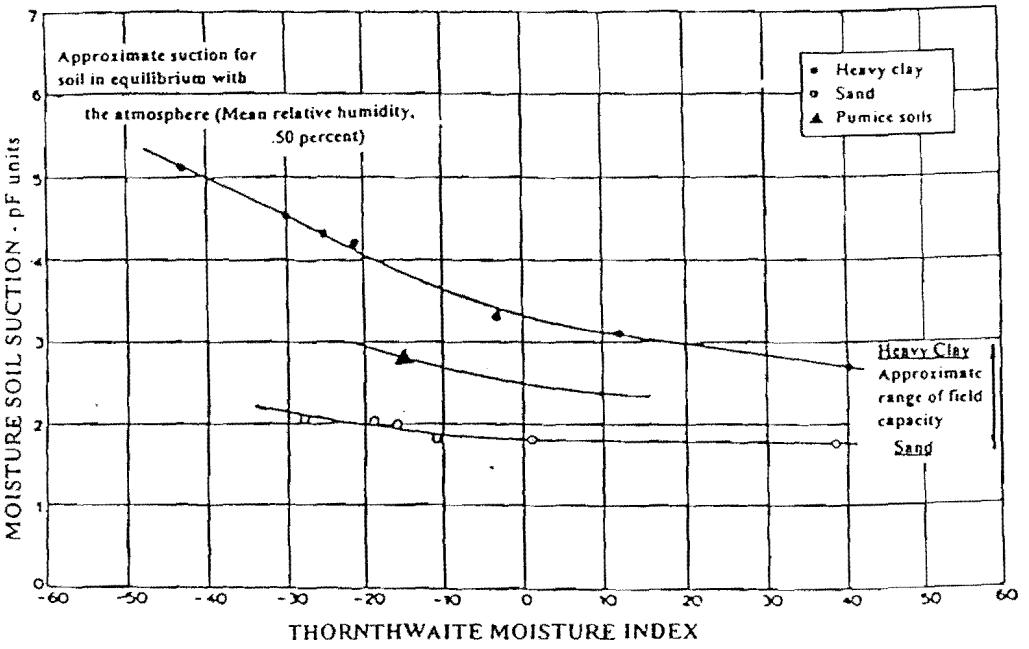


Figure 11. Variation of Soil Suction of Road Subgrade with Thornthwaite Moisture Index (after Russam and Coleman, 1961).

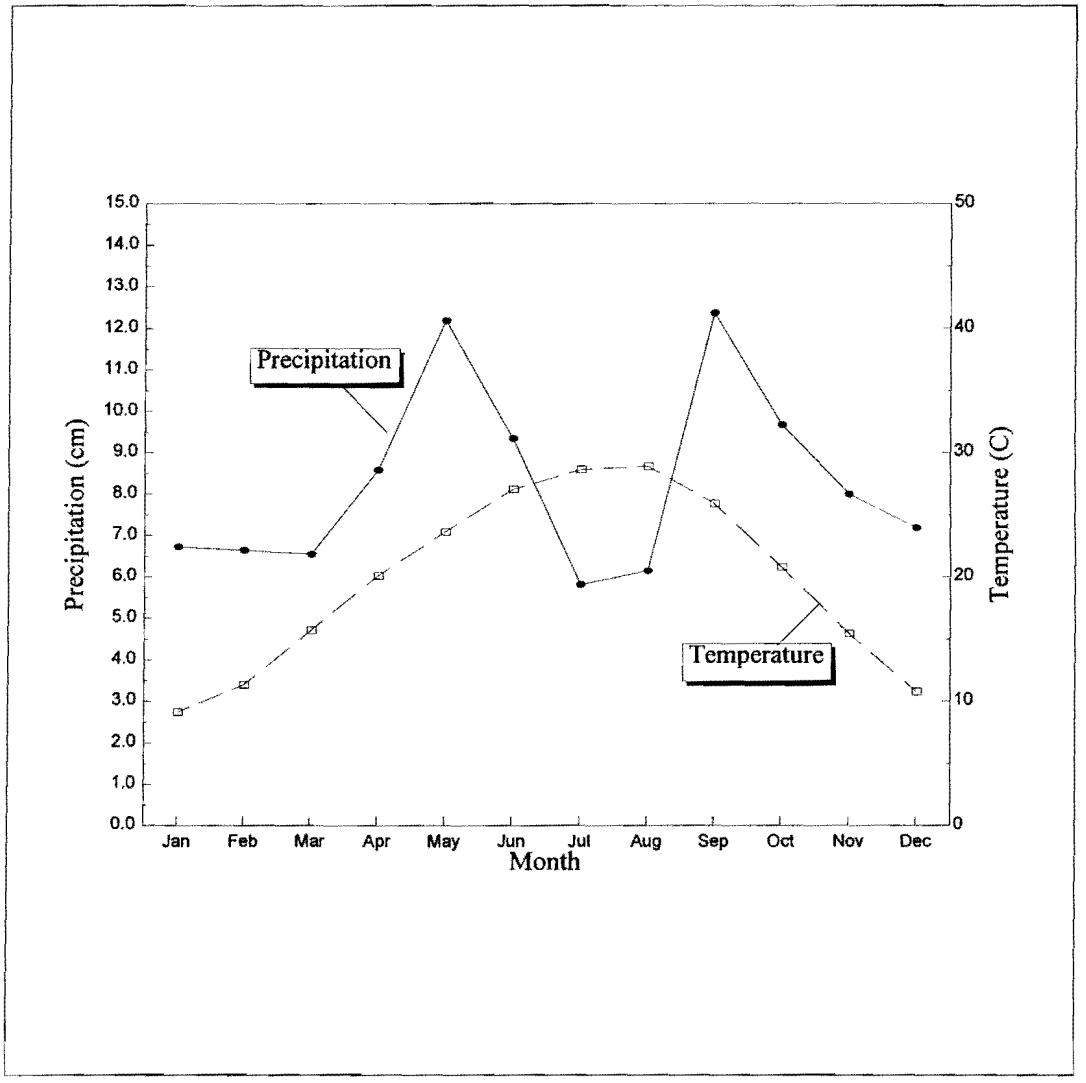


Figure 12. Mean Monthly Precipitation and Temperature in Brazos and Burleson Counties.

Figure 13(a). The Soil Boring at SH 21 Site.

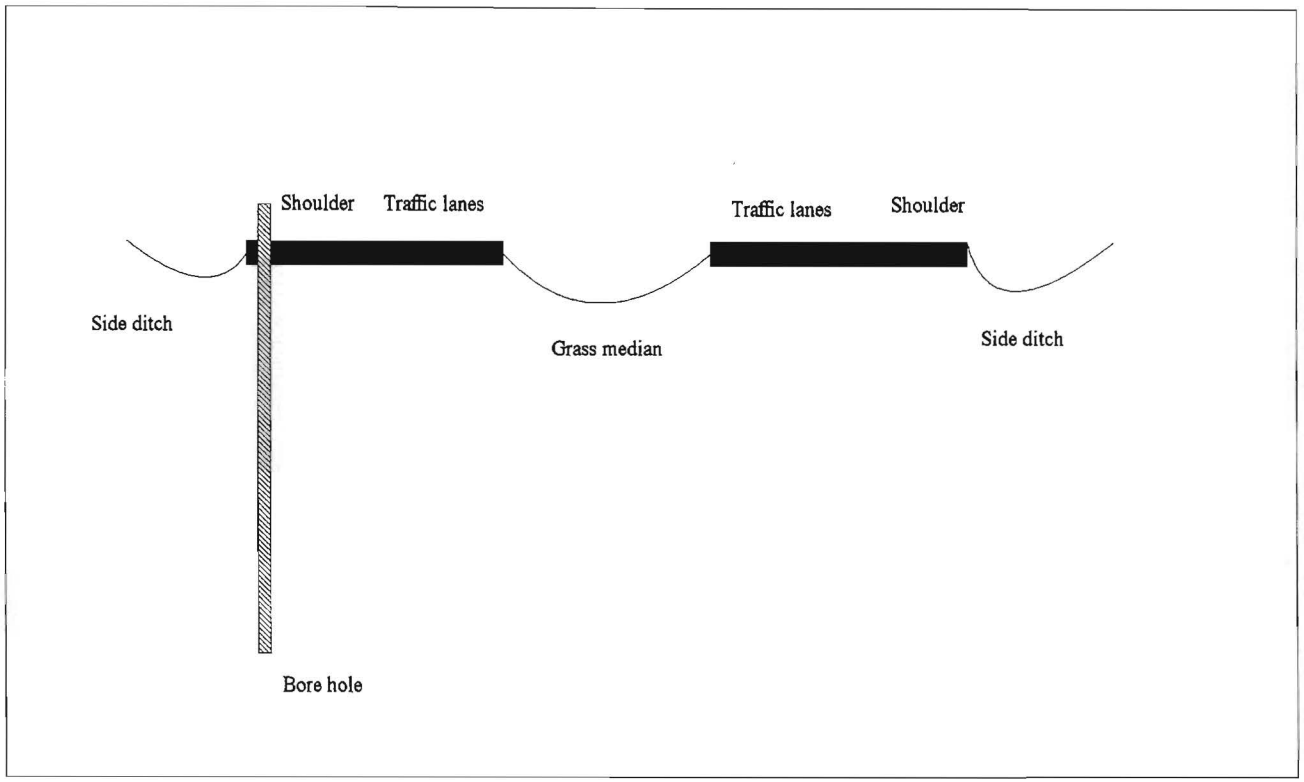


Figure 13 (b). Cross Section of Pavements Where the Borings were Made.

Figure 14. Radar Survey Using Ground Coupled Antenna at SH 21 Site.

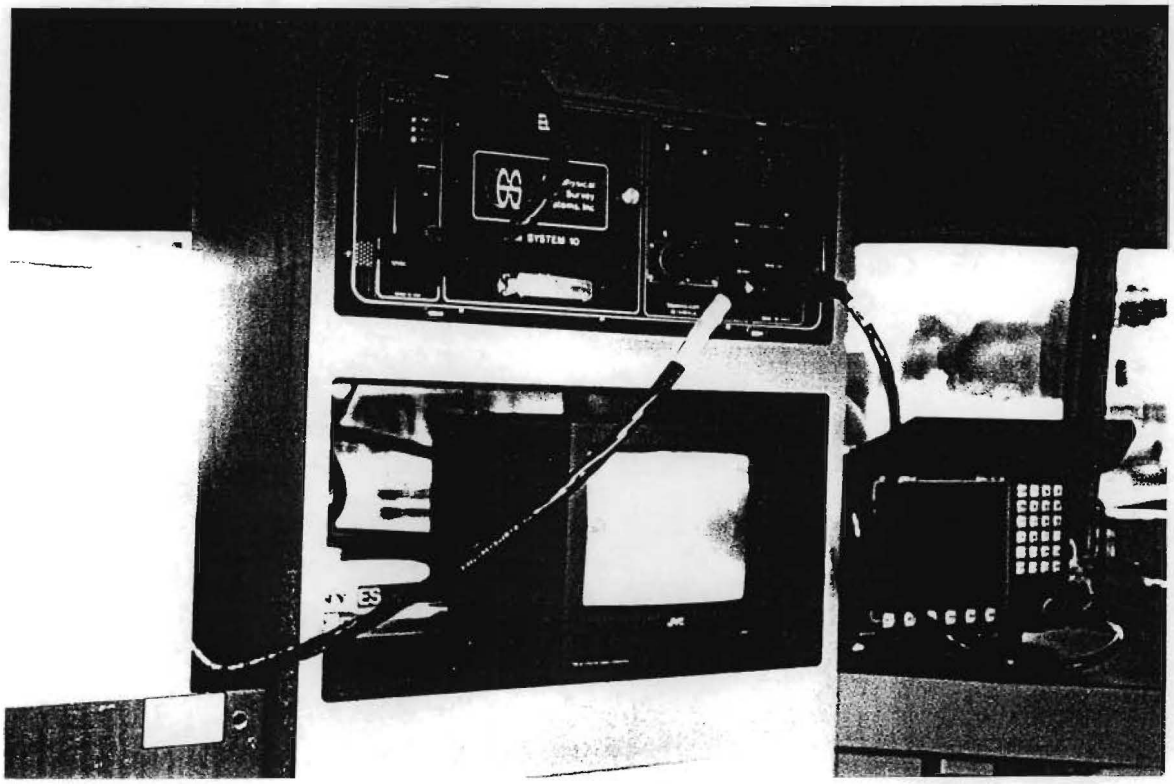

Figure 15. SIR 10 A Control Unit (GSSI, Inc.).

Based on information from soil survey maps and the first survey trial, the central frequency was found to be too low to successfully differentiate thin layers in the subgrade soils. In an attempt to obtain better resolution in the predominantly clay environment in the project sites, the wave propagation of GPR was minimized. A higher frequency antenna of 500 MHz was used in place of the 100 MHz device. However, the clay subsoil was highly attenuating because the highly montmorillonitic clays which comprise the major soil types in the project areas have relatively high water contents. The high water contents impede penetration of the GPR signals into the soil and thus prevented the observation of any deep, water-bearing lenses of granular materials. An example of the test result is shown in Appendix C.

## LABORATORY TESTS AND RESULTS

### Sulfate Content Test

Currently, there is no standard test for sulfate content testing of soils. Extraction of the soluble sulfates was performed using the EPA procedure (1979), and sample saturation was performed in accordance with the USDA method (Richards et al. 1954). Two different soil-to-water ratios (saturated soil paste and 1:20 by weight) were used. The saturated soil paste was allowed to set overnight and then the sulfate was extracted. Nine samples from SH 6 and SH 21 near the surface where lime stabilization was used were tested and the results are shown in Tables 5 through 8.

The sulfate test results in Tables 5 and 6 show that there is a large amount of soluble sulfate in the soil at the SH 6 site. There was sufficient sulfate in the soil to warrant the use of alternatives to lime in providing a working table for construction equipment during the construction of the pavement.

On the other hand, Tables 7 and 8 show that much less soluble sulfate is present in the subgrade soil at the SH 21 site. This level of sulfate is considered to be low enough to eliminate concern about a lime-sulfate swell problem.

Table 5. Sulfate Content of Soils from SH 6 Using Saturated Paste.

| | Sulfate content | | | | |
|---|---|---|---|---|---|
| | Test 1 | | Test 2 | | Avg. |
| Sample | (ppm) | (meq / l) | (ppm) | (meq / l) | (meq / l) |
| NB1-1A | 182 | 3.8 | 163 | 3.4 | 3.6 |
| NB2-1A | 4453 | 92.7 | 4410 | 91.8 | 92.3 |
| NB2-2A | 4522 | 94.1 | 4499 | 93.7 | 93.9 |
| SB1-1A | 2034 | 42.3 | 2038 | 42.4 | 42.4 |
| SB1-2A | 3527 | 73.4 | 3495 | 72.8 | 73.1 |
| SB2-1A | 819 | 17.1 | 743 | 15.5 | 16.3 |

Table 6. Sulfate Content of Soils from SH 6 Using 1:20 Soil Water Ratio.

| | Sulfate content | | | | |
|---|---|---|---|---|---|
| | Test 1 | | Test 2 | | Avg. |
| Sample | (ppm) | (meq / l) | (ppm) | (meq / l) | (meq / l) |
| NB1-1A | 756 | 15.7 | 758 | 15.8 | 15.8 |
| NB2-1A | 15870 | 330.4 | 15820 | 329.4 | 329.9 |
| NB2-2A | 14090 | 293.4 | 14110 | 293.8 | 293.6 |
| SB1-1A | 4451 | 92.7 | 4457 | 92.8 | 92.7 |
| SB1-2A | 13220 | 275.2 | 13260 | 276.1 | 275.7 |
| SB2-1A | 1160 | 24.2 | 1147 | 23.9 | 24.0 |

Table 7. Sulfate Content of Soils from SH 21 Using Saturated Paste.

| | Sulfate content | | | | |
|---|---|---|---|---|---|
| | Test 1 | | Test 2 | | Avg. |
| Sample | (ppm) | (meq / l) | (ppm) | (meq / l) | (meq / l) |
| EB1-1A | 75 | 1.6 | 95 | 2.0 | 1.8 |
| EB1-2A | 78 | 1.6 | 78 | 1.6 | 1.6 |
| EB1-3A | 45 | 0.9 | 48 | 1.0 | 1.0 |

Table 8. Sulfate Content of Soils from SH 21 Using 1:20 Soil Water Ratio.

| | Sulfate content | | | | |
|---|---|---|---|---|---|
| | Test 1 | | Test 2 | | Avg. |
| Sample | (ppm) | (meq / l) | (ppm) | (meq / l) | (meq / l) |
| EB1-1A | 192 | 4.0 | 194 | 4.0 | 4.0 |
| EB1-2A | 343 | 7.1 | 347 | 7.2 | 7.2 |
| EB1-3A | 197 | 4.1 | 193 | 4.0 | 4.1 |

**Electrical Conductivity Test**

Electrical conductivity measurements were performed in an attempt to estimate the sulfate content in the soils. The test was performed in accordance with a procedure developed by Bredenkemp et al. (1994). Figures 16 and 17 show a conductivity probe and a test view. The procedure is performed by using the following.

- Obtain 5 gm of soil.
- Weigh approximately 5 gm of each soil sample into a plastic container. If the soil is wet, break up any lumps and dry the soil.
- Record the dry weight of the sample and add a mass of distilled water equal to 20 times the weight of the dry soil in a plastic container.
- Tightly close the lid of the container and shake until the soil and water forms a homogeneous mixture.
- Calibrate the conductivity meter.
- Record the reading in milli Siemens (mS).

Table 9 gives a result of the electrical conductivity measurements from SH 6 and SH 21. The measurements of electrical conductivity shown in Table 9 correlate with the soluble sulfate test data shown in Tables 5 through 8. The high conductivity values (SH 6 site) indicate large levels of soluble sulfates. Low conductivities (SH 21 site) indicate low sulfate contents.


Figure 16. Hand Held Electrical Conductivity Meter.

Figure 17. Test View of Electrical Conductivity Meter.

Table 9. Electrical Conductivity Test Results from SH 6 and SH 21.

| SH 6 | | SH 21 | | SH 21 | | SH 21 | |
|---|---|---|---|---|---|---|---|
| Sample | (mS) | Sample | (mS) | Sample | (mS) | Sample | (mS) |
| NB1-1A | 0.11 | EB1-1A | 0.14 | EB1-2A | 0.06 | EB1-3A | 0.05 |
| NB1-2A | 0.10 | EB1-1F | 0.08 | EB1-2B | 0.07 | EB1-3B | 0.09 |
| NB2-1A | 0.31 | EB1-1H | 0.06 | EB1-2C | 0.14 | EB1-3C | 0.08 |
| NB2-2A | 0.48 | | | EB1-2D | 0.06 | EB1-3D | 0.09 |
| SB1-1A | 0.43 | | | EB1-2E | 0.09 | EB1-3E | 0.05 |
| SB1-2A | 0.26 | | | EB1-2F | 0.10 | EB1-3F | 0.09 |
| SB1-3A | 0.21 | | | EB1-2G | 0.09 | EB1-3G | 0.08 |
| SB2-1A | 0.28 | | | EB1-2H | 0.08 | EB1-3H | 0.09 |
| SB2-2A | 0.11 | | | EB1-2I | 0.11 | EB1-3I | 0.08 |

**Fine Particle Size Analysis**

Particle size analysis of soils finer than 75 μm was conducted in accordance with test method TEX-238-F (TxDOT 1996). TxDOT's Horiba laser diffraction particle size distribution analyzer, LA-500, and spinned micro riffler were used as described in Figures 18 and 19. The detection range of the Horiba LA-500 includes 0.1 μm to 200 μm particles. The fluid suspension is composed of sample (soils), distilled water, and dispersing agent. For this test, 96% distilled water and 4% sodium hexametaphosphate ($Na_2 PO_3$), as dispersant, were designated. The proper sample size can be determined by experimentation based on the translucence of the fluid suspension.

Typically, a sample size from 0.02 gm to 1.00 gm and under 75 μm particle size is required. Agitation by cavitation of water induced by ultrasound is effective in breaking up conglomerated particles. One minute of fluid suspension circulation and 5 minutes of ultrasonic agitation were performed before reading outputs. The results are generated as frequency and cumulative distribution graphs and a table. Typical printouts are provided in Appendix D.

**Atterberg Limits Test**

Atterberg limits (liquid and plastic limits) and the plasticity index were determined in accordance with ASTM D 4318-87. Soils passing the 425 μm sieve size were used, and liquid limit was determined by a multi-point test. The soil samples were prepared in accordance with ASTM D 2217 as follows:

- Soak in distilled water for 24 hours and then wet sieve through a 425 μm sieve,
- Dry at 105° C after wet sieving,
- Grind to pass the 425 μm sieve,
- Add distilled water to dry soil, and
- Test immediately.

According to the USCS (Unified Soil Classification System) plasticity chart in Figures 20 and 21, most of the soils are highly plastic and active regarding swelling. The Atterberg limits for the SH 6 site on both sides of the road show soils that are very highly expansive clays

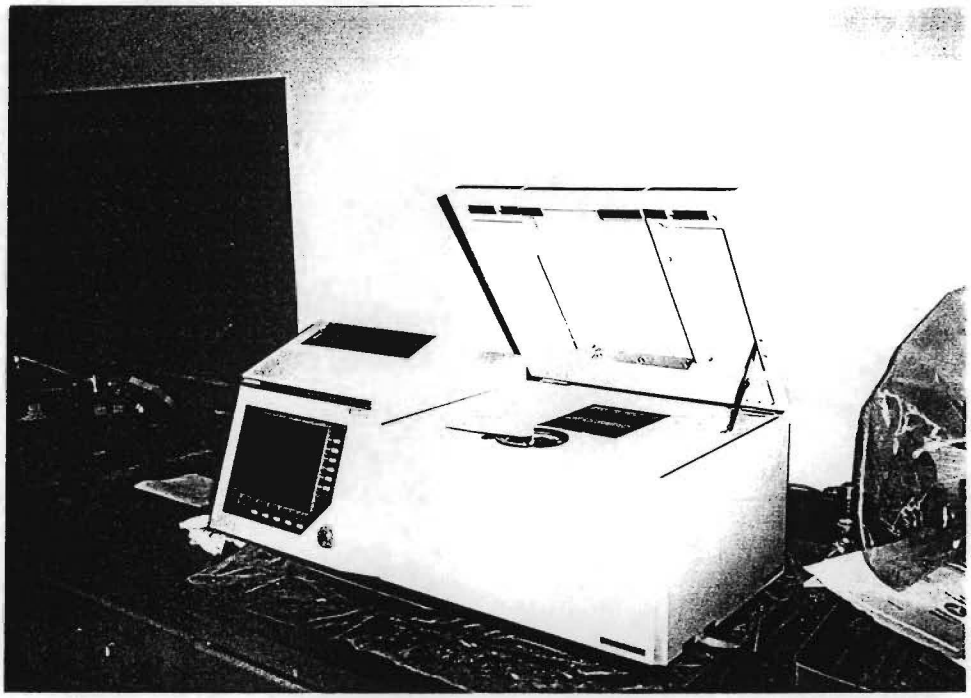

Figure 18. Horiba Laser Diffraction Particle Size Distribution Analyzer.

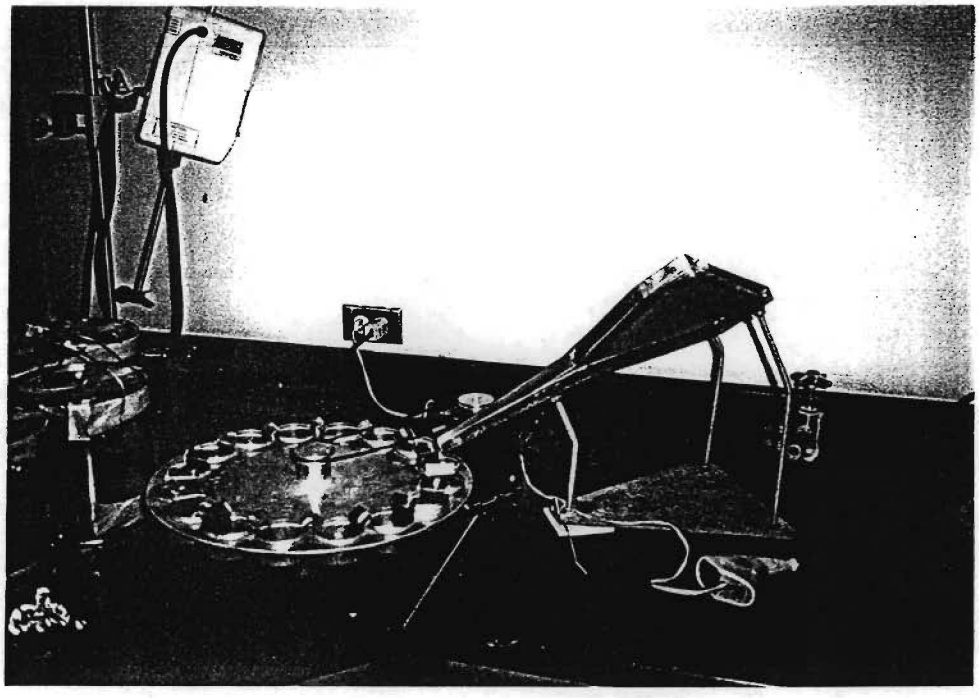

Figure 19. Spinned Micro Riffler.

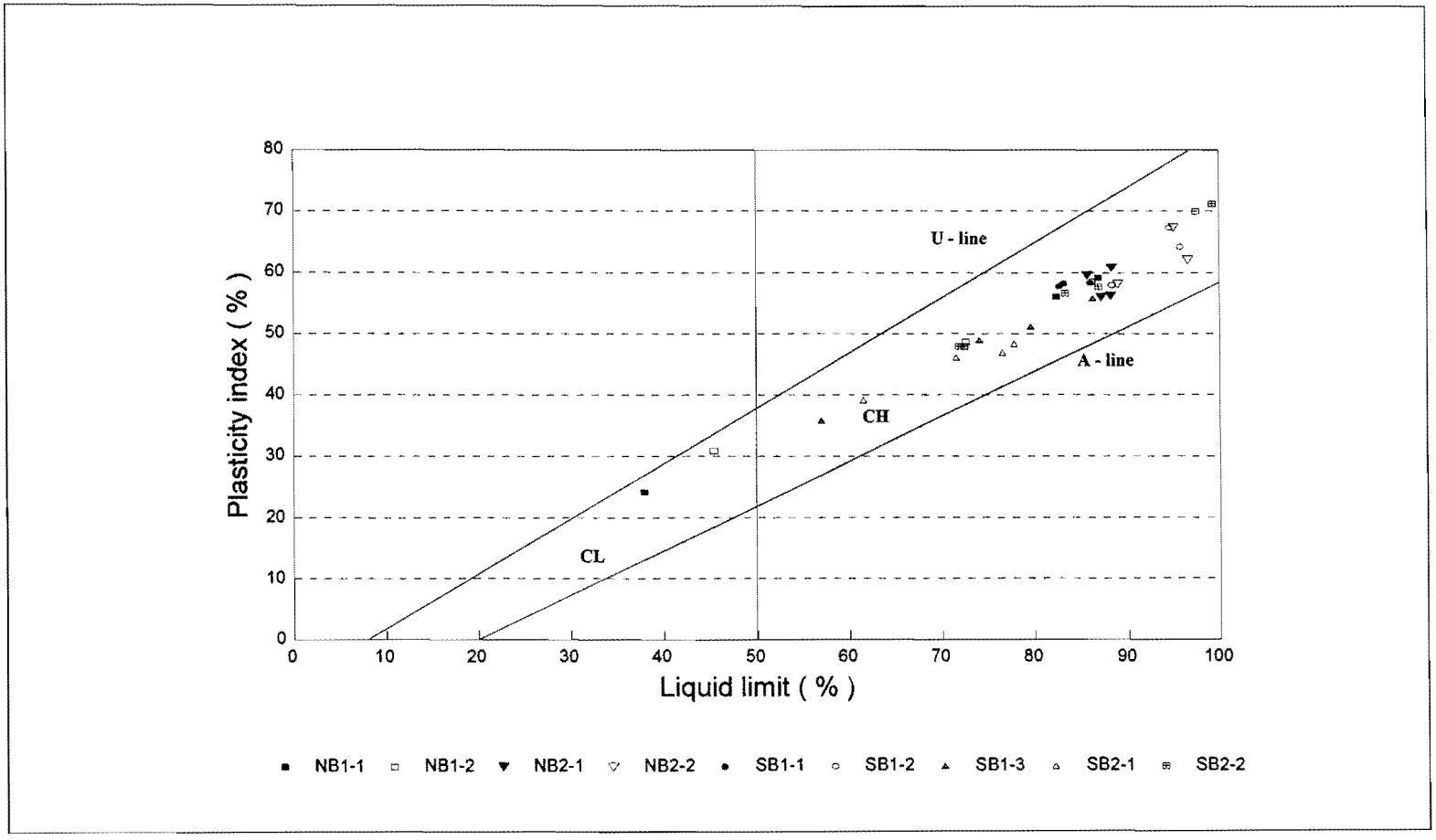


Figure 20. Plasticity Chart for SH 6 Soil Samples.

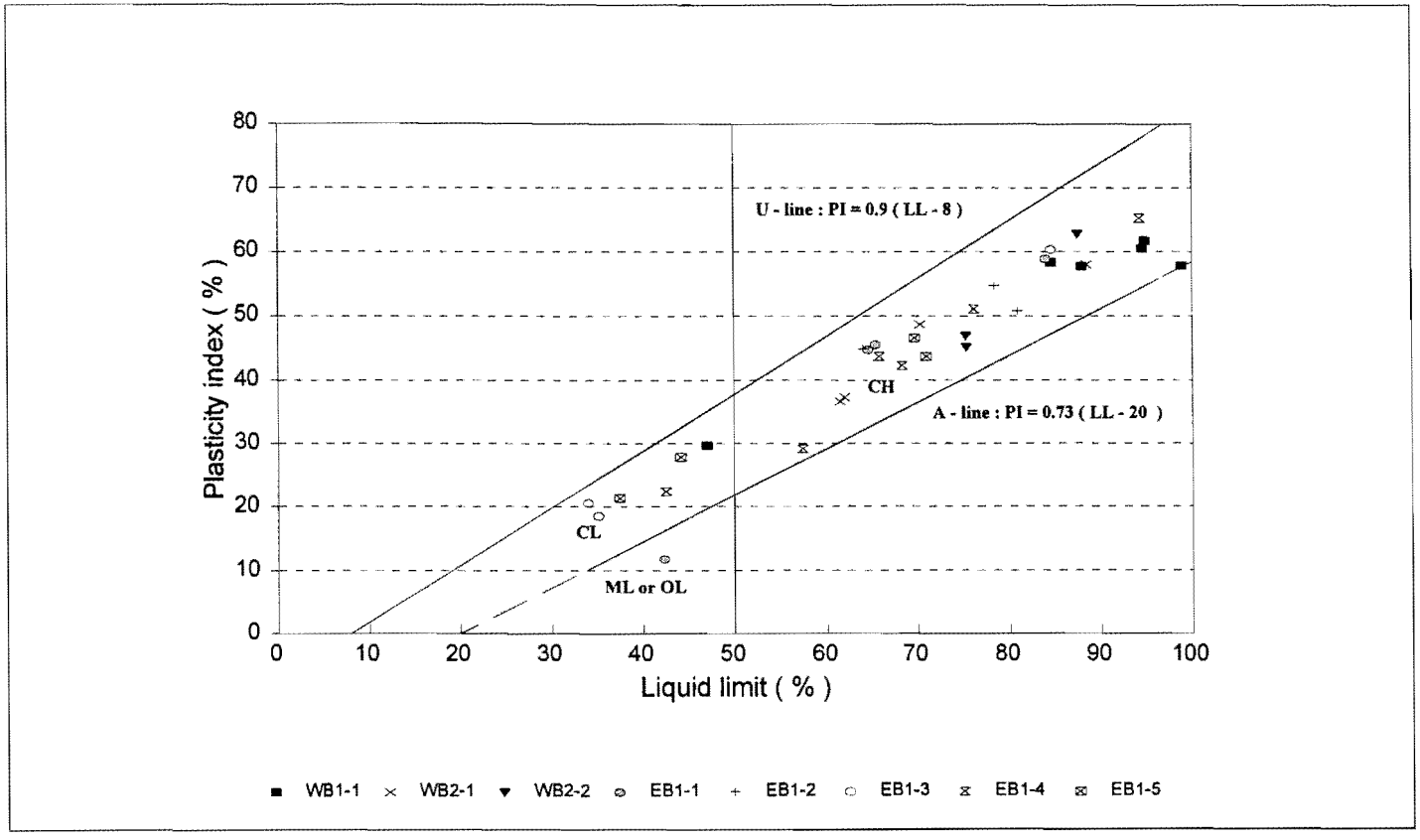


Figure 21. Plasticity Chart for SH 21 Soil Samples.

with liquid limits generally above 70%. On the other hand, the SH 21 site exhibits Atterberg limits that are much more variable with a substantial number of samples classified as low plastic clays and silts.

This means that roughness along the SH 6 site is more likely due to water getting into deep shrinkage cracks within the upper 2.5 to 3 m of the soil. The roughness of the SH 21 site is more likely due to the variability of the shrinkage and swelling of the soils along the length of the pavement. The more active soils will heave higher and shrink lower than the alternating more active and less active soils.

**Soil Suction Test**

*Filter Paper Method*

Both total and matric suction were determined using filter papers in accordance with ASTM D5298 and the method described by Jayatilaka et al. (1993). Each sample was taken from a Shelby thin-walled tube. When measuring total suction (non-contact method), a rubber stopper or spacer was placed on top of the soil sample and then the filter paper was placed on the spacer. For matric suction, the filter paper was placed on or between 2 soil samples. Figure 22 shows setups for both suction measurements. The filter paper is initially required to be dry. A sealable plastic container with a tight fitting lid and tape are used to provide an air tight condition.

The test time required is typically about 7 to 10 days. Drier samples require longer to reach equilibrium. When equilibrium was reached, the container was opened and the filter paper weighed to the nearest 0.0001 gm. After drying the filter paper, its moisture content was determined. From the calibration curve between the soil suction and the moisture content, total and matric suctions were determined. Figure 23 presents a fitted calibration curve for filter papers. The calibration procedure for the filter paper method is listed below.

- Prepare 200 ml of different reagent grade sodium chloride (NaCl) solutions which have different concentrations corresponding to suction values.
- 20 ml of each of the NaCl solutions are put into sealable plastic containers with a spacer at the center of the containers.

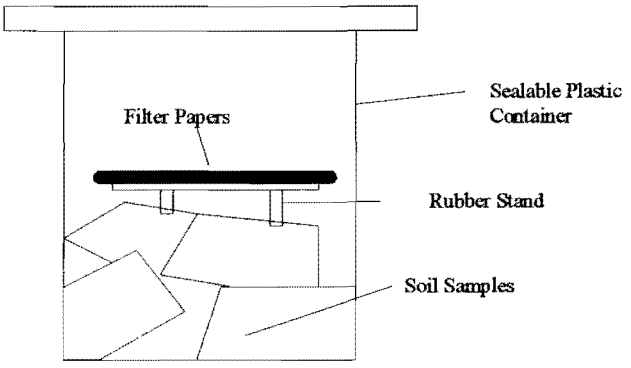


A) Total Suction Measurement

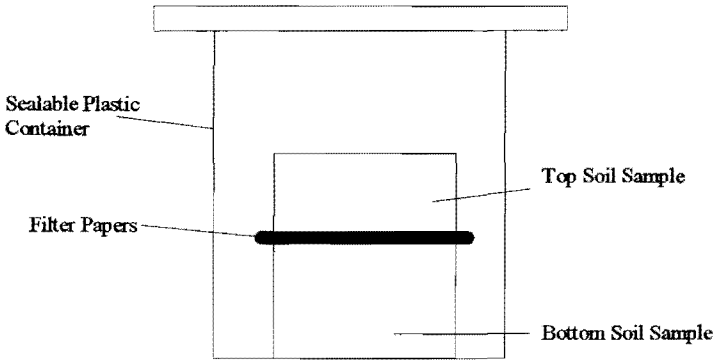


B) Matric Suction Measurement

Figure 22. Suction Measurements Using Filter Paper.

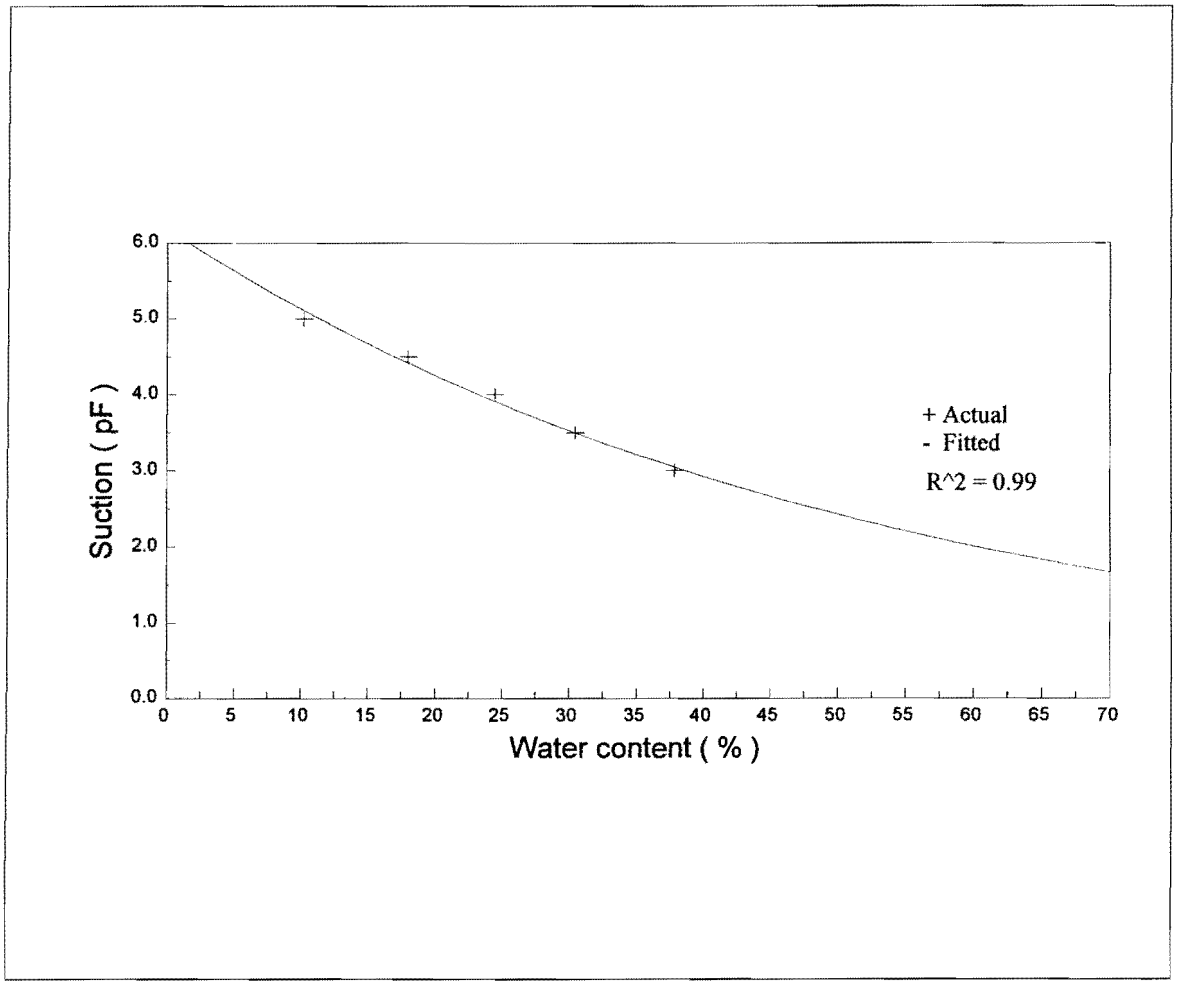


Figure 23. Calibration Curve for Filter Paper Method.

- Place 3 filter papers on the spacer, and keep the sealed containers in a temperature controlled room for 7 to 10 days.
- Determine the moisture content of the filter paper to an accuracy 0.0001 gm, and obtain the suction value corresponding to each NaCl concentration.

Tables 18 through 26 summarize suction measurements using the filter paper method at each borehole.

*Transistor Psychrometer*

A transistor psychrometer, originally developed in Australia, was also used to measure total suction. This state-of-the-art equipment consists of 3 main parts as shown in Figure 24: a thermally insulated container, the psychrometer probes, and a logger for recording the output. In the probe, a wet transistor measures the temperature depression and amplifies it. For calibration and zeroing of the transistor, standard salt solutions are needed. The pF 2.0 solution is used for the zeroing and pF 3.0 to 5.0 solutions for calibration. The zeroing process should be performed before calibration and measurement of soil suction.

Calibration of each probe should be done within a day. A linear calibration line between the suction pF values and log mV is based upon a set of calibration tests within pF 3.0 to 5.0. Calibration charts are given in Appendix E. Listed below is the procedure for measuring soil suction.

- Soil samples are trimmed using a 10 mm high sampling ring.
- This soil sample is then cut to obtain a smaller 15 mm diameter by 10 mm high specimen.
- The soil sample is sealed and contained in wooden plate.
- Each sampling tube containing a soil specimen is inserted into the thermally insulated container.
- The soil within the probe will stabilize in about 1 hour after placing the samples.
- Total suction of soil is obtained using the calibration line from linear regression for each probe.

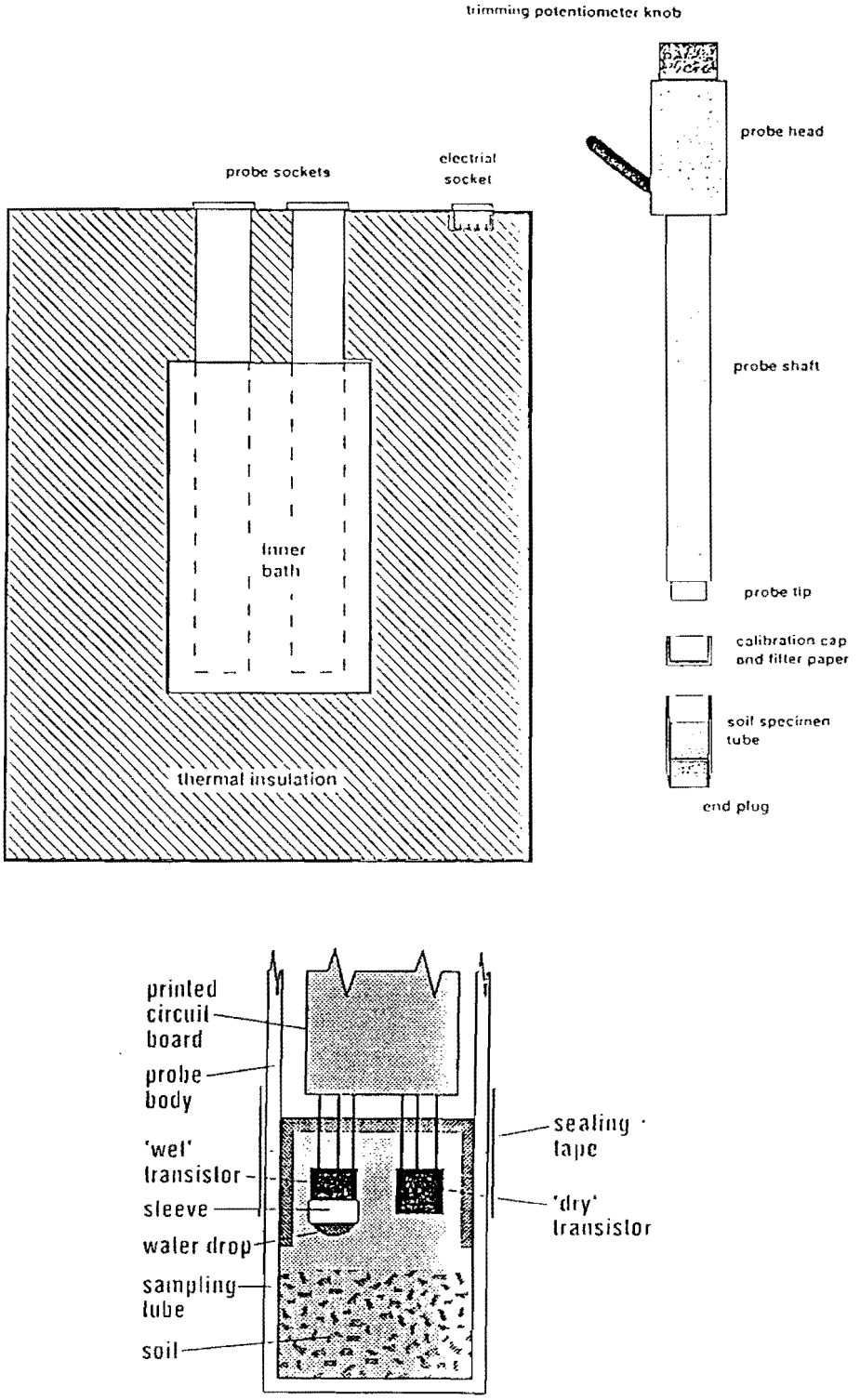


Figure 24. Transistor Psychrometer (Woodburn, 1993).

Tables 10 through 26 show the results of total suction measurements using the transistor psychrometer on samples from each borehole from SH 6 and SH 21. The transistor psychrometer consistently measured total suctions about 0.172 pF smaller than the filter paper as illustrated in Figure 25. This difference is due entirely to calibration, and the transistor psychrometer is considered to be the more accurate of the 2 measurements.

## VOLUME CHANGE AND FLOW PROPERTIES IN SUBGRADE SOILS

The diffusion coefficients and the permeabilities of the soils were estimated using the equations described in Chapter 2. For calculating the unsaturated permeability, knowledge of parameters such as the activity of clays, cation exchange capacity, and fine clay content are required for the estimation of the suction compression index (Jayatilaka et al. 1993). The suction compression index is the volume change per unit change of suction in pF units. This parameter can be obtained from a chart which was developed originally for the FAA (McKeen 1981) using the relationship between the clay activity and the cation exchange activity. The chart and the suction compression index are given in Figure 26, and Table 27 shows the mineralogical composition. The suction compression indexes and the slopes of the $\log_{10}$ (suction)-versus-water content curves that were determined from these relationships are shown in Tables 28 through 35, arranged by boring numbers and depth. The soil properties for the SH 6 site are shown in Tables 28 through 31 and those for the SH 21 site are in Tables 32 through 35.

These tables also show the soil properties that were used to derive these volume change characteristics of the soil, namely, the fine clay activity ratio, the estimated cation exchange capacity (CEC), and the fine clay cation exchange activity ratio (CEAc). The fine clay activity ratio is given by:

$$AC = \frac{PI, \%}{\% \ Fine \ Clay}$$

Table 10. Measured Suction Using Transistor Psychrometer at WB1-1.

| Test Hole | Depth (m) | Natural Water Content (%) | Transistor Psychrometer Total Suction ( pF) | Transistor Psychrometer Total Suction (cm) |
|---|---|---|---|---|
| WB1-1 | -0.4 | 23.18 | 3.33 | 2138 |
| | -0.8 | 24.84 | 3.72 | 5248 |
| | -1.2 | 31.13 | 3.72 | 5248 |
| | -1.4 | 36.56 | 3.71 | 5128 |
| | -1.6 | 33.43 | 3.77 | 5888 |
| | -1.8 | 36.12 | 3.92 | 8317 |
| | -2.0 | 34.37 | 3.73 | 5370 |
| | -2.4 | 36.82 | 3.70 | 5011 |

Table 11. Measured Suction Using Transistor Psychrometer at WB2-1.

| Test Hole | Depth (m) | Natural Water Content (%) | Transistor Psychrometer Total Suction ( pF) | Transistor Psychrometer Total Suction (cm) |
|---|---|---|---|---|
| WB2-1 | -0.4 | 30.73 | 3.59 | 3890 |
| | -0.8 | 31.33 | 3.54 | 3467 |
| | -1.2 | 28.27 | 3.71 | 5128 |
| | -1.4 | 40.54 | 3.42 | 2630 |
| | -1.6 | 33.80 | 3.58 | 3801 |
| | -2.0 | 37.72 | 3.65 | 4466 |
| | -2.4 | 34.47 | 3.75 | 5623 |
| | -2.8 | 33.33 | 3.64 | 4365 |

Table 12. Measured Suction Using Transistor Psychrometer at WB2-2.

| Test Hole | Depth (m) | Natural Water Content (%) | Transistor Psychrometer Total Suction ( pF) | Transistor Psychrometer Total Suction (cm) |
|---|---|---|---|---|
| WB2-2 | -0.4 | 26.60 | 3.75 | 5623 |
| | -0.8 | 38.86 | 3.63 | 4265 |
| | -1.2 | 37.03 | 3.53 | 3388 |
| | -1.6 | 38.12 | 3.54 | 3467 |
| | -2.0 | 36.31 | 3.50 | 3162 |
| | -2.4 | 32.08 | 3.29 | 1950 |

Table 13. Measured Suction Using Transistor Psychrometer at EB1-1.

| Test Hole | Depth (m) | Natural Water Content (%) | Transistor Psychrometer Total Suction ( pF) | Transistor Psychrometer Total Suction (cm) |
|---|---|---|---|---|
| EB1-1 | -0.4 | 32.40 | 3.56 | 3630 |
| | -0.8 | 26.35 | 3.34 | 2188 |
| | -1.2 | 25.47 | 3.37 | 2344 |
| | -1.6 | 23.41 | 3.44 | 2754 |
| | -2.0 | 25.38 | 3.62 | 4168 |
| | -2.4 | 28.65 | 3.56 | 3630 |
| | -2.8 | 30.99 | 3.51 | 3236 |
| | -3.2 | 31.59 | 3.52 | 3311 |

Table 14. Measured Suction Using Transistor Psychrometer at EB1-2.

| Test Hole | Depth (m) | Natural Water Content (%) | Transistor Psychrometer Total Suction ( pF) | Transistor Psychrometer Total Suction (cm) |
|---|---|---|---|---|
| EB1-2 | -0.4 | 26.98 | 3.47 | 2951 |
| | -0.8 | 25.30 | 3.37 | 2344 |
| | -1.2 | 22.96 | 3.56 | 3630 |
| | -1.6 | 25.39 | 3.59 | 3890 |
| | -2.0 | 25.61 | 3.51 | 3236 |
| | -2.4 | 37.15 | 3.64 | 4365 |
| | -2.8 | 31.07 | 3.45 | 2818 |
| | -3.2 | 32.91 | 3.66 | 4570 |
| | -3.6 | 27.36 | 3.51 | 3236 |

Table 15. Measured Suction Using Transistor Psychrometer at EB1-3.

| Test Hole | Depth (m) | Natural Water Content (%) | Transistor Psychrometer Total Suction ( pF) | Transistor Psychrometer Total Suction (cm) |
|---|---|---|---|---|
| EB1-3 | -0.4 | 21.62 | 3.50 | 3162 |
| | -0.8 | 22.73 | 3.25 | 1778 |
| | -1.2 | 25.40 | 3.49 | 3090 |
| | -1.6 | 30.09 | 3.52 | 3311 |
| | -2.0 | 36.25 | 3.27 | 1862 |
| | -2.4 | 37.78 | 3.39 | 2454 |
| | -2.8 | 24.42 | 3.71 | 5128 |
| | -3.2 | 35.35 | 3.43 | 2691 |
| | -3.6 | 25.48 | 3.62 | 4168 |

Table 16. Measured Suction Using Transistor Psychrometer at EB1-4.

| Test Hole | Depth (m) | Natural Water Content (%) | Transistor Psychrometer Total Suction ( pF) | Transistor Psychrometer Total Suction (cm) |
|---|---|---|---|---|
| EB1-4 | -0.4 | 27.05 | 3.33 | 2138 |
| | -0.8 | 26.51 | 2.94 | 871 |
| | -1.2 | 27.04 | 3.31 | 2042 |
| | -1.6 | 31.16 | 3.26 | 1820 |
| | -2.0 | | 3.52 | 3311 |
| | -2.4 | 34.70 | 3.58 | 3801 |
| | -2.8 | 20.81 | 3.62 | 4168 |

Table 17. Measured Suction Using Transistor Psychrometer at EB1-5.

| Test Hole | Depth (m) | Natural Water Content (%) | Transistor Psychrometer Total Suction ( pF) | Transistor Psychrometer Total Suction (cm) |
|---|---|---|---|---|
| EB1-5 | -0.4 | 27.61 | 3.40 | 2512 |
| | -0.8 | 27.57 | 2.94 | 871 |
| | -1.2 | 26.78 | 3.44 | 2754 |
| | -1.6 | 34.48 | 3.44 | 2754 |
| | -2.0 | 33.07 | 3.62 | 4168 |
| | -2.4 | 30.45 | 3.60 | 3981 |
| | -2.8 | 29.67 | 3.83 | 6760 |

Table 18. Measured Suction Using Transistor Psychrometer and Filter Paper at NB1-1.

| Test Hole | Depth (m) | Natural Water Content (%) | Transistor Psychrometer Total Suction (pF) | Transistor Psychrometer Total Suction (cm) | Filter Paper Total Suction (pF) | Filter Paper Total Suction (cm) | Filter Paper Matric Suction (pF) | Filter Paper Matric Suction (cm) |
|---|---|---|---|---|---|---|---|---|
| NB1-1 | -0.4 | 15.86 | 3.25 | 1782 | 3.65 | 4425 | 2.88 | 766 |
| | -0.8 | 26.21 | 3.59 | 3890 | 3.53 | 3388 | 3.27 | 1849 |
| | -1.2 | 21.34 | 3.55 | 3540 | - | - | - | - |
| | -1.6 | 38.24 | 3.75 | 5623 | 3.85 | 7014 | 3.45 | 2786 |
| | -2.0 | 32.07 | 3.67 | 4720 | - | - | - | - |
| | -2.4 | 35.68 | 3.76 | 5754 | 3.84 | 6949 | 3.60 | 4008 |
| | -2.8 | 38.73 | 3.00 | 1005 | - | - | - | - |
| | -3.3 | 32.14 | 3.78 | 6011 | 4.01 | 10208 | 3.73 | 5382 |



Table 19. Measured Suction Using Transistor Psychrometer and Filter Paper at NB1-2.

| Test Hole | Depth (m) | Natural Water Content (%) | Transistor Psychrometer Total Suction (pF) | Transistor Psychrometer Total Suction (cm) | Filter Paper Total Suction (pF) | Filter Paper Total Suction (cm) | Filter Paper Matric Suction (pF) | Filter Paper Matric Suction (cm) |
|---|---|---|---|---|---|---|---|---|
| NB1-2 | -0.4 | 15.32 | 2.53 | 339 | 3.42 | 2630 | 3.13 | 1355 |
| | -0.8 | 12.66 | 3.70 | 5058 | 4.02 | 10446 | - | - |
| | -1.2 | 25.63 | 3.70 | 5011 | - | - | - | - |
| | -1.6 | 11.69 | 3.95 | 8850 | 4.32 | 21084 | 4.13 | 13519 |
| | -2.0 | 11.34 | 3.44 | 2754 | - | - | - | - |
| | -2.4 | 31.58 | 3.84 | 6854 | 4.35 | 22591 | 4.01 | 10255 |
| | -2.8 | 42.10 | 3.68 | 4742 | - | - | - | - |
| | -3.3 | 38.36 | 3.68 | 4764 | 3.94 | 8709 | 3.92 | 8259 |

Table 20. Measured Suction Using Transistor Psychrometer and Filter Paper at NB2-1.

| Test Hole | Depth (m) | Natural Water Content (%) | Transistor Psychrometer Total Suction (pF) | Transistor Psychrometer Total Suction (cm) | Filter Paper Total Suction (pF) | Filter Paper Total Suction (cm) | Filter Paper Matric Suction (pF) | Filter Paper Matric Suction (cm) |
|---|---|---|---|---|---|---|---|---|
| NB2-1 | -0.4 | 44.96 | 3.61 | 4064 | 3.44 | 2773 | 2.85 | 713 |
| | -0.8 | 39.63 | 3.78 | 6053 | - | - | - | - |
| | -1.2 | 38.46 | 3.75 | 5571 | 3.74 | 5507 | 3.09 | 1225 |
| | -1.6 | 36.11 | 3.79 | 6165 | - | - | - | - |
| | -2.0 | 32.86 | 3.84 | 6949 | 3.88 | 7498 | 3.80 | 6265 |
| | -2.4 | 36.52 | 3.71 | 5140 | 3.79 | 6151 | 3.54 | 3443 |
| | -2.8 | 30.25 | 3.92 | 8355 | - | - | - | - |
| | -3.3 | 41.26 | 3.93 | 8550 | - | - | - | - |



Table 21. Measured Suction Using Transistor Psychrometer and Filter Paper at NB2-2.

| Test Hole | Depth (m) | Natural Water Content (%) | Transistor Psychrometer Total Suction (pF) | Transistor Psychrometer Total Suction (cm) | Filter Paper Total Suction (pF) | Filter Paper Total Suction (cm) | Filter Paper Matric Suction (pF) | Filter Paper Matric Suction (cm) |
|---|---|---|---|---|---|---|---|---|
| NB2-2 | -0.4 | 36.96 | 4.04 | 10938 | 3.77 | 5901 | 3.48 | 2985 |
| | -0.8 | 35.56 | 4.01 | 10279 | - | - | - | - |
| | -1.2 | 34.09 | 4.04 | 10989 | 3.68 | 4819 | - | - |
| | -1.6 | 32.76 | 4.13 | 13334 | - | - | - | - |
| | -2.0 | 30.36 | 4.08 | 12077 | 4.06 | 11349 | 3.92 | 8336 |
| | -2.4 | 31.81 | 4.09 | 12217 | - | - | - | - |
| | -2.8 | 32.19 | 4.03 | 10591 | 3.83 | 6776 | - | - |
| | -3.3 | 19.80 | 4.04 | 10838 | - | - | - | - |

Table 22. Measured Suction Using Transistor Psychrometer and Filter Paper at SB1-1.

| Test Hole | Depth (m) | Natural Water Content (%) | Transistor Psychrometer Total Suction (pF) | Transistor Psychrometer Total Suction (cm) | Filter Paper Total Suction (pF) | Filter Paper Total Suction (cm) | Filter Paper Matric Suction (pF) | Filter Paper Matric Suction (cm) |
|---|---|---|---|---|---|---|---|---|
| SB1-1 | -0.4 | 37.30 | 3.49 | 3119 | 3.78 | 6039 | 3.35 | 2254 |
| | -0.8 | 34.02 | 3.61 | 4045 | - | - | - | - |
| | -1.2 | 39.00 | 3.62 | 4149 | 3.77 | 5834 | 3.28 | 1883 |
| | -1.6 | 38.94 | 3.63 | 4226 | - | - | - | - |
| | -2.0 | 40.80 | 3.62 | 4149 | 3.86 | 7177 | 3.64 | 4405 |
| | -2.4 | 40.39 | 3.83 | 6791 | - | - | - | - |
| | -2.8 | 38.17 | 3.71 | 5069 | 3.98 | 9637 | 3.64 | 4315 |
| | -3.3 | 34.12 | 3.77 | 5929 | - | - | - | - |
| | -3.7 | 38.28 | 3.52 | 3311 | 3.99 | 9659 | 3.76 | 5741 |
| | -4.1 | 39.25 | 3.79 | 6208 | - | - | - | - |



Table 23. Measured Suction Using Transistor Psychrometer and Filter Paper at SB1-2.

| Test Hole | Depth (m) | Natural Water Content (%) | Transistor Psychrometer Total Suction (pF) | Transistor Psychrometer Total Suction (cm) | Filter Paper Total Suction (pF) | Filter Paper Total Suction (cm) | Filter Paper Matric Suction (pF) | Filter Paper Matric Suction (cm) |
|---|---|---|---|---|---|---|---|---|
| SB1-2 | -0.4 | 40.52 | 3.56 | 3605 | 3.75 | 5584 | 3.21 | 1633 |
| | -0.8 | 38.31 | 3.52 | 3342 | 4.29 | 19631 | 3.53 | 3388 |
| | -1.6 | 42.74 | 3.33 | 2143 | - | - | - | - |
| | -2.0 | 37.49 | 3.49 | 3119 | 3.69 | 4886 | 3.44 | 2754 |
| | -2.4 | 34.32 | 3.69 | 4864 | 3.67 | 4677 | 3.36 | 2285 |
| | -2.8 | 36.22 | 3.74 | 5482 | - | - | - | - |
| | -3.3 | 33.79 | 3.89 | 7833 | 3.92 | 8394 | 3.62 | 4197 |

Table 24. Measured Suction Using Transistor Psychrometer and Filter Paper at SB1-3.

| Test Hole | Depth (m) | Natural Water Content (%) | Transistor Psychrometer Total Suction (pF) | Transistor Psychrometer Total Suction (cm) | Filter Paper Total Suction (pF) | Filter Paper Total Suction (cm) | Filter Paper Matric Suction (pF) | Filter Paper Matric Suction (cm) |
|---|---|---|---|---|---|---|---|---|
| SB1-3 | -0.4 | 46.21 | 3.27 | 1858 | 3.43 | 2710 | 3.28 | 1905 |
| | -0.8 | 41.11 | 3.52 | 3273 | - | - | - | - |
| | -1.2 | 42.51 | 3.60 | 3935 | 3.76 | 5701 | 3.18 | 1496 |
| | -1.6 | 44.71 | 3.61 | 4045 | - | - | - | - |
| | -2.0 | 34.67 | 3.55 | 3507 | 3.79 | 6151 | 3.51 | 3228 |
| | -2.4 | 37.58 | 3.55 | 3540 | - | - | - | - |
| | -2.8 | 36.08 | 3.38 | 2371 | 3.68 | 4753 | 3.55 | 3572 |
| | -3.7 | 36.49 | 3.55 | 3540 | 3.78 | 6039 | 3.58 | 3775 |



Table 25. Measured Suction Using Transistor Psychrometer and Filter Paper at SB2-1.

| Test Hole | Depth (m) | Natural Water Content (%) | Transistor Psychrometer Total Suction (pF) | Transistor Psychrometer Total Suction (cm) | Filter Paper Total Suction (pF) | Filter Paper Total Suction (cm) | Filter Paper Matric Suction (pF) | Filter Paper Matric Suction (cm) |
|---|---|---|---|---|---|---|---|---|
| SB2-1 | -0.8 | 25.19 | 3.95 | 8891 | 4.10 | 12646 | 4.09 | 12188 |
| | -1.2 | 30.79 | 4.03 | 10616 | 4.40 | 24943 | 4.13 | 13613 |
| | -1.6 | 29.58 | 3.98 | 9571 | 4.20 | 15666 | 4.17 | 14755 |
| | -2.0 | 31.64 | 4.06 | 11427 | - | - | - | - |
| | -2.4 | 26.43 | 3.97 | 9267 | 4.07 | 11694 | - | - |

Table 26. Measured Suction Using Transistor Psychrometer and Filter Paper at SB2-2.

| Test Hole | Depth (m) | Natural Water Content (%) | Transistor Psychrometer Total Suction (pF) | Transistor Psychrometer Total Suction (cm) | Filter Paper Total Suction (pF) | Filter Paper Total Suction (cm) | Filter Paper Matric Suction (pF) | Filter Paper Matric Suction (cm) |
|---|---|---|---|---|---|---|---|---|
| SB2-2 | -0.4 | 32.60 | 3.47 | 2971 | 3.07 | 1161 | 2.33 | 216 |
| | -0.8 | 36.59 | 3.32 | 2099 | - | - | - | - |
| | -1.2 | 32.61 | 3.75 | 5584 | 3.81 | 6516 | 3.76 | 5754 |
| | -1.6 | 34.36 | 3.42 | 2606 | - | - | - | - |
| | -2.0 | 34.40 | 3.49 | 3119 | 3.63 | 4295 | - | - |
| | -2.4 | 8.08 | 3.38 | 2421 | - | - | - | - |
| | -2.8 | 36.39 | 3.27 | 1879 | 3.60 | 3935 | - | - |
| | -3.3 | 21.19 | 3.48 | 3006 | 3.71 | 5116 | - | - |
| | -3.7 | 33.75 | 3.37 | 2323 | - | - | - | - |
| | -4.1 | 36.06 | 3.05 | 1117 | 3.79 | 6222 | 3.52 | 3281 |
| | -4.5 | 34.95 | 3.53 | 3349 | 3.23 | 1679 | 2.04 | 110 |

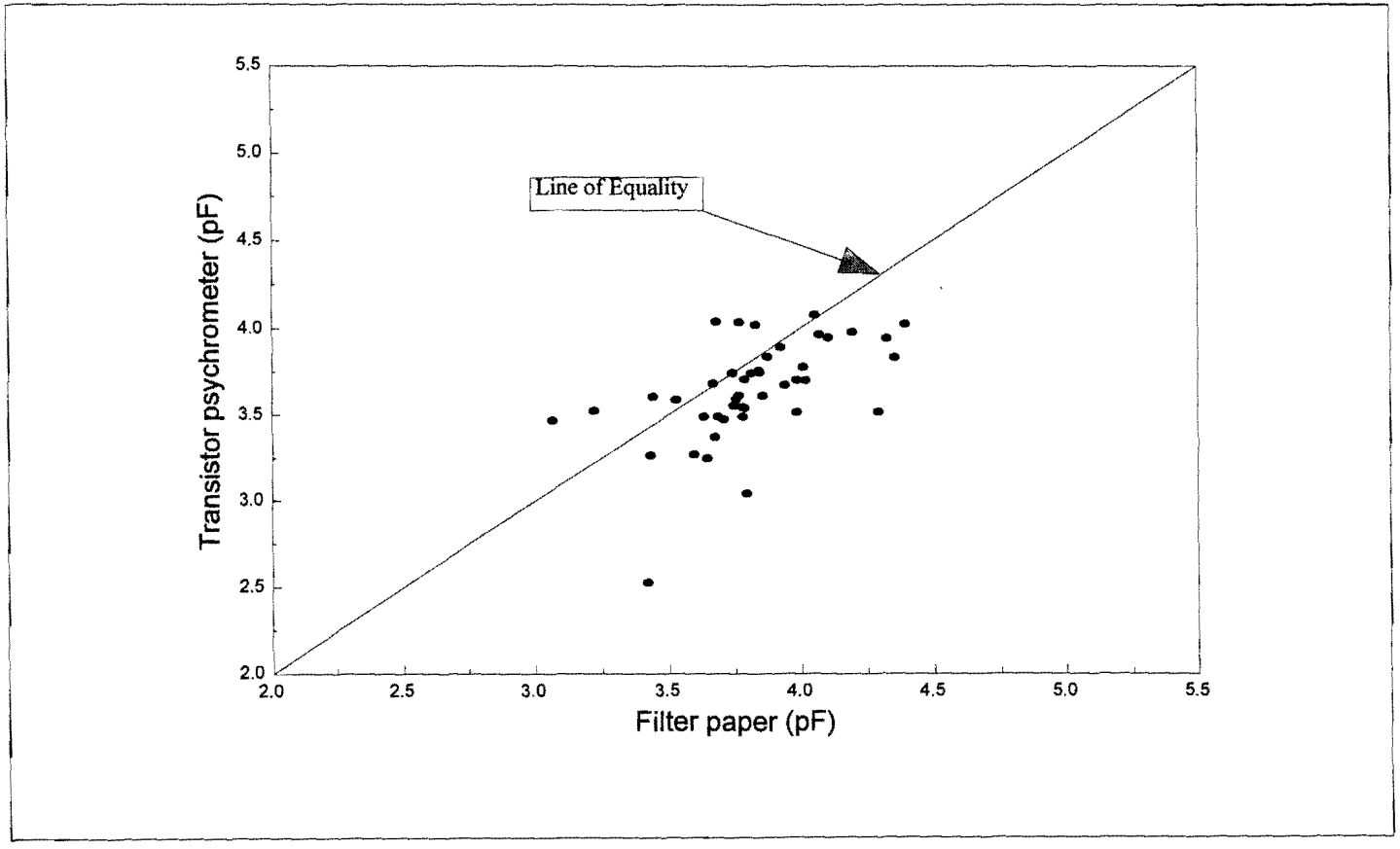


Figure 25. Filter Paper Versus Transistor Psychrometer.

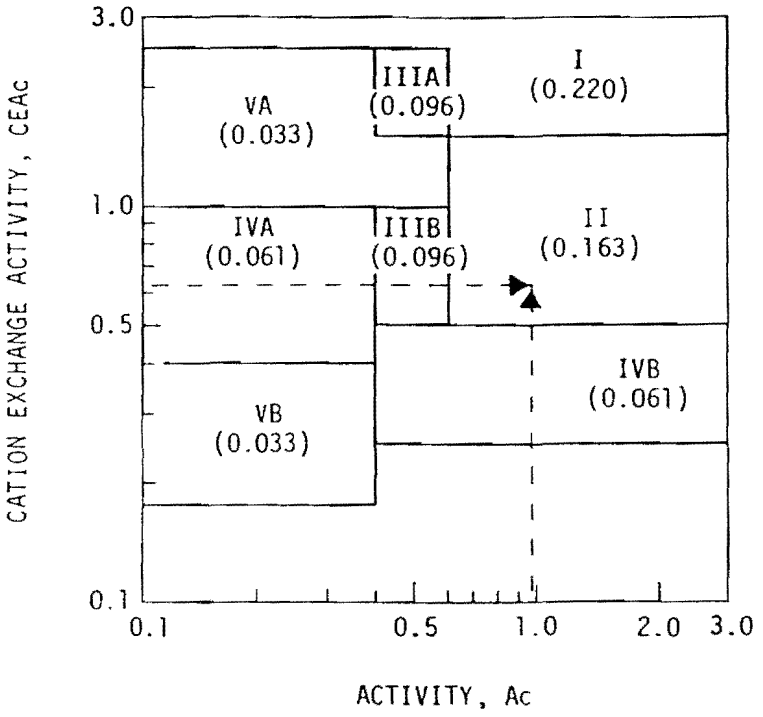


Figure 26. Chart for Suction Compression Index (after McKeen 1981).

Table 27. Region Mineralogical Composition (after McKeen 1981).

| Region | Smectite | Illite | Kaolinite | Vermiculite |
|---|---|---|---|---|
| I | >50 | N | N | N |
| II | >50 | Tr - 25 | Tr - 25 | N |
| IIIA | 25 - 50 | 10 - 25 | 5 - 10 | N |
| IIIB | 5 - 50 | 5 - 25 | Tr - 25 | N |
| IVA | Tr - 10 | 5 - 25 | 5 - 50 | N |
| IVB | Tr | 10 - 25 | 5 - 50 | N |
| VA | N | Tr - 25 | 5 - 50 | Tr - 25 |
| VB | N | N | 10 - 25 | Tr |

- All values expressed as percent of the clay fraction.

N = none
Tr = trace, >5 percent.

Table 28. Estimated SCI Values at NB1-1 and NB1-2.

| Test Hole | Depth (m) | Activity Ratio | Cation Exchange Capacity (meq / 100 gm) | Cation Exchange Activity Ratio | Suction Water Content Slope | SCI for 100% Fine Clay | Suction Compression Index (actual) |
|---|---|---|---|---|---|---|---|
| NB1-1 | -0.4 | - | - | - | - | - | - |
| | -0.8 | 1.11 | 21.38 | 0.97 | -11.68 | 0.163 | 0.036 |
| | -1.6 | 2.03 | 45.65 | 1.65 | -7.79 | 0.220 | 0.061 |
| | -2.4 | 1.39 | 48.72 | 1.14 | -6.96 | 0.163 | 0.070 |
| NB1-2 | -0.4 | - | - | - | - | - | - |
| | -1.6 | 1.68 | 22.66 | 1.23 | -11.14 | 0.163 | 0.030 |
| | -2.4 | 0.49 | 41.20 | 0.41 | -7.88 | 0.061 | 0.061 |
| | -3.3 | 0.71 | 48.10 | 0.48 | -6.56 | 0.061 | 0.061 |



Table 29. Estimated SCI Values at NB2-1 and NB2-2.

| Test Hole | Depth (m) | Activity Ratio | Cation Exchange Capacity (meq / 100 gm) | Cation Exchange Activity Ratio | Suction Water Content Slope | SCI for 100% Fine Clay | Suction Compression Index (actual) |
|---|---|---|---|---|---|---|---|
| NB2-1 | -0.4 | 1.39 | 57.47 | 1.42 | -6.49 | 0.163 | 0.066 |
| | -1.2 | 1.40 | 55.79 | 1.39 | -6.78 | 0.163 | 0.065 |
| | -2.4 | 1.54 | 45.44 | 1.17 | -7.15 | 0.163 | 0.063 |
| | -3.3 | 1.84 | 48.10 | 1.46 | -7.05 | 0.163 | 0.054 |
| NB2-2 | -0.4 | 1.41 | 62.77 | 1.43 | -6.38 | 0.163 | 0.072 |
| | -1.2 | 0.70 | 48.51 | 0.50 | -6.82 | 0.163 | 0.157 |
| | -2.0 | 1.67 | 65.13 | 1.64 | -5.48 | 0.220 | 0.087 |
| | -3.3 | 1.49 | 54.95 | 1.41 | -6.72 | 0.163 | 0.064 |

Table 30. Estimated SCI Values at SB1-1, SB1-2, and SB1-3.

| Test Hole | Depth (m) | Activity Ratio | Cation Exchange Capacity (meq / 100 gm) | Cation Exchange Activity Ratio | Suction Water Content Slope | SCI for 100% Fine Clay | Suction Compression Index (actual) |
|---|---|---|---|---|---|---|---|
| SB1-1 | -0.4 | 0.87 | 43.01 | 0.64 | -7.53 | 0.163 | 0.109 |
| | -1.2 | 1.77 | 43.01 | 1.30 | -7.55 | 0.163 | 0.054 |
| | -2.4 | 1.50 | 79.51 | 2.05 | -5.07 | 0.220 | 0.085 |
| | -3.7 | 0.63 | 48.51 | 0.52 | -7.39 | 0.163 | 0.152 |
| SB1-2 | -0.4 | 1.30 | 48.51 | 1.07 | -7.72 | 0.163 | 0.074 |
| | -1.6 | 1.53 | 53.90 | 1.42 | -6.78 | 0.163 | 0.062 |
| | -2.4 | 1.65 | 47.69 | 1.17 | -6.72 | 0.163 | 0.067 |
| | -2.8 | 0.72 | 56.63 | 0.63 | -6.79 | 0.163 | 0.146 |
| SB1-3 | -0.4 | 0.84 | 35.43 | 0.83 | -10.19 | 0.163 | 0.070 |
| | -1.2 | 1.27 | 43.41 | 1.13 | -8.58 | 0.163 | 0.063 |
| | -2.4 | 1.20 | 50.16 | 1.17 | -7.60 | 0.163 | 0.070 |
| | -3.7 | 0.56 | 54.32 | 0.55 | -6.65 | 0.096 | 0.095 |

Table 31. Estimated SCI Values at SB2-1 and SB2-2.

| Test Hole | Depth (m) | Activity Ratio | Cation Exchange Capacity (meq / 100 gm) | Cation Exchange Activity Ratio | Suction Water Content Slope | SCI for 100% Fine Clay | Suction Compression Index (actual) |
|---|---|---|---|---|---|---|---|
| SB2-1 | -0.8 | 0.43 | 38.00 | 0.42 | -8.93 | 0.061 | 0.056 |
| | -1.6 | 2.37 | 52.86 | 2.67 | -7.10 | 0.220 | 0.044 |
| | -2.0 | 0.76 | 52.44 | 0.82 | -7.44 | 0.163 | 0.104 |
| | -2.4 | 1.78 | 44.02 | 1.69 | -8.10 | 0.220 | 0.057 |
| SB2-2 | -0.4 | 1.84 | 40.99 | 1.57 | -8.81 | 0.220 | 0.057 |
| | -0.8 | 1.50 | 51.61 | 1.34 | -6.93 | 0.163 | 0.063 |
| | -1.6 | 2.04 | 49.34 | 1.41 | -6.41 | 0.163 | 0.057 |
| | -2.8 | 1.56 | 46.67 | 1.28 | -7.21 | 0.163 | 0.059 |
| | -4.1 | 0.49 | 42.20 | 0.43 | -7.94 | 0.061 | 0.060 |
| | -4.9 | 1.02 | 24.89 | 0.30 | -9.31 | 0.061 | 0.050 |

Table 32. Estimated SCI Values at WB1-1 and WB2-1.

| Test Hole | Depth (m) | Activity Ratio | Cation Exchange Capacity (meq / 100 gm) | Cation Exchange Activity Ratio | Suction Water Content Slope | SCI for 100% Fine Clay | Suction Compression Index (actual) |
|---|---|---|---|---|---|---|---|
| WB1-1 | -0.4 | 1.01 | 28.09 | 0.95 | -10.89 | 0.163 | 0.048 |
| | -0.8 | 1.59 | 45.85 | 1.25 | -7.36 | 0.163 | 0.060 |
| | -1.2 | - | 60.22 | - | - | - | - |
| | -1.6 | 1.62 | 53.90 | 1.51 | -6.60 | 0.220 | 0.078 |
| | -2.0 | 1.93 | 61.92 | 1.97 | -5.90 | 0.220 | 0.069 |
| | -2.4 | 2.34 | 77.08 | 3.12 | -5.06 | 0.220 | 0.054 |
| WB2-1 | -0.4 | 1.66 | 36.42 | 1.24 | -8.52 | 0.163 | 0.048 |
| | -0.8 | 1.27 | 42.40 | 1.43 | -8.26 | 0.163 | 0.048 |
| | -1.6 | 1.07 | 42.81 | 1.25 | -8.99 | 0.163 | 0.056 |
| | -2.8 | 1.29 | 54.32 | 1.21 | -7.94 | 0.163 | 0.073 |



Table 33. Estimated SCI Values at WB2-2 and EB1-1.

| Test Hole | Depth (m) | Activity Ratio | Cation Exchange Capacity (meq / 100 gm) | Cation Exchange Activity Ratio | Suction Water Content Slope | SCI for 100% Fine Clay | Suction Compression Index (actual) |
|---|---|---|---|---|---|---|---|
| WB2-2 | -0.4 | 1.67 | 42.60 | 1.13 | -7.47 | 0.163 | 0.061 |
| | -1.2 | 1.15 | 49.96 | 1.22 | -7.71 | 0.163 | 0.067 |
| | -2.0 | 1.32 | 54.11 | 1.58 | -7.95 | 0.163 | 0.056 |
| EB1-1 | -0.4 | 3.05 | 54.32 | 13.94 | - | - | - |
| | -1.2 | 1.36 | 32.89 | 0.98 | -9.88 | 0.163 | 0.055 |
| | -2.0 | 1.23 | 32.89 | 0.90 | -10.04 | 0.163 | 0.059 |
| | -2.8 | 1.82 | 43.41 | 1.34 | -7.53 | 0.163 | 0.053 |

Table 34. Estimated SCI Values at EB1-2 and EB1-3.

| Test Hole | Depth (m) | Activity Ratio | Cation Exchange Capacity (meq / 100 gm) | Cation Exchange Activity Ratio | Suction Water Content Slope | SCI for 100% Fine Clay | Suction Compression Index (actual) |
|---|---|---|---|---|---|---|---|
| EB1-2 | -0.4 | 2.16 | 31.54 | 1.52 | -9.64 | 0.220 | 0.046 |
| | -2.0 | 1.16 | 40.59 | 0.86 | -8.92 | 0.163 | 0.077 |
| | -2.4 | 1.74 | 49.34 | 1.08 | -6.56 | 0.163 | 0.074 |
| | -3.6 | 1.16 | 53.69 | 1.22 | -7.16 | 0.163 | 0.072 |
| EB1-3 | -0.4 | 1.74 | 20.83 | 1.76 | -12.27 | 0.220 | 0.026 |
| | -0.8 | 1.34 | 26.76 | 1.93 | -11.44 | 0.220 | 0.030 |
| | -2.0 | 1.89 | 41.80 | 1.31 | -7.48 | 0.163 | 0.052 |
| | -2.8 | 1.42 | 43.01 | 1.19 | -8.02 | 0.163 | 0.059 |
| | -3.6 | 1.89 | 51.41 | 1.49 | -6.52 | 0.163 | 0.056 |



Table 35. Estimated SCI Values at EB1-4 and EB1-5.

| Test Hole | Depth (m) | Activity Ratio | Cation Exchange Capacity (meq / 100 gm) | Cation Exchange Activity Ratio | Suction Water Content Slope | SCI for 100% Fine Clay | Suction Compression Index (actual) |
|---|---|---|---|---|---|---|---|
| EB1-4 | -0.4 | 1.64 | 33.28 | 2.42 | -10.58 | 0.220 | 0.030 |
| | -1.6 | 1.42 | 37.21 | 1.20 | -9.15 | 0.163 | 0.050 |
| | -2.0 | 1.62 | 49.54 | 2.74 | -8.10 | 0.220 | 0.040 |
| | -2.4 | 1.90 | 45.04 | 2.02 | -8.08 | 0.220 | 0.049 |
| EB1-5 | -0.4 | 1.73 | 25.63 | 2.07 | -11.30 | 0.220 | 0.027 |
| | -1.2 | 2.11 | 26.01 | 1.96 | -10.97 | 0.220 | 0.029 |
| | -1.6 | 1.09 | 39.19 | 0.91 | -9.48 | 0.163 | 0.070 |
| | -2.8 | 1.91 | 47.69 | 2.08 | -7.90 | 0.220 | 0.050 |

and

$$\%\ Fine\ Clay = \frac{\%\ < 2\mu m}{\%\ < 75\mu m}$$

The estimated cation exchange capacity is due to Mojekwu (1979), and is given by

$$CEC\ \left(\frac{meq}{100\ gm\ of\ dry\ soil}\right) \cong (PL\%)^{1.17}$$

The fine clay cation exchange activity ratio is given by

$$CEAc = CEC\ \frac{\left(\frac{meq}{100\ gm\ dry\ soil}\right)}{\%\ Fine\ Clay}$$

where,

PI = plasticity index

PL = plastic limit (%).

The soils information from which these soils properties were estimated is shown in Tables 36 through 39. The liquid limits, plasticity indexes, amount percent passing the 75 μm sieve and fine clay content for the SH 6 sites are shown in Tables 36 and 37. The same information for the SH 21 site is shown in Tables 38 and 39.

Further estimates may be made of the diffusion coefficient of the soils at each depth in each boring using the relationships given in Chapter 2. From these coefficients, Mitchell's unsaturated permeabilities, p, can be determined and are tabulated in Tables 40 through 47. The results for the SH 6 site are in Tables 40 through 43 and for the SH 21 site are in Tables 44 through 47.

All the soils in the project areas are classified as medium cracked or moderately permeable soils which have a Mitchell's unsaturated permeability greater than 0.00005 $cm^2/sec$ and smaller than 0.001$cm^2/sec$.

Table 36. Index Test Results from SH 6 Northbound.

| Test Hole | Depth (m) | Liquid Limit (%) | Plasticity Index (%) | Passing No. 200 Sieve (%) | Fine Clay Content (%) |
|---|---|---|---|---|---|
| NB1-1 | -0.4 | 15.6 | NP | 43.3 | 37.7 |
| | -0.8 | 38.0 | 24.3 | 81.2 | 21.9 |
| | -1.6 | 82.4 | 56.2 | 91.8 | 27.7 |
| | -2.4 | 86.9 | 59.2 | 98.8 | 42.7 |
| NB1-2 | -0.4 | 19.5 | NP | 44.0 | 23.2 |
| | -1.6 | 45.4 | 31.0 | 83.7 | 18.4 |
| | -2.4 | 72.7 | 48.7 | 99.7 | 99.7 |
| | -3.3 | 97.5 | 70.1 | 99.3 | 99.3 |
| NB2-1 | -0.4 | 88.2 | 56.3 | 97.8 | 40.4 |
| | -1.2 | 87.2 | 56.1 | 95.5 | 40.1 |
| | -2.4 | 85.7 | 59.6 | 99.4 | 38.7 |
| | -3.3 | 88.3 | 60.9 | 97.2 | 33.0 |
| NB2-2 | -0.4 | 96.6 | 62.2 | 90.4 | 44.0 |
| | -1.2 | 95.1 | 67.5 | 96.5 | 96.4 |
| | -2.0 | 101.8 | 66.3 | 98.7 | 39.6 |
| | -3.3 | 89.0 | 58.3 | 96.1 | 39.0 |

Table 37. Index Test Results from SH 6 Southbound.

| Test Hole | Depth (m) | Liquid Limit (%) | Plasticity Index (%) | Passing No. 200 Sieve (%) | Fine Clay Content (%) |
|---|---|---|---|---|---|
| SB1-1 | -0.4 | 82.7 | 57.8 | 97.6 | 66.7 |
| | -1.2 | 83.2 | 58.3 | 97.0 | 33.0 |
| | -2.4 | 100.1 | 58.0 | 94.5 | 38.7 |
| | -3.7 | 86.0 | 58.4 | 93.2 | 93.2 |
| SB1-2 | -0.4 | 86.2 | 58.6 | 88.2 | 45.3 |
| | -1.6 | 88.3 | 58.1 | 96.4 | 38.0 |
| | -2.4 | 94.6 | 67.4 | 98.9 | 40.9 |
| | -2.8 | 95.8 | 64.3 | 89.8 | 89.8 |
| SB1-3 | -0.4 | 57.0 | 35.9 | 79.7 | 42.7 |
| | -1.2 | 74.1 | 49.0 | 86.7 | 38.5 |
| | -2.4 | 79.7 | 51.3 | 92.3 | 42.8 |
| | -3.7 | 86.3 | 55.9 | 99.0 | 99.0 |
| SB2-1 | -0.8 | 61.6 | 39.2 | 93.2 | 91.4 |
| | -1.6 | 76.6 | 46.9 | 99.1 | 19.8 |
| | -2.0 | 77.9 | 48.4 | 93.8 | 63.9 |
| | -2.4 | 71.6 | 46.2 | 94.6 | 26.0 |
| SB2-2 | -0.4 | 71.9 | 48.0 | 86.7 | 26.1 |
| | -0.8 | 86.9 | 57.8 | 96.8 | 38.6 |
| | -1.6 | 99.3 | 71.3 | 99.4 | 35.0 |
| | -2.8 | 83.4 | 56.7 | 98.8 | 36.3 |
| | -4.1 | 72.5 | 48.0 | 98.0 | 97.6 |
| | -4.9 | 98.9 | 83.3 | 78.4 | 81.9 |

Table 38. Index Test Results from SH 21 Westbound.

| Test Hole | Depth (m) | Liquid Limit (%) | Plasticity Index (%) | Passing No. 200 Sieve (%) | Fine Clay Content (%) |
|---|---|---|---|---|---|
| WB1-1 | -0.4 | 47.0 | 29.8 | 81.7 | 24.1 |
| | -0.8 | 84.7 | 58.4 | 96.5 | 35.6 |
| | -1.2 | 94.9 | 61.8 | - | 33.9 |
| | -1.6 | 88.0 | 57.8 | 99.2 | 35.4 |
| | -2.0 | 94.6 | 60.6 | 99.2 | 31.2 |
| | -2.4 | 98.9 | 57.9 | 97.1 | 24.0 |
| WB2-1 | -0.4 | 70.3 | 48.8 | 95.9 | 28.2 |
| | -0.8 | 62.0 | 37.4 | 99.1 | 29.3 |
| | -1.6 | 61.5 | 36.8 | 88.6 | 30.4 |
| | -2.8 | 88.5 | 58.1 | 79.0 | 35.6 |
| WB2-2 | -0.4 | 87.6 | 62.8 | 96.0 | 36.2 |
| | -1.2 | 75.3 | 47.0 | 93.3 | 38.1 |
| | -2.0 | 75.4 | 45.2 | 86.5 | 29.7 |

Table 39. Index Test Results from SH 21 Eastbound.

| Test Hole | Depth (m) | Liquid Limit (%) | Plasticity Index (%) | Passing No. 200 Sieve (%) | Fine Clay Content (%) |
|---|---|---|---|---|---|
| EB1-1 | -0.4 | 42.3 | 11.9 | 70.6 | 2.8 |
| | -1.2 | 65.4 | 45.6 | 81.6 | 27.4 |
| | -2.0 | 64.6 | 44.8 | 79.7 | 29.1 |
| | -2.8 | 84.1 | 59.0 | 96.5 | 31.2 |
| EB1-2 | -0.4 | 64.1 | 45.0 | 87.1 | 18.1 |
| | -2.0 | 78.5 | 54.8 | 81.7 | 38.8 |
| | -2.4 | 107.5 | 79.5 | 92.5 | 42.2 |
| | -3.6 | 81.0 | 50.9 | 95.0 | 41.8 |
| EB1-3 | -0.4 | 34.0 | 20.6 | 75.3 | 8.9 |
| | -0.8 | 35.2 | 18.6 | 81.3 | 11.3 |
| | -2.0 | 84.7 | 60.4 | 98.2 | 31.4 |
| | -2.8 | 76.2 | 51.2 | 93.9 | 33.9 |
| | -3.6 | 94.3 | 65.3 | 98.9 | 34.2 |
| EB1-4 | -0.4 | 42.5 | 22.5 | 84.0 | 11.6 |
| | -1.6 | 65.8 | 43.8 | 88.4 | 27.3 |
| | -2.0 | 57.4 | 29.3 | 98.0 | 17.7 |
| | -2.4 | 68.3 | 42.4 | 96.0 | 21.4 |
| EB1-5 | -0.4 | 37.5 | 21.5 | 83.0 | 10.3 |
| | -1.2 | 44.1 | 28.0 | 84.0 | 11.2 |
| | -1.6 | 69.7 | 46.7 | 79.6 | 34.2 |
| | -2.8 | 71.0 | 43.8 | 94.8 | 21.7 |

Table 40. Estimated Flow Properties of Soils at NB1-1 and NB1-2.

| Test Hole | Depth (m) | Diffusion Coefficient (cm^2/sec) | Mitchell's Unsaturated Permeability p (cm^2/sec) | Saturated Permeability ko (cm/sec) | Gardner's Permeability k (cm/sec) | Mitchell's Permeability k (cm/sec) |
|---|---|---|---|---|---|---|
| NB1-1 | -0.4 | - | - | - | - | - |
| | -0.8 | 4.36E-03 | 5.97E-04 | 2.59E-06 | 4.33E-08 | 6.66E-08 |
| | -1.6 | 3.42E-03 | 7.02E-04 | 3.05E-06 | 1.71E-08 | 5.42E-08 |
| | -2.4 | 3.18E-03 | 7.30E-04 | 3.17E-06 | 1.66E-08 | 5.51E-08 |
| NB1-2 | -0.4 | - | - | - | - | - |
| | -1.6 | 4.34E-03 | 6.23E-04 | 2.71E-06 | 3.90E-09 | 3.06E-08 |
| | -2.4 | 3.43E-03 | 6.98E-04 | 3.03E-06 | 9.38E-09 | 4.42E-08 |
| | -3.3 | 3.22E-03 | 7.87E-04 | 3.42E-06 | 3.13E-08 | 7.17E-08 |

Table 41. Estimated Flow Properties of Soils at NB2-1 and NB2-2.

| Test Hole | Depth (m) | Diffusion Coefficient (cm^2/sec) | Mitchell's Unsaturated Permeability p (cm^2/sec) | Saturated Permeability ko (cm/sec) | Gardner's Permeability k (cm/sec) | Mitchell's Permeability k (cm/sec) |
|---|---|---|---|---|---|---|
| NB2-1 | -0.4 | 3.15E-03 | 7.76E-04 | 3.37E-06 | 4.95E-08 | 8.29E-08 |
| | -1.2 | 3.20E-03 | 7.56E-04 | 3.28E-06 | 1.89E-08 | 5.89E-08 |
| | -2.4 | 3.29E-03 | 7.36E-04 | 3.19E-06 | 2.34E-08 | 6.21E-08 |
| | -3.3 | 3.39E-03 | 7.68E-04 | 3.34E-06 | 5.33E-09 | 3.90E-08 |
| NB2-2 | -0.4 | 3.06E-03 | 7.67E-04 | 3.33E-06 | 2.54E-09 | 3.05E-08 |
| | -1.2 | 2.09E-03 | 4.90E-04 | 2.13E-06 | 1.60E-09 | 1.94E-08 |
| | -2.0 | 2.73E-03 | 7.95E-04 | 3.45E-06 | 1.96E-09 | 2.86E-08 |
| | -3.3 | 3.21E-03 | 7.65E-04 | 3.32E-06 | 2.61E-09 | 3.07E-08 |

Table 42. Estimated Flow Properties of Soils at SB1-1, SB1-2, and SB1-3.

| Test Hole | Depth (m) | Diffusion Coefficient (cm^2/sec) | Mitchell's Unsaturated Permeability p (cm^2/sec) | Saturated Permeability ko (cm/sec) | Gardner's Permeability k (cm/sec) | Mitchell's Permeability k (cm/sec) |
|---|---|---|---|---|---|---|
| SB1-1 | -0.4 | 2.79E-03 | 5.94E-04 | 2.58E-06 | 8.23E-08 | 8.27E-08 |
| | -1.2 | 3.47E-03 | 7.35E-04 | 3.19E-06 | 4.41E-08 | 7.69E-08 |
| | -2.4 | 2.68E-03 | 8.46E-04 | 3.68E-06 | 1.17E-08 | 5.41E-08 |
| | -3.7 | 2.24E-03 | 4.86E-04 | 2.11E-06 | 5.66E-08 | 6.37E-08 |
| SB1-2 | -0.4 | 3.25E-03 | 6.73E-04 | 2.92E-06 | 6.11E-08 | 8.11E-08 |
| | -1.6 | 3.24E-03 | 7.65E-04 | 3.32E-06 | 3.07E-07 | 1.55E-07 |
| | -2.4 | 3.18E-03 | 7.57E-04 | 3.29E-06 | 2.83E-08 | 6.76E-08 |
| | -2.8 | 2.21E-03 | 5.22E-04 | 2.27E-06 | 1.37E-08 | 4.13E-08 |
| SB1-3 | -0.4 | 3.70E-03 | 5.81E-04 | 2.53E-06 | 3.41E-07 | 1.36E-07 |
| | -1.2 | 3.52E-03 | 6.57E-04 | 2.85E-06 | 4.61E-08 | 7.25E-08 |
| | -2.4 | 3.28E-03 | 6.91E-04 | 3.00E-06 | 6.61E-08 | 8.47E-08 |
| | -3.7 | 2.82E-03 | 6.78E-04 | 2.94E-06 | 6.49E-08 | 8.32E-08 |

Table 43. Estimated Flow Properties of Soils at SB2-1 and SB2-2.

| Test Hole | Depth (m) | Diffusion Coefficient (cm^2/sec) | Mitchell's Unsaturated Permeability p (cm^2/sec) | Saturated Permeability ko (cm/sec) | Gardner's Permeability k (cm/sec) | Mitchell's Permeability k (cm/sec) |
|---|---|---|---|---|---|---|
| SB2-1 | -0.8 | 3.67E-03 | 6.57E-04 | 2.85E-06 | 4.05E-09 | 3.21E-08 |
| | -1.6 | 3.52E-03 | 7.93E-04 | 3.44E-06 | 3.92E-09 | 3.60E-08 |
| | -2.0 | 2.84E-03 | 6.10E-04 | 2.65E-06 | 1.77E-09 | 2.32E-08 |
| | -2.4 | 3.51E-03 | 6.94E-04 | 3.01E-06 | 3.78E-09 | 3.25E-08 |
| SB2-2 | -0.4 | 3.63E-03 | 6.59E-04 | 2.86E-06 | 1.05E-07 | 9.63E-08 |
| | -0.8 | 3.25E-03 | 7.51E-04 | 3.26E-06 | 3.19E-07 | 1.55E-07 |
| | -1.6 | 3.24E-03 | 8.09E-04 | 3.52E-06 | 1.88E-07 | 1.35E-07 |
| | -2.8 | 3.35E-03 | 7.42E-04 | 3.22E-06 | 4.22E-07 | 1.72E-07 |
| | -4.1 | 3.46E-03 | 6.97E-04 | 3.03E-06 | 1.27E-06 | 2.71E-07 |
| | -4.9 | 3.80E-03 | 6.53E-04 | 2.84E-06 | - | - |

Table 44. Estimated Flow Properties of Soils at WB1-1 and WB2-1.

| Test Hole | Depth (m) | Diffusion Coefficient (cm^2/sec) | Mitchell's Unsaturated Permeability p (cm^2/sec) | Saturated Permeability ko (cm/sec) | Gardner's Permeability k (cm/sec) | Mitchell's Permeability k (cm/sec) |
|---|---|---|---|---|---|---|
| WB1-1 | -0.4 | 4.08E-03 | 5.99E-04 | 2.60E-06 | 2.42E-07 | 1.22E-07 |
| | -0.8 | 3.36E-03 | 7.30E-04 | 3.17E-06 | 2.18E-08 | 6.04E-08 |
| | -1.2 | - | - | - | - | - |
| | -1.6 | 3.01E-03 | 7.31E-04 | 3.17E-06 | 1.55E-08 | 5.39E-08 |
| | -2.0 | 3.01E-03 | 8.16E-04 | 3.55E-06 | 2.28E-08 | 6.60E-08 |
| | -2.4 | 3.06E-03 | 9.66E-04 | 4.20E-06 | 3.31E-08 | 8.37E-08 |
| WB2-1 | -0.4 | 3.70E-03 | 6.94E-04 | 3.01E-06 | 5.04E-08 | 7.75E-08 |
| | -0.8 | 3.65E-03 | 7.07E-04 | 3.07E-06 | 7.20E-08 | 8.86E-08 |
| | -1.6 | 3.67E-03 | 6.54E-04 | 2.84E-06 | 5.08E-08 | 7.47E-08 |
| | -2.8 | 3.29E-03 | 6.63E-04 | 2.88E-06 | 3.42E-08 | 6.60E-08 |

Table 45. Estimated Flow Properties of Soils at WB2-2 and EB1-1.

| Test Hole | Depth (m) | Diffusion Coefficient (cm^2/sec) | Mitchell's Unsaturated Permeability p (cm^2/sec) | Saturated Permeability ko (cm/sec) | Gardner's Permeability k (cm/sec) | Mitchell's Permeability k (cm/sec) |
|---|---|---|---|---|---|---|
| WB2-2 | -0.4 | 3.36E-03 | 7.20E-04 | 3.13E-06 | 1.75E-08 | 5.56E-08 |
| | -1.2 | 3.34E-03 | 6.92E-04 | 3.01E-06 | 7.54E-08 | 8.88E-08 |
| | -2.0 | 3.51E-03 | 7.05E-04 | 3.06E-06 | 9.39E-08 | 9.69E-08 |
| EB1-1 | -0.4 | - | - | - | - | - |
| | -1.2 | 3.83E-03 | 6.21E-04 | 2.70E-06 | 1.94E-07 | 1.15E-07 |
| | -2.0 | 3.80E-03 | 6.06E-04 | 2.63E-06 | 3.58E-08 | 6.31E-08 |
| | -2.8 | 3.48E-03 | 7.39E-04 | 3.21E-06 | 9.20E-08 | 9.91E-08 |

Table 46. Estimated Flow Properties of Soils at EB1-2 and EB1-3.

| Test Hole | Depth (m) | Diffusion Coefficient (cm^2/sec) | Mitchell's Unsaturated Permeability p (cm^2/sec) | Saturated Permeability ko (cm/sec) | Gardner's Permeability k (cm/sec) | Mitchell's Permeability k (cm/sec) |
|---|---|---|---|---|---|---|
| EB1-2 | -0.4 | 3.90E-03 | 6.48E-04 | 2.81E-06 | 1.05E-07 | 9.53E-08 |
| | -2.0 | 3.40E-03 | 6.10E-04 | 2.65E-06 | 7.60E-08 | 8.19E-08 |
| | -2.4 | 3.06E-03 | 7.45E-04 | 3.24E-06 | 3.85E-08 | 7.41E-08 |
| | -3.6 | 3.19E-03 | 7.12E-04 | 3.09E-06 | 8.86E-08 | 9.55E-08 |
| EB1-3 | -0.4 | 4.57E-03 | 5.96E-04 | 2.59E-06 | 7.94E-08 | 8.19E-08 |
| | -0.8 | 4.38E-03 | 6.13E-04 | 2.66E-06 | 4.02E-07 | 1.50E-07 |
| | -2.0 | 3.48E-03 | 7.44E-04 | 3.23E-06 | 4.33E-07 | 1.73E-07 |
| | -2.8 | 3.48E-03 | 6.94E-04 | 3.02E-06 | 2.22E-08 | 5.88E-08 |
| | -3.6 | 3.27E-03 | 8.02E-04 | 3.48E-06 | 4.75E-08 | 8.36E-08 |

Table 47. Estimated Flow Properties of Soils at EB1-4 and EB1-5.

| Test Hole | Depth (m) | Diffusion Coefficient (cm^2/sec) | Mitchell's Unsaturated Permeability p (cm^2/sec) | Saturated Permeability ko (cm/sec) | Gardner's Permeability k (cm/sec) | Mitchell's Permeability k (cm/sec) |
|---|---|---|---|---|---|---|
| EB1-4 | -0.4 | 4.24E-03 | 6.42E-04 | 2.79E-06 | 2.59E-07 | 1.30E-07 |
| | -1.6 | 3.77E-03 | 6.59E-04 | 2.86E-06 | 4.07E-07 | 1.57E-07 |
| | -2.0 | 3.73E-03 | 7.36E-04 | 3.20E-06 | 8.57E-08 | 9.66E-08 |
| | -2.4 | 3.61E-03 | 7.15E-04 | 3.11E-06 | 5.55E-08 | 8.17E-08 |
| EB1-5 | -0.4 | 4.40E-03 | 6.23E-04 | 2.70E-06 | 1.61E-07 | 1.08E-07 |
| | -1.2 | 4.32E-03 | 6.30E-04 | 2.74E-06 | 1.25E-07 | 9.94E-08 |
| | -1.6 | 3.58E-03 | 6.04E-04 | 2.63E-06 | 1.20E-07 | 9.53E-08 |
| | -2.8 | 3.57E-03 | 7.22E-04 | 3.14E-06 | 1.01E-08 | 4.64E-08 |

Tables 40 through 47 show the estimated saturated permeabilities, $k_o$, and the Gardner's and Mitchell's permeabilities for the level of suction measured at the recorded depth in each boring. The difference between the 2 permeabilities is that Gardner's permeability is that of the intact soil, and Mitchell's permeability is that of the soil mass, including the effects of cracks.

# CHAPTER 4
# IDENTIFICATION OF PROBLEMS

## SOIL SUCTION PROFILES AND THEIR INTERPRETATION

Figures 27 through 44 are the measured suction profiles at the SH 6 site, whereas Figures 45 through 52 are the suction profiles at the SH 21 site. Suction was measured by two methods at the SH 6 site using the transistor psychrometer and the filter paper method. Only the transistor psychrometer was used to measure suction at the SH 21 site. The transistor psychrometer is capable of measuring only the total suction while the filter paper method measures both the total and matric suction. The difference between the two is the osmotic suction which is tabulated in Tables 48 and 49 and will be discussed subsequently.

The transistor psychrometer and filter paper suction profiles are plotted in pairs for each boring so that the patterns of suction variation with depth can be compared. Another comparison can be made between the borings that were taken at the peaks and the foot of heave patterns in the pavement. Samples taken from borings beneath the peaks of the heaves should be wetter and have a lower suction than those at the foot of the heaves. The pattern of suction variation with depth indicates the source of the water which caused the heave. All of this will be seen in detail by reviewing each set of borings.

## SUCTION PROFILES FOR BORINGS AT THE SH 6 SITE

Boring NB1-1 was made at the peak of the heave, and boring NB1-2 was made at the foot of the heave. The suction profiles for boring NB1-1 are shown in Figures 27 and 28. The "equilibrium suction" line shown on both graphs was taken from the Thornthwaite Moisture Index - versus - suction graph that is shown in Figure 11 and result from the experimental work of Russam and Coleman (1961) on clay subgrades. This line is drawn on all of the graphs of suction profiles at both sites (SH 6 and SH 21) to show how the suction measurements made at these sites compare with the published information. The fact that all suction values, both matric and total suction, at depths of several meters below the ground are higher than the published value is evidence that the clays on these two projects have higher fine clay content and higher osmotic suction values than in the original published suction values.

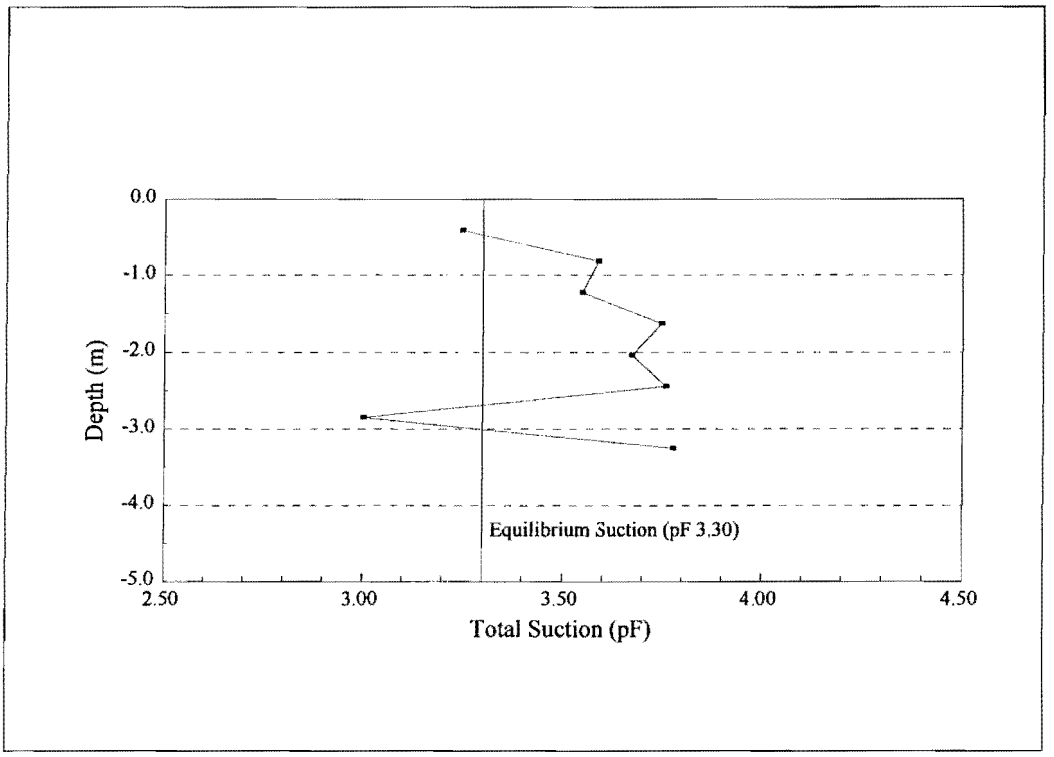


Figure 27. Total Suction Profile for NB1-1 Using Transistor Psychrometer.

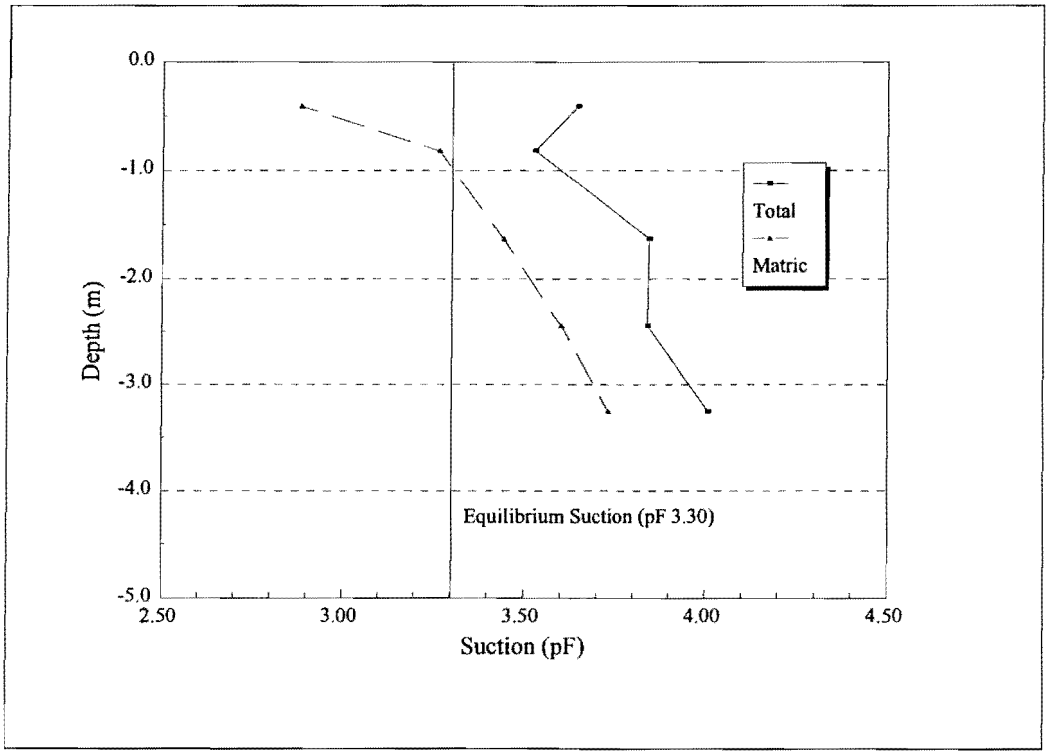


Figure 28. Total and Matric Suction Profile for NB1-1 Using Filter Paper.

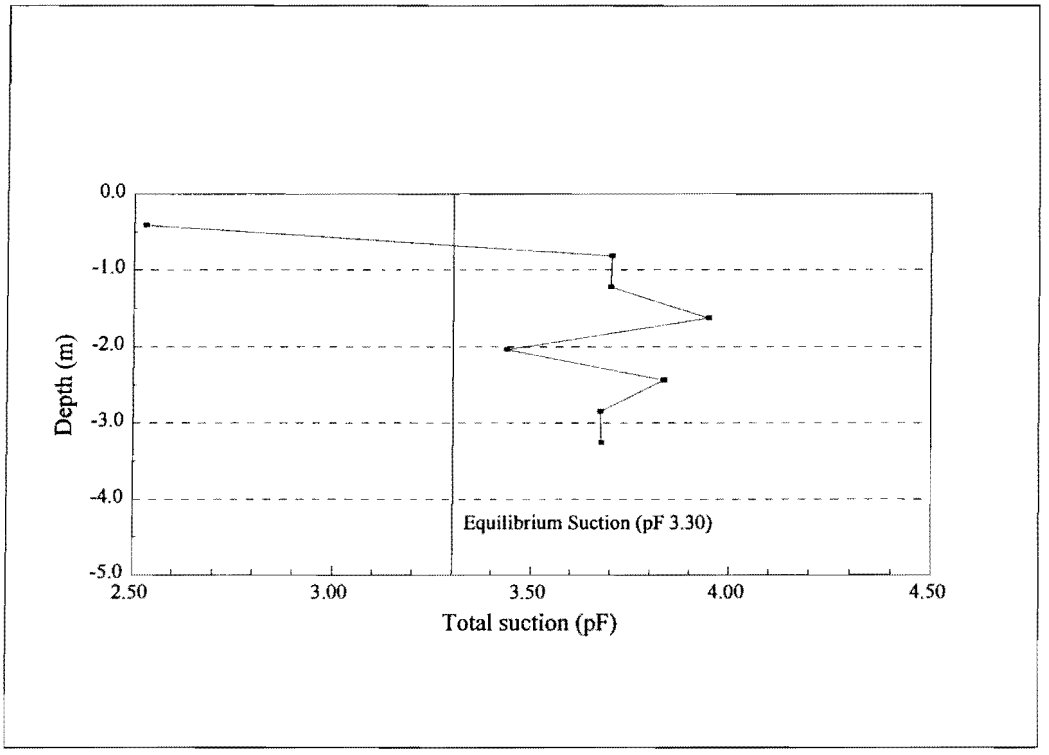


Figure 29. Total Suction Profile for NB1-2 Using Transistor Psychrometer.

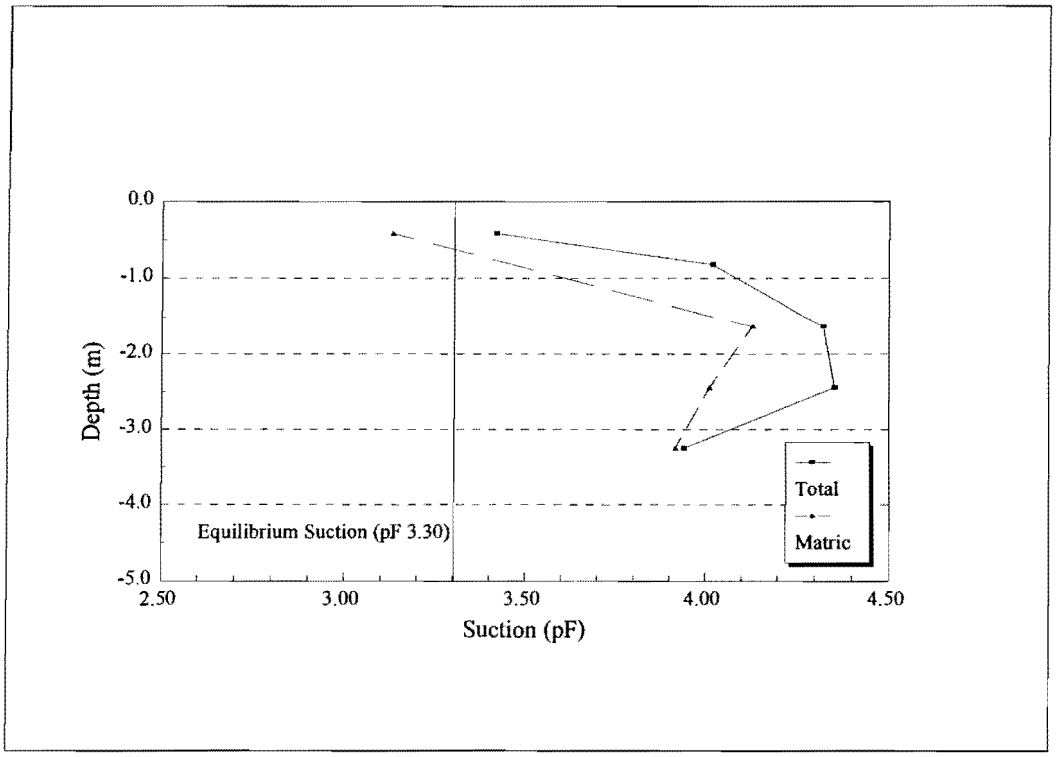


Figure 30. Total and Matric Suction Profile for NB1-2 Using Filter Paper.

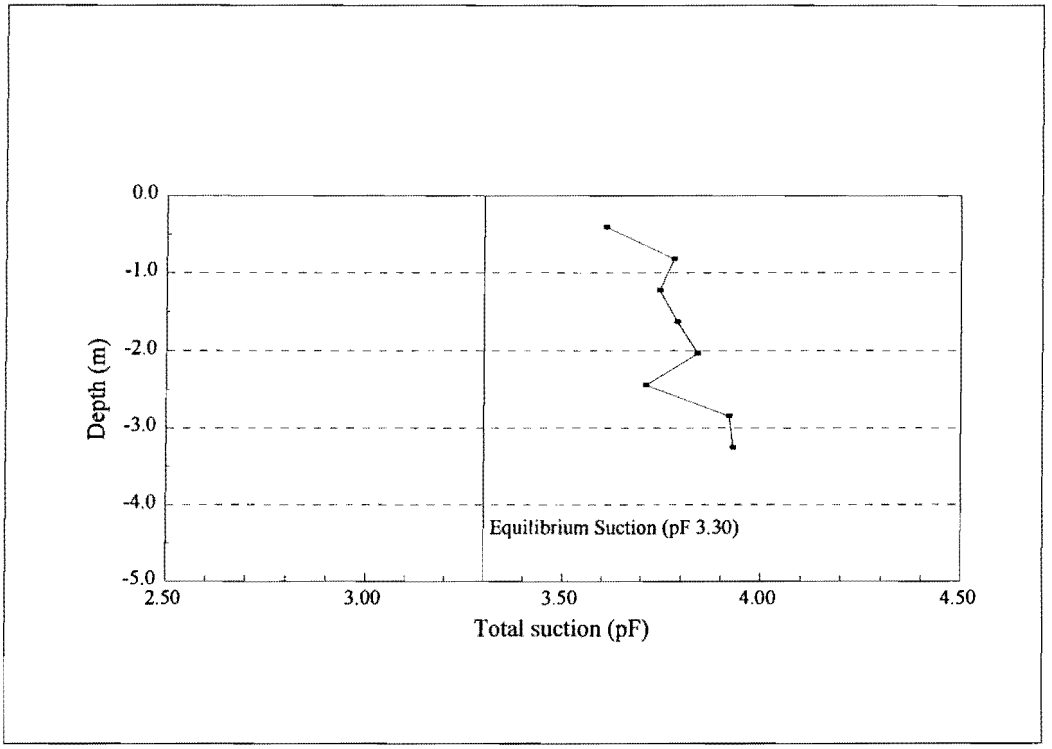


Figure 31. Total Suction Profile for NB2-1 Using Transistor Psychrometer.

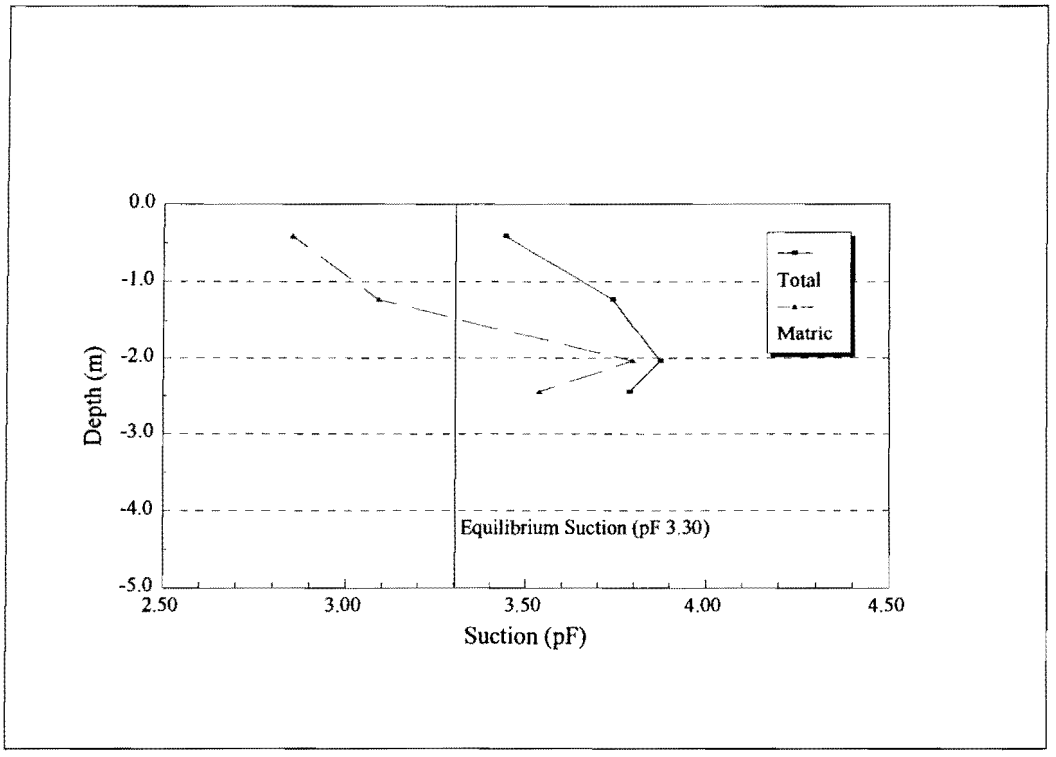


Figure 32. Total and Matric Suction Profile for NB2-1 Using Filter Paper.

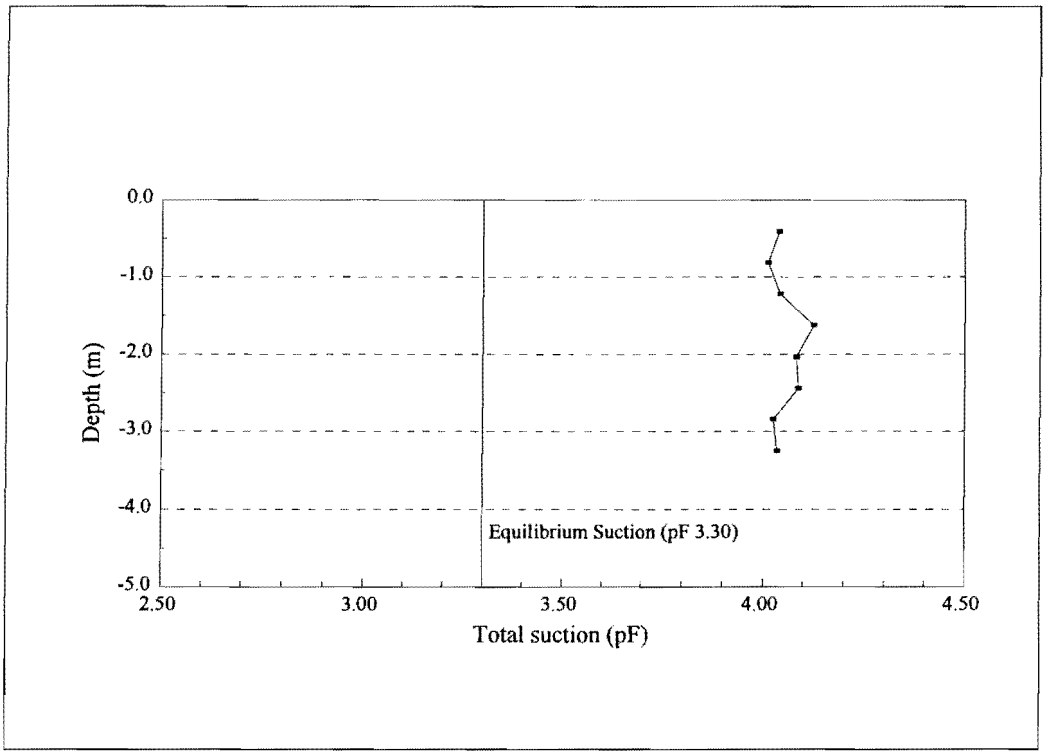


Figure 33. Total Suction Profile for NB2-2 Using Transistor Psychrometer.

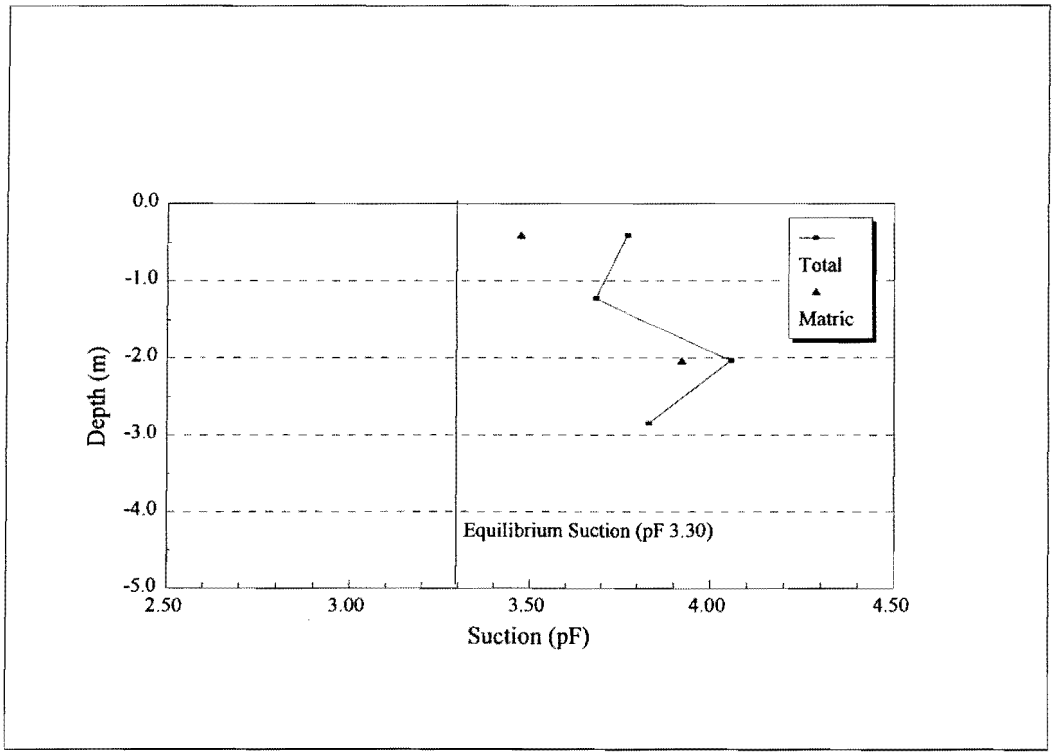


Figure 34. Total and Matric Suction Profile for NB2-2 Using Filter Paper.

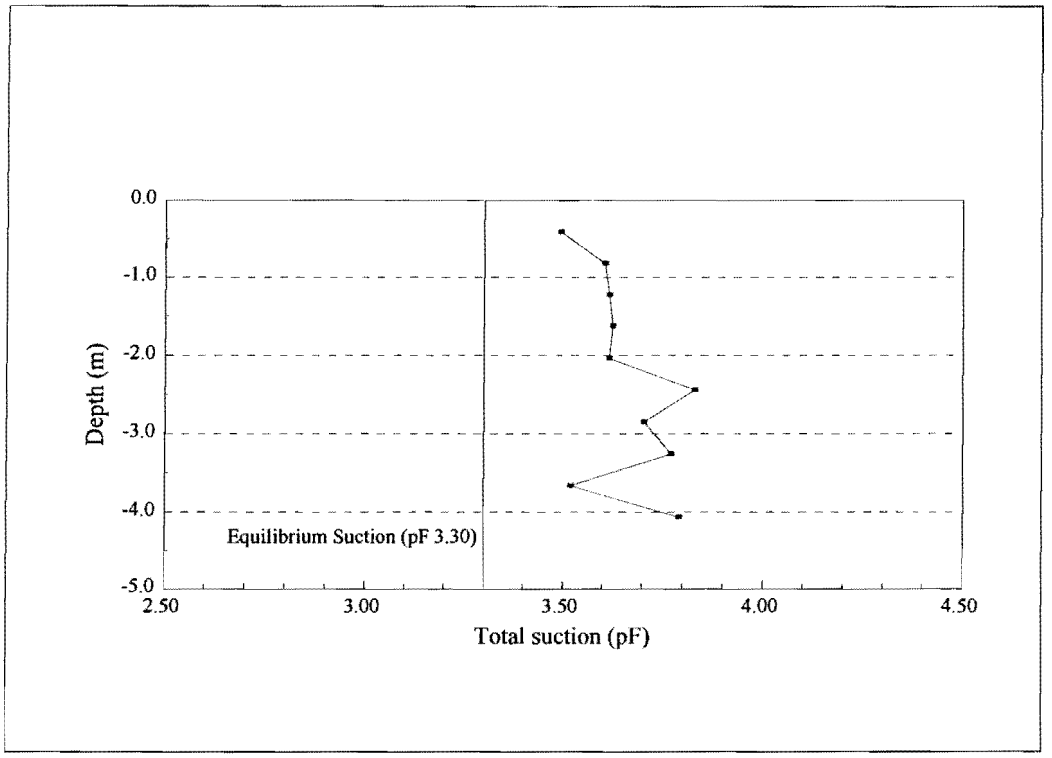


Figure 35. Total Suction Profile for SB1-1 Using Transistor Psychrometer.

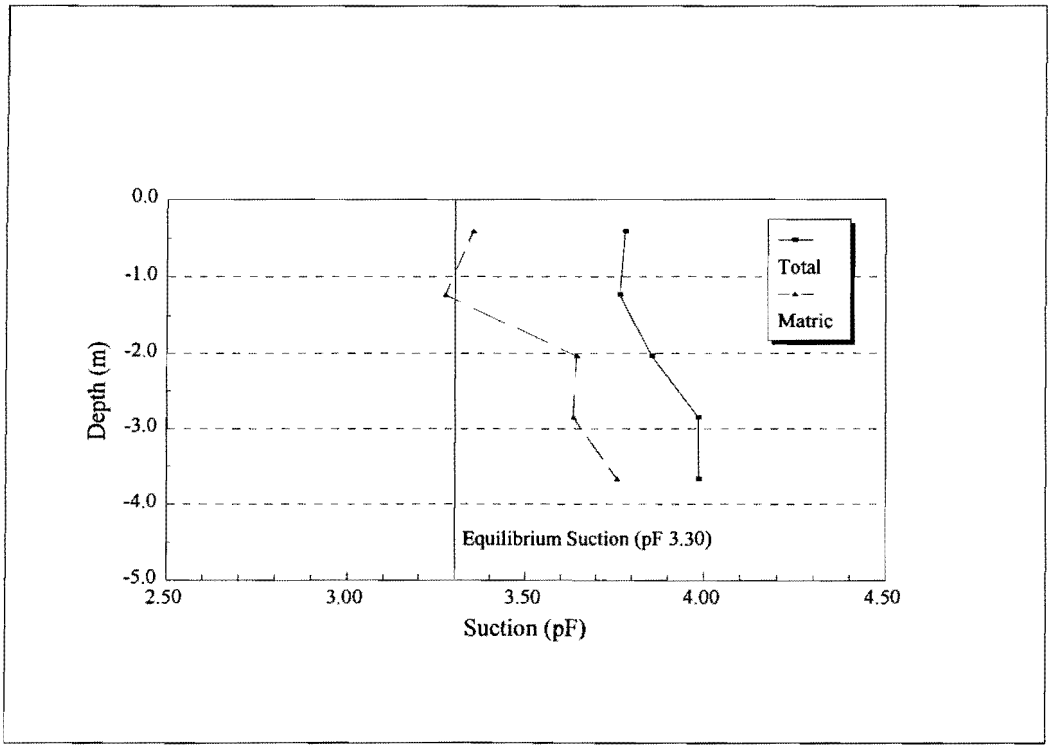


Figure 36. Total and Matric Suction Profile for SB1-1 Using Filter Paper.

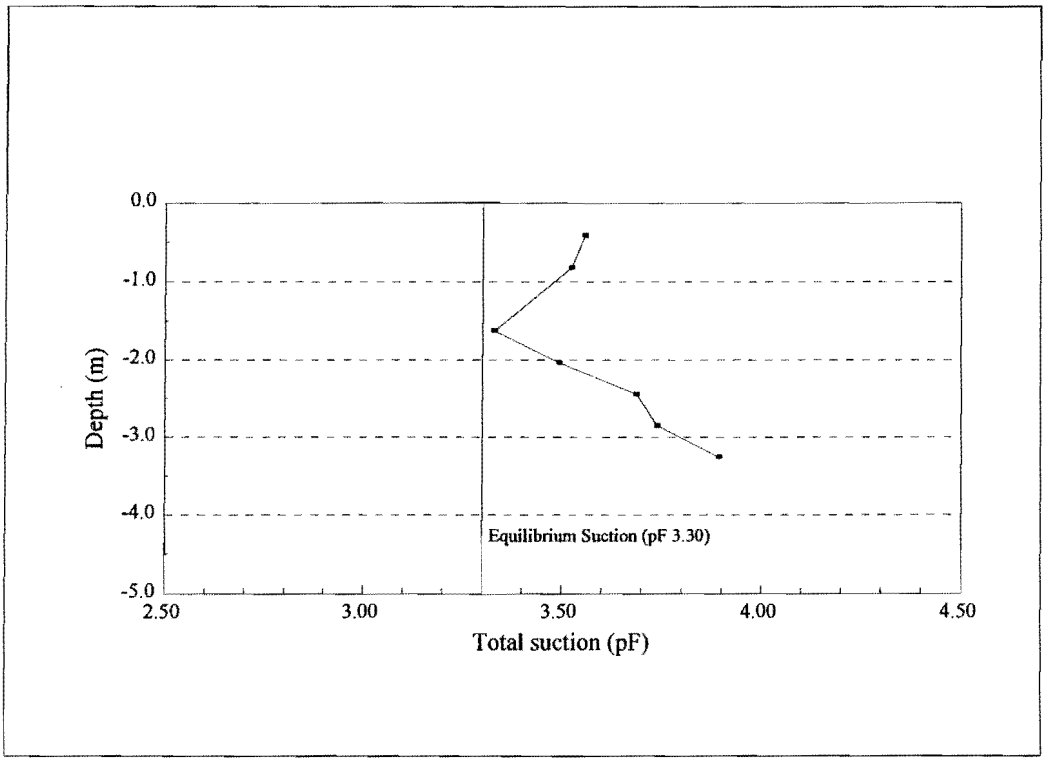


Figure 37. Total Suction Profile for SB1-2 Using Transistor Psychrometer.

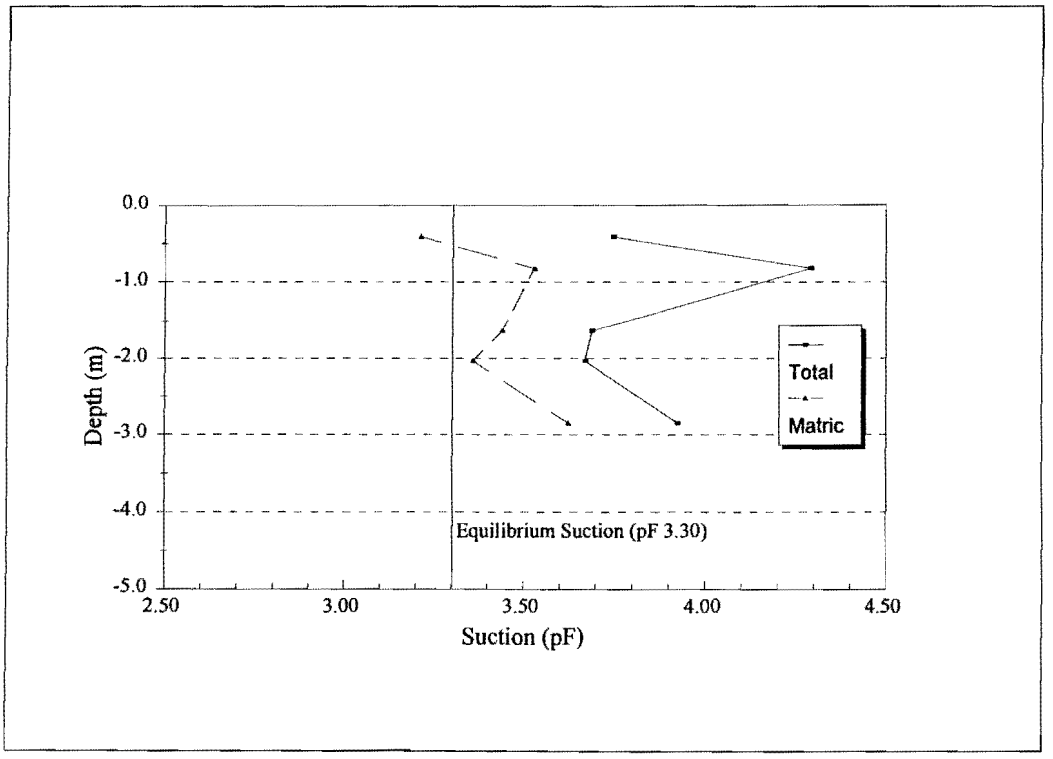


Figure 38. Total and Matric Suction Profile for SB1-2 Using Filter Paper.

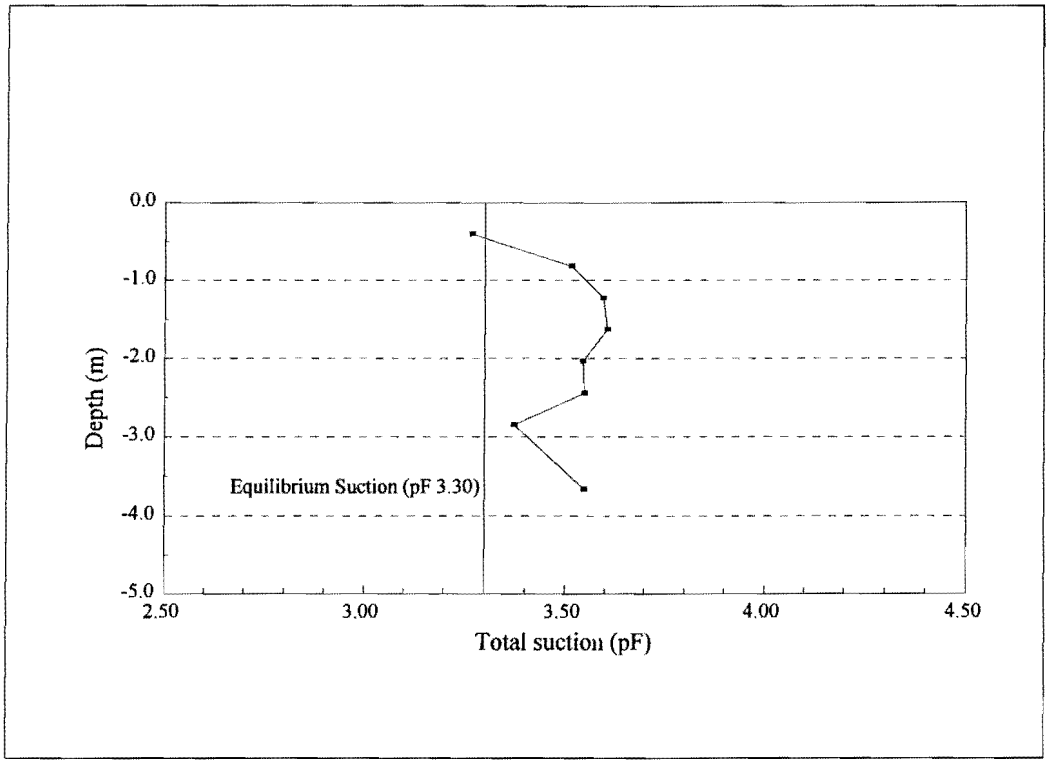


Figure 39. Total Suction Profile for SB1-3 Using Transistor Psychrometer.

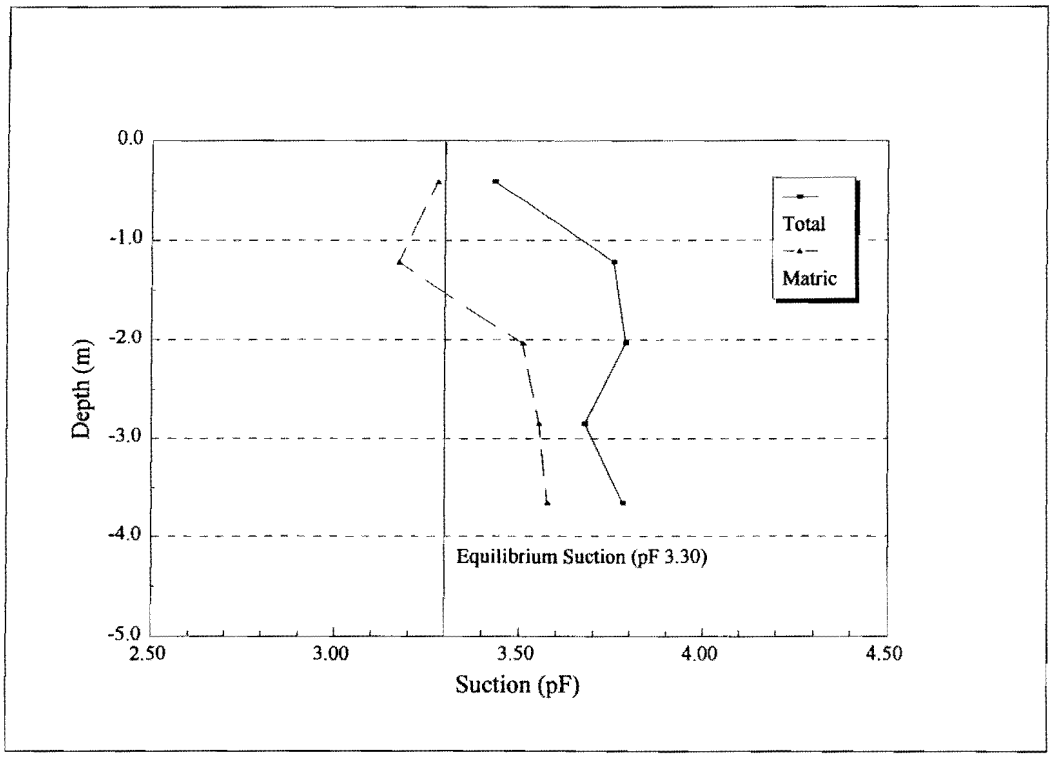


Figure 40. Total and Matric Suction Profile for SB1-3 Using Filter Paper.

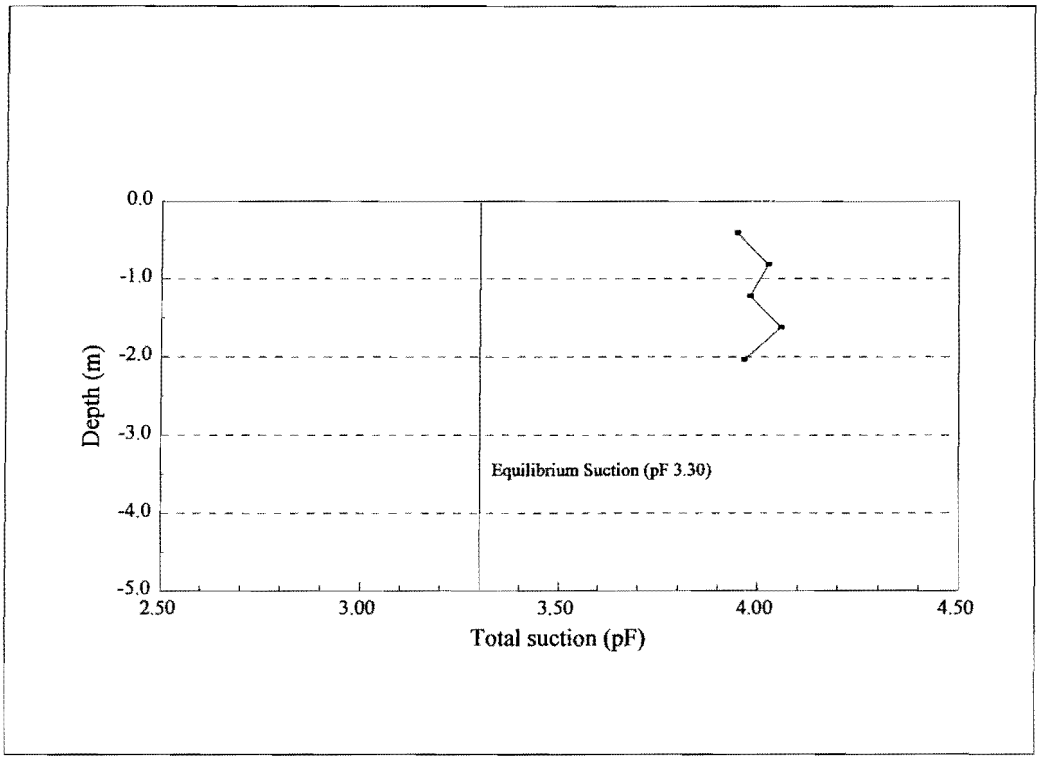


Figure 41. Total Suction Profile for SB2-1 Using Transistor Psychrometer.

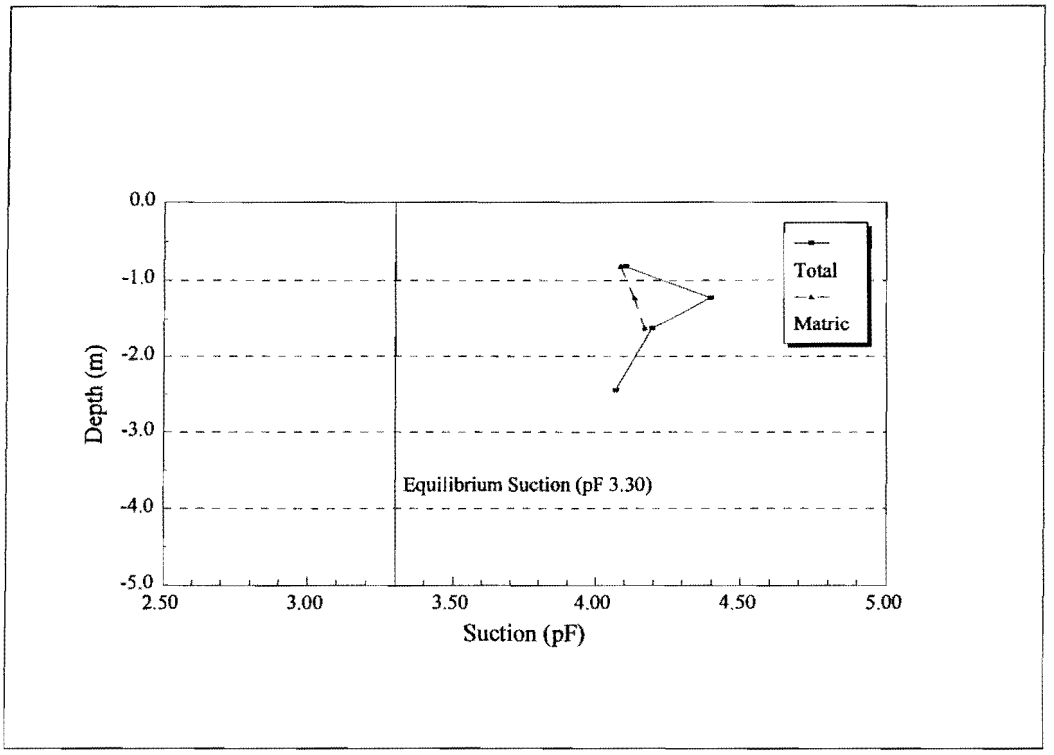


Figure 42. Total and Matric Suction Profile for SB2-1 Using Filter Paper.

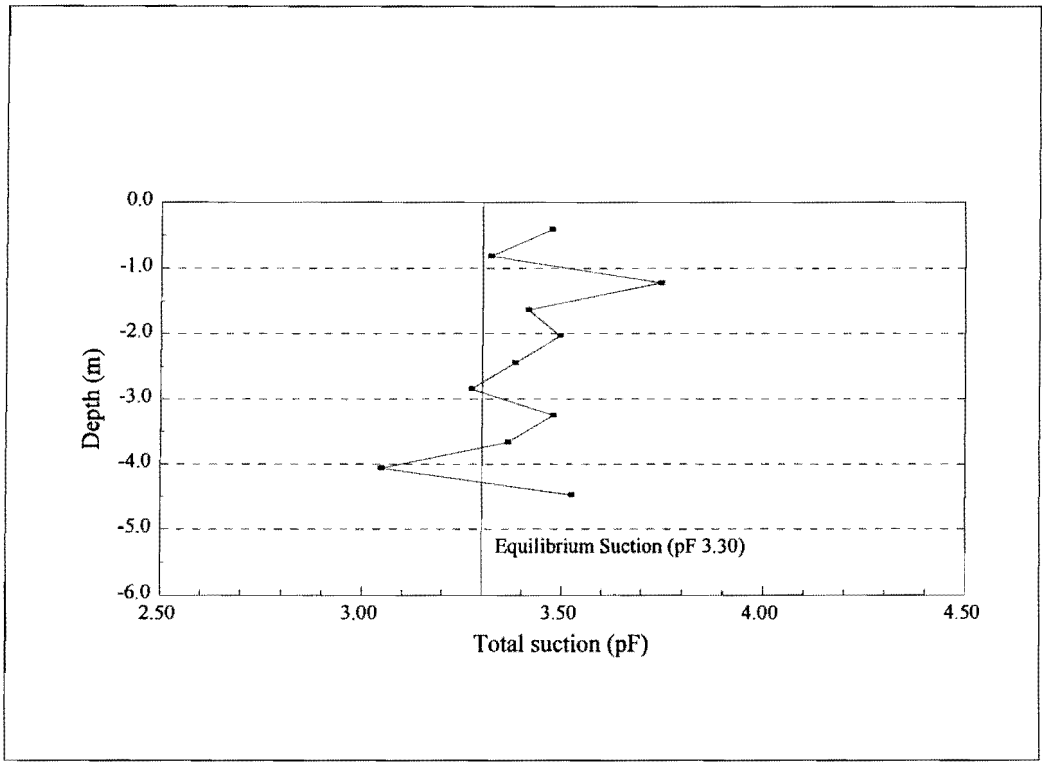


Figure 43. Total Suction Profile for SB2-2 Using Transistor Psychrometer.

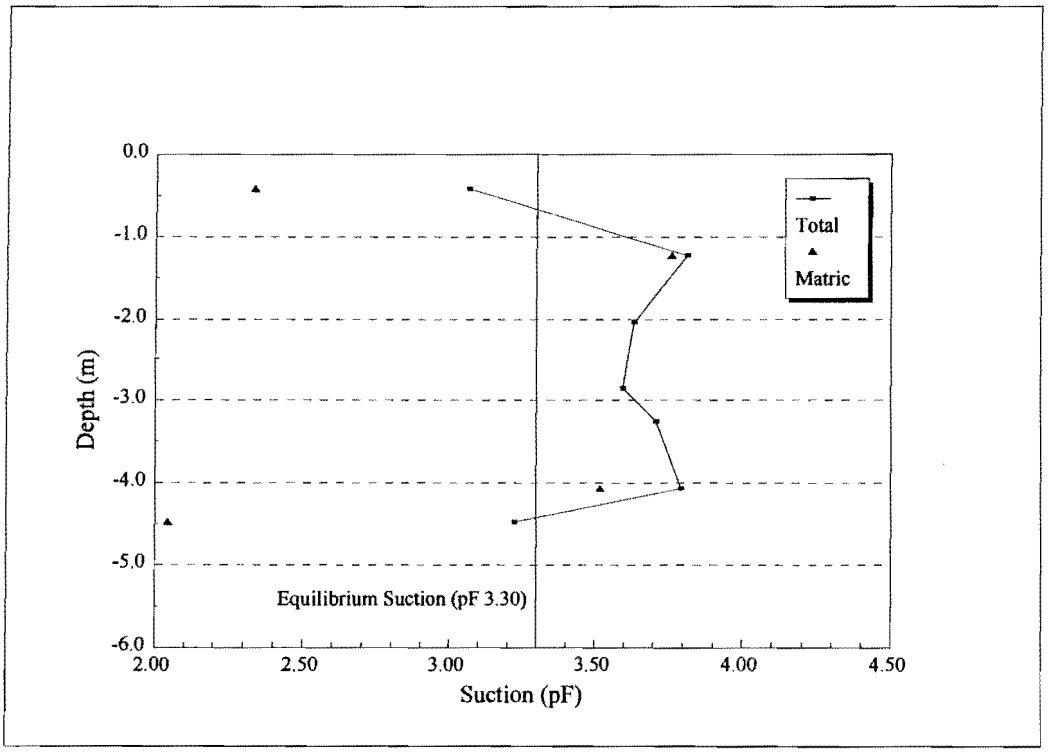


Figure 44. Total and Matric Suction Profile for SB2-2 Using Filter Paper.

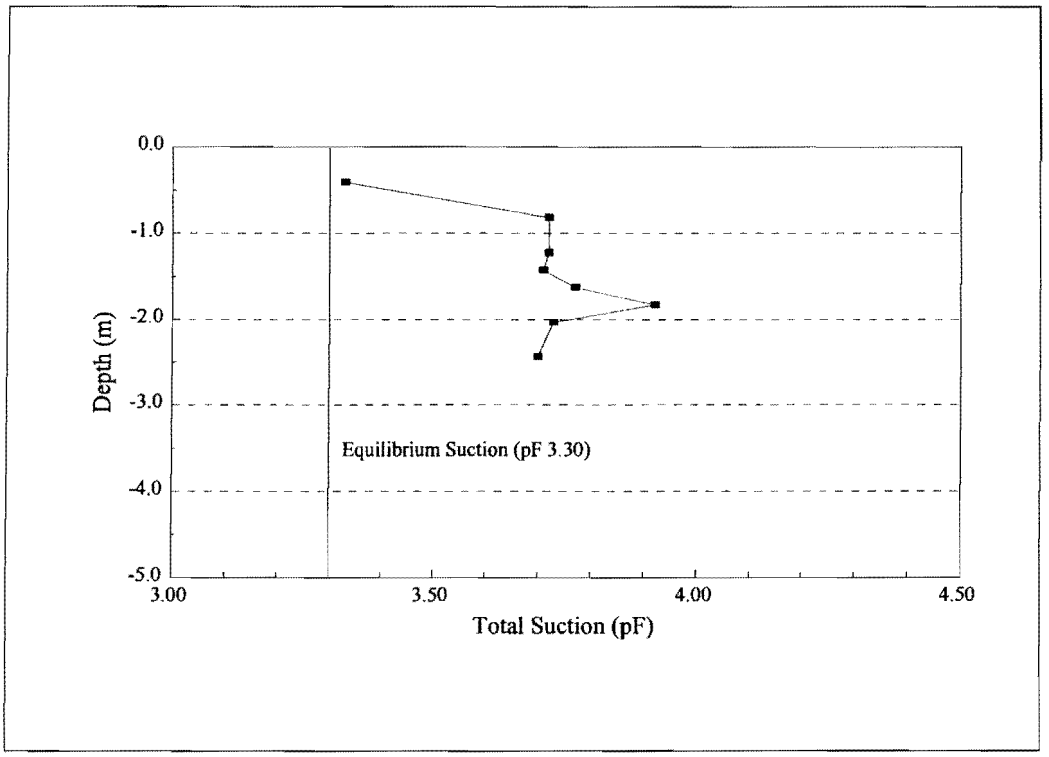


Figure 45. Total Suction Profile for WB1-1 Using Transistor Psychrometer.

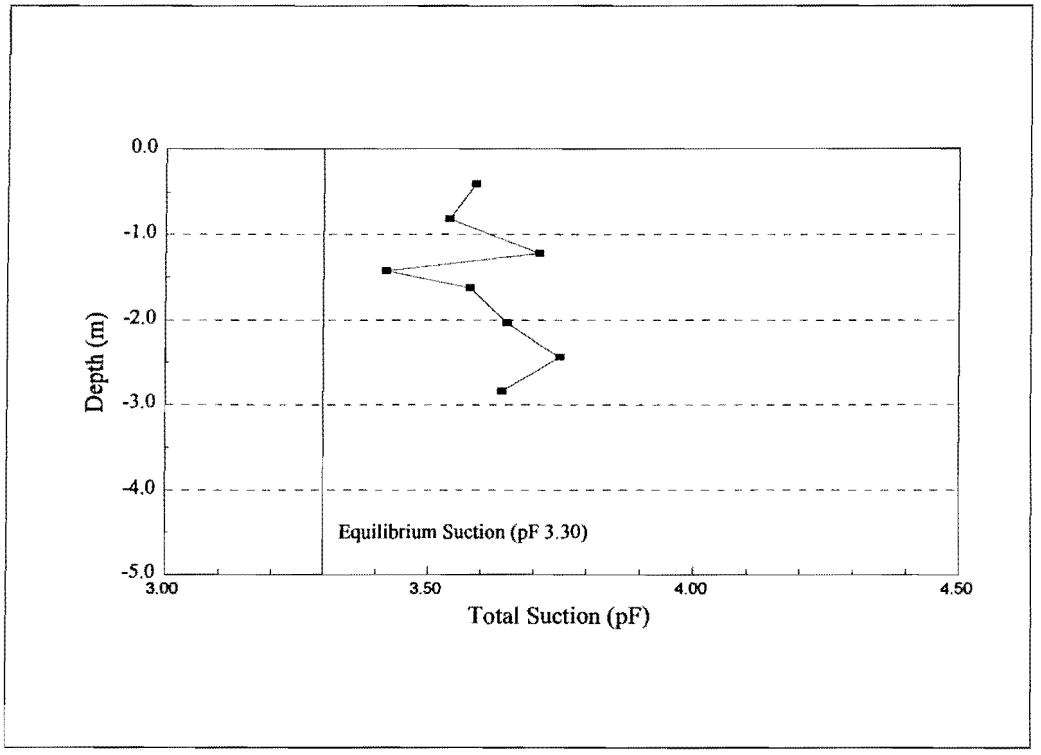


Figure 46. Total Suction Profile for WB2-1 Using Transistor Psychrometer.

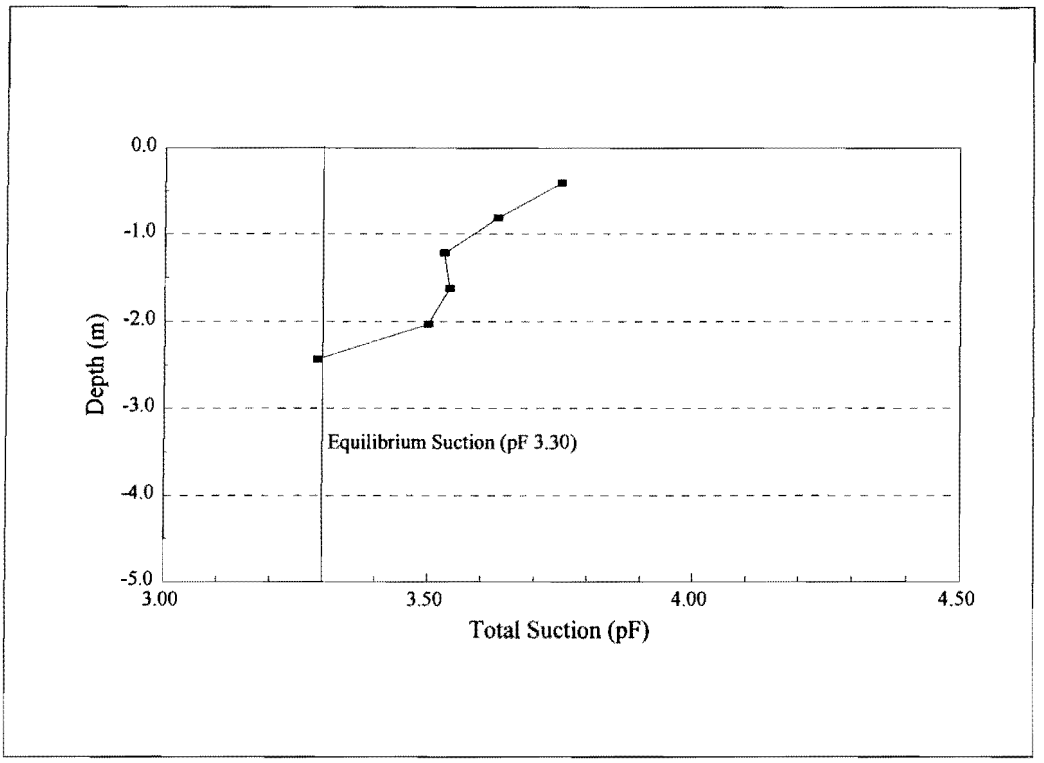


Figure 47. Total Suction Profile for WB2-2 Using Transistor Psychrometer.

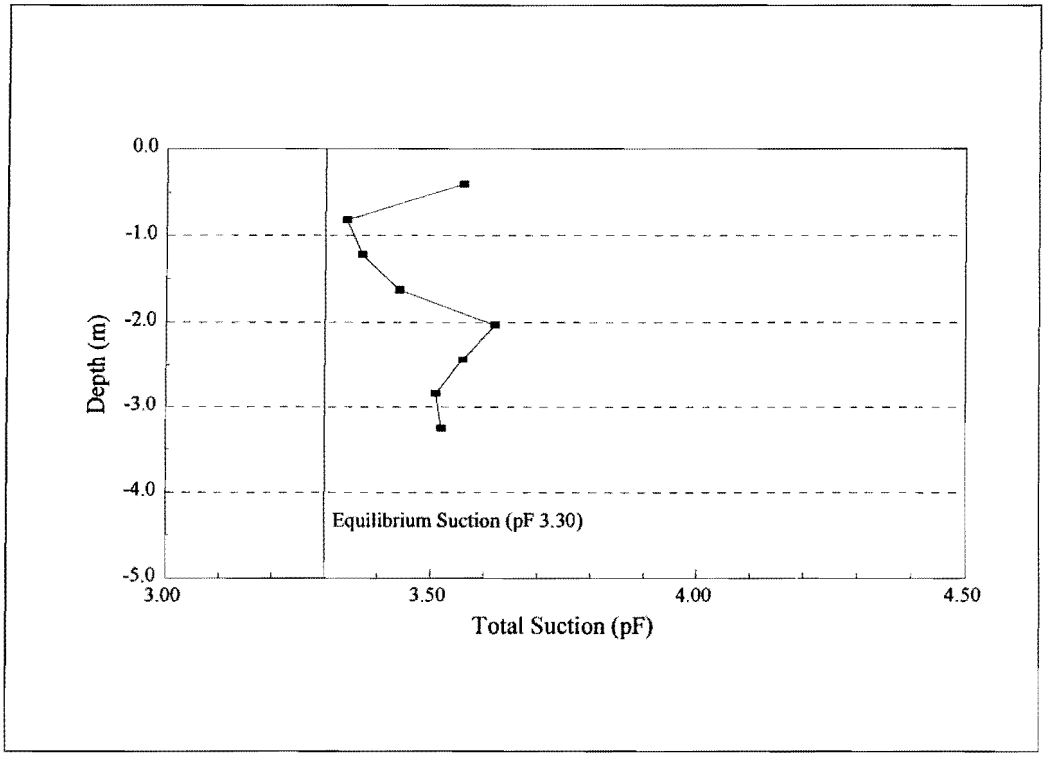


Figure 48. Total Suction Profile for EB1-1 Using Transistor Psychrometer.

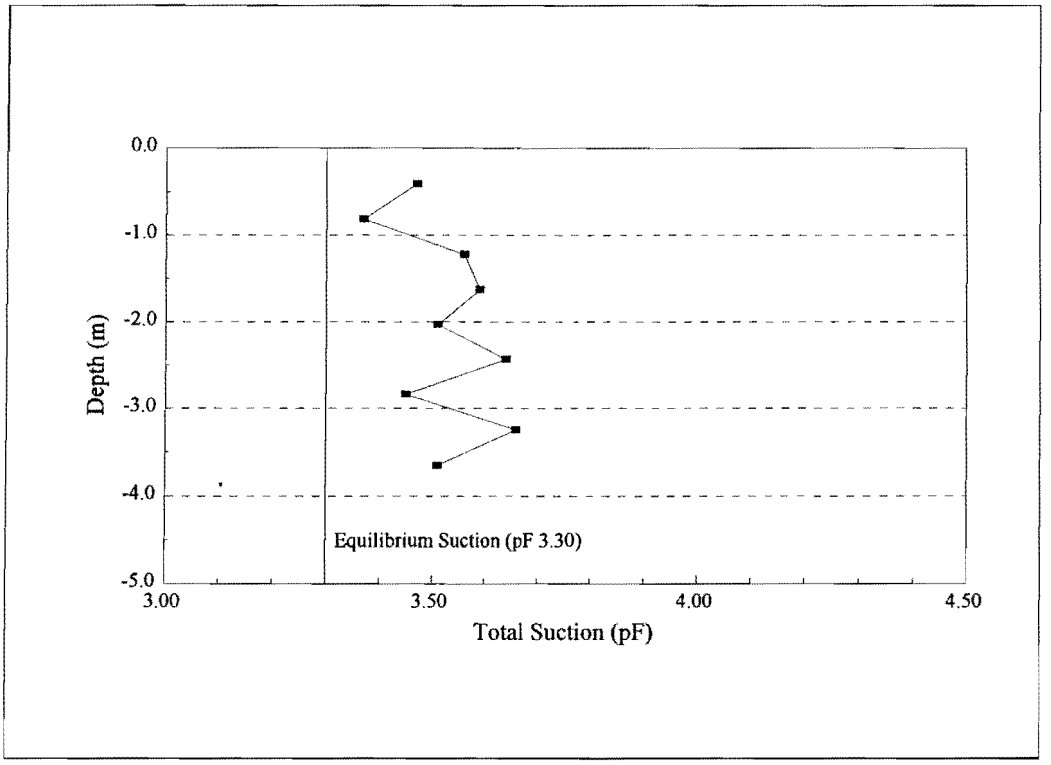


Figure 49. Total Suction Profile for EB1-2 Using Transistor Psychrometer.

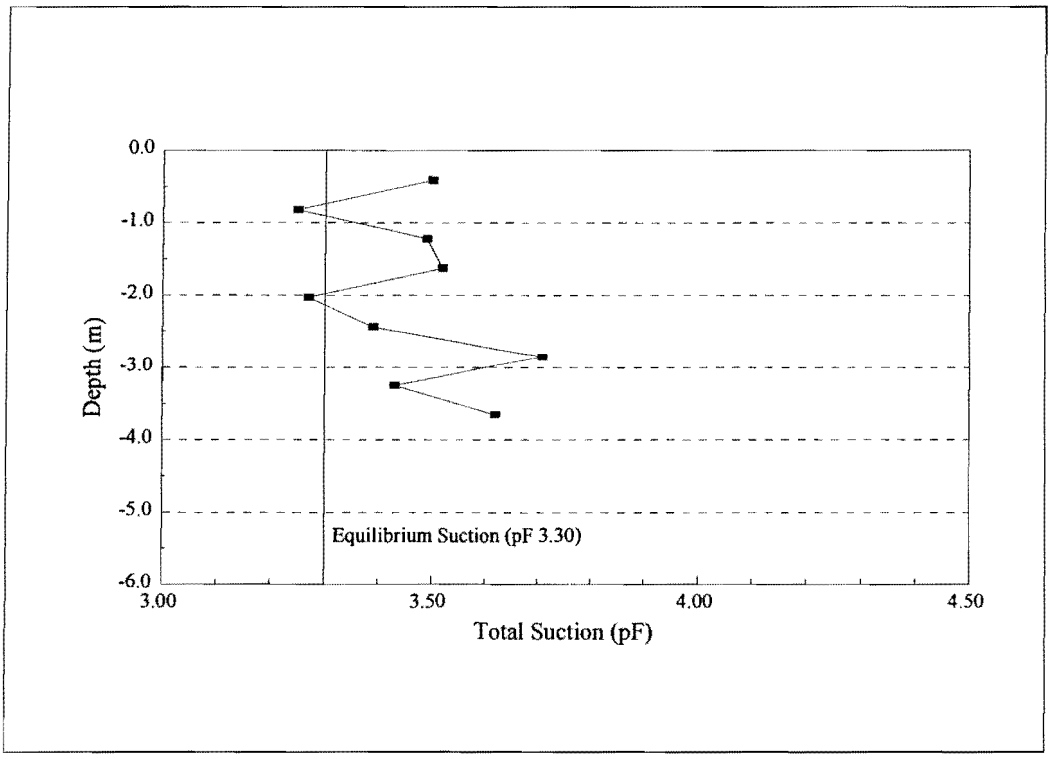


Figure 50. Total Suction Profile for EB1-3 Using Transistor Psychrometer.

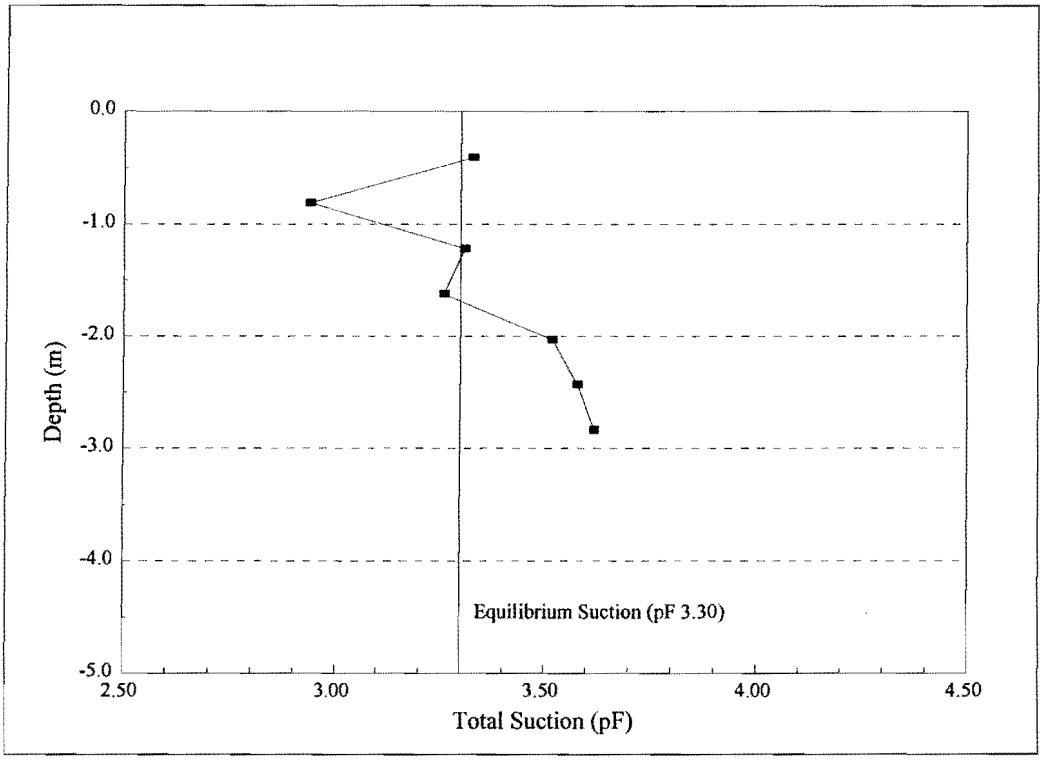


Figure 51. Total Suction Profile for EB1-4 Using Transistor Psychrometer.

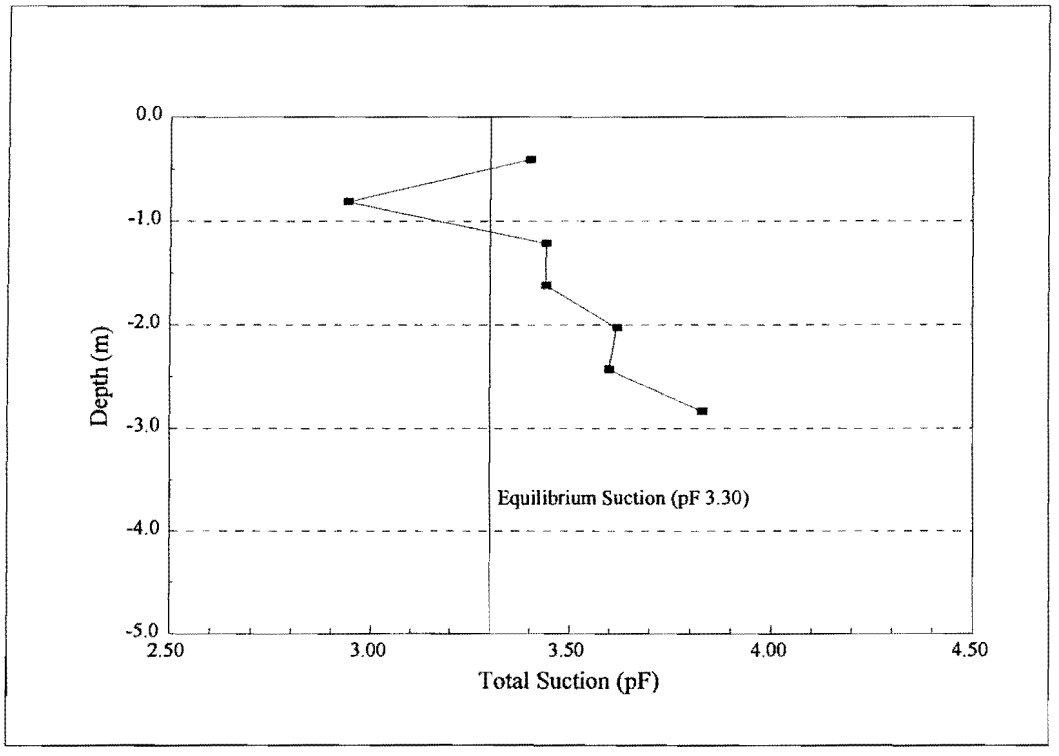


Figure 52. Total Suction Profile for EB1-5 Using Transistor Psychrometer.

Table 48. Estimated Calcium Sulfate at SH 6 Northbound.

| Test Hole | Depth (m) | Osmotic Suction (pF) | Osmotic Suction (cm) | Molar Concentration (moles / liter) | Estimated Calcium Sulfate (mg / l) |
|---|---|---|---|---|---|
| NB1-1 | -0.4 | 3.56 | 3660 | 0.00015 | 20 |
| | -0.8 | 3.19 | 1539 | 0.00006 | 8 |
| | -1.6 | 3.63 | 4228 | 0.00017 | 23 |
| | -2.4 | 3.47 | 2941 | 0.00012 | 16 |
| | -3.3 | 3.68 | 4826 | 0.00019 | 26 |
| NB1-2 | -0.4 | 3.11 | 1275 | 0.00005 | 7 |
| | -1.6 | 3.88 | 7565 | 0.00030 | 41 |
| | -2.4 | 4.09 | 12336 | 0.00050 | 68 |
| | -3.3 | 2.65 | 449 | 0.00002 | 2 |
| NB2-1 | -0.4 | 3.31 | 2060 | 0.00008 | 11 |
| | -1.2 | 3.63 | 4283 | 0.00017 | 23 |
| | -2.0 | 3.09 | 1233 | 0.00005 | 7 |
| | -2.4 | 3.43 | 2708 | 0.00011 | 15 |
| NB2-2 | -0.4 | 3.46 | 2916 | 0.00012 | 16 |
| | -2.0 | 3.48 | 3013 | 0.00012 | 17 |

Table 49. Estimated Calcium Sulfate at SH 6 Southbound.

| Test Hole | Depth (m) | Osmotic Suction (pF) | Osmotic Suction (cm) | Molar Concentration (moles / liter) | Estimated Calcium Sulfate (mg / l) |
|---|---|---|---|---|---|
| SB1-1 | -0.4 | 3.58 | 3785 | 0.00015 | 21 |
| | -1.2 | 3.60 | 3950 | 0.00016 | 22 |
| | -2.0 | 3.44 | 2772 | 0.00011 | 15 |
| | -2.8 | 3.73 | 5322 | 0.00021 | 29 |
| | -3.7 | 3.59 | 3919 | 0.00016 | 21 |
| SB1-2 | -0.4 | 3.60 | 3951 | 0.00016 | 22 |
| | -0.8 | 4.21 | 16243 | 0.00065 | 89 |
| | -2.0 | 3.33 | 2132 | 0.00009 | 12 |
| | -2.4 | 3.38 | 2391 | 0.00010 | 13 |
| | -3.3 | 3.62 | 4196 | 0.00017 | 23 |
| SB1-3 | -0.4 | 2.91 | 805 | 0.00003 | 4 |
| | -1.2 | 3.62 | 4205 | 0.00017 | 23 |
| | -2.0 | 3.47 | 2923 | 0.00012 | 16 |
| | -2.8 | 3.07 | 1180 | 0.00005 | 6 |
| | -3.7 | 3.35 | 2263 | 0.00009 | 12 |
| SB2-1 | -0.8 | 2.66 | 457 | 0.00002 | 3 |
| | -1.2 | 4.05 | 11330 | 0.00046 | 62 |
| | -1.6 | 2.96 | 910 | 0.00004 | 5 |
| SB2-2 | -0.4 | 2.98 | 946 | 0.00004 | 5 |
| | -1.2 | 2.88 | 762 | 0.00003 | 4 |
| | -4.1 | 3.47 | 2942 | 0.00012 | 16 |
| | -4.5 | 3.20 | 1568 | 0.00006 | 9 |

In boring NB1-1, both suction measurement methods indicate an increase of total suction with depth to a value around pF 3.8 to 4.0 at about 3.5 m. The matric suction also increases with depth to a value of about pF 3.7 at 3.5 m depth. The pattern is a classic one showing that the water that is entering this profile is entering from the surface.

The same pattern holds for boring NB1-2 at the foot of the heave. The suction at the surface is smaller than that at depth, indicating that here also, at the foot of the heave, water is also entering the soil profile from the surface. A comparison of the 2 profiles shows that the suction in boring NB1-1 is smaller than that in boring NB1-2, indicating that the soil has heaved more at NB1-1 than at NB1-2. This is consistent with the observed heave pattern.

In boring NB2-1, the total suction and matric suction values increase with depth, indicating once more that water is entering the profile from the surface. The entire suction profile at NB2-1 is wetter than that at boring NB2-2, which was made at the foot of the heave. This is consistent with the observed heave pattern. The matric suction is smaller at the surface than at depth, whereas, the total suction profile in the top meter indicates a recent drying trend.

The borings along the south bound lanes were made with SB1-2 at the peak and SB1-1 and SB1-3 at the feet of the heave. The suction values in all borings indicate an increase with depth, with a peculiar v-shape in the suction pattern beneath the peak of the heave in boring SB1-2. The general pattern of increasing suction with depth indicates water entering the soil from the surface. However, an additional source of moisture is indicated at a 2-m depth in boring SB1-2 beneath the heave peak. This is the typical suction pattern formed by a lens or seam that carries water.

Borings SB2-1 and SB2-2 show that the suction profile beneath boring SB2-2 is wetter than that in boring SB2-1 at the foot of the heave. This is consistent with the observed heave pattern. The suction profile in boring SB2-2 gets larger with depth indicating that water enters this profile from the surface. There is a possibility that cannot be confirmed with the existing data, that there is another source of moisture at about a 4 - 4.5 m depth. This is suggested by the v-shape at that depth in the suction profile in boring SB2-2. If so, this is consistent with water flowing in a granular seam of sand or gravel in a river alluvium. It is too deep to have been seen by the ground penetrating radar survey.

## SUCTION PROFILES FOR THE BORINGS AT THE SH 21 SITE

There were 3 sets of borings on the SH 21 site, 2 along the westbound lanes and 1 set along the eastbound lanes.

One boring, WB1-1 was made to the east of the intersection of SH 21 with FM 1362, and the rest were made to the west of that intersection. The suction pattern in boring WB1-1 (Figure 45) indicates the suction increasing with depth in the top 2 meters and decreasing below that level. Because the suction profile does not continue deeper than 2.5 meters, it is impossible to tell whether the decreasing suction with depth below the 2-meter depth indicates a deep source of water entering the profile or not. The recollection of the crew taking the borings was that the boring was stopped at the 2.5 m depth because of the high stiffness and strength of the soil encountered at that depth. Taking this information as factual, the suction profile in boring WB1-1 is consistent with water entering from the surface with another possible source of water in a seam of the hard, intact soil (called a "clay pan") below the 2 meter level. This water in the intact soil would not contribute to the heave of the soil above the 2 m level. This is because the intact soil is cemented and water penetrates it very slowly, moving with a permeability of 2-3 x $10^{-8}$ cm/sec as noted on Table 46. Thus, the water movement in the profile of boring WB1-1 is from the surface downwards, and the heave is occurring in the upper 2 m.

The suction profiles in borings WB2-1 and WB2-2 in Figures 46 and 47 show that the wetter profile above 1.5 m is WB2-1 and below 1.5 m is clearly WB2-2. The oscillating pattern of suction with depth in boring WB2-1 indicates that the soil above the 2.5 m depth is reflecting the suction changes at the soil surface over the previous 2 wet seasons. The rainfall pattern in this area is bimodal, i.e., there are 2 rainy seasons each year as shown in Figure 12. Peak rainfalls occur in May and September with a dry summer in between. The wet suction values at 0.8 m and 1.5 m depths reflect the rainfall in the previous September and May. The soil in boring WB2-1 responds rapidly to water supplied to it from the roadside ditch. The remainder of the suction profile increases with depth to a depth of 2.5 m indicating that water enters this profile from the surface.

The suction profile in boring WB2-2 (Figure 47) shows clearly the water flowing upward from a source that is below ground level and is likely to be below the 2.5 m depth. Water from this depth will not cause as much heave as will water flowing downward from the surface as in boring WB2-1. It is for this reason that the suction profile of WB2-1 is consistent with the peak of the heave pattern that was observed at the WB2-1 boring. The source of water in the WB2-2 boring does not need to be a lens of granular material. Instead, the total suction at the 2.5 m level is consistent with the equilibrium suction that would be expected from the Thornthwaite Moisture Index relation in Figure 11. It may simply reflect the presence of a soil at the 2.5 m level that is similar to the clay soil used in the original work by Russam and Coleman (1961). If this is so, the suction profile in boring WB2-2 indicates a steady loss of moisture from the soil profile by evaporation and transpiration with only slight alternations due to seasonal wetting and drying. This soil would not heave at all.

The suction profiles for borings EB1-1, EB1-2, EB1-3, EB1-4, and EB1-5 are shown in Figures 48 through 51. The wettest profile is in boring EB1-4 which is consistent with the peak of the observed heave pattern. All of the suction profile patterns are consistent with water entering from the surface, and all show that the borings were made after a drying season which raised the suction in the top 0.8 meters. This is the consistent pattern in borings EB1-1 EB1-4, and EB1-5. The other 2 borings differ from this pattern somewhat and require further description.

The suction profile in boring EB1-3 (Figure 50) is interesting because it shows that there is a source of water at the 2 m depth, in addition to water entering the profile from the surface. Because the measured suction at 2 meters in wetter than the value expected from the Thornthwaite Moisture Index relation of Figure 11, it is a candidate for a granular soils lens that carries water at that depth.

The suction profile in boring EB1-2 oscillates with depth, all suctions being drier than that expected from the Thornthwaite Moisture Index relation of Figure 11. Very likely, the oscillation is real, rather than reflecting experimental error, and it indicates a transient response of the suction to the wetting and drying seasons of the previous 2 years. It also indicates the presence of cracking patterns in the soil capable of carrying water to such depths.

## OSMOTIC SUCTION PROFILES AT THE SH 6 SITE

Tables 48 and 49 give the osmotic suction values that were derived from the filter paper tests on the samples taken at the SH 6 site. These osmotic suction values measure the amount of dissolved salts in the pore water of the soil. The levels of osmotic suction in all of the borings are high, ranging between pF 2.66 in boring SB2-1 and pF 4.21 in boring SB1-2. No correlation could be found between the measured amounts of soluble sulfate in these borings (Tables 49) and the level of the osmotic suction at the same location. This failure to correlate emphasizes the fact that osmotic suction is due to the concentration of all dissolved salts in the pore water and not just due to the presence or absence of soluble sulfate salts.

The osmotic suction is related to the molar concentration of dissolved salts by the Van't Hoff equation as follows:

$$\pi = R\ T\ C$$

where $\pi$ = the osmotic suction, cm,

R = the universal gas constant $8.475 \times 10^4$ ergs / K-mol,

T = the absolute temperature, degrees Kelvin (273 + °C), and

C = molar concentration of dissolved salt (solute), moles per liter.

The osmotic suction (pF) at 25°C is related to the molar concentration of the solute by the following:

$$\log_{10} \pi = pF = 7.40 + \log_{10} C$$

The molar concentration of solute is given by

$$C = \frac{(x)\ \dfrac{gm}{1000\ cm^3}}{(y)\ \dfrac{gm}{mole}}$$

where x = the weight in gm of the substance dissolved in 1000 $cm^3$ of a solution

and y = the molecular weight of the substance in gm/mole.

These relationships were used to construct Tables 48 and 49. An example will illustrate. The osmotic suction in boring NB1-2 at 2.4 m depth is shown in Table 50 to be 12,336 cm. In pF units, this is equal to

$$\log_{10} \pi = 4.09$$

The molar concentration corresponding to the osmotic suction is

$$C = \frac{\pi}{RT}$$

$$C = \frac{12{,}336\ cm}{8.475x10^4 \frac{erg}{k\text{-}mol} \times 273+25°C}$$

$$C = 48.8 \times 10^{-5} \frac{moles}{liter}$$

If all of the osmotic suction were due to dissolved calcium sulfate (gypsum), calcium sulfate in milligrams per liter is given by

$$= 48.8 \times 10^{-5} \frac{moles}{liter} \times 136.14 \times 10^3 \frac{mg}{mole}$$

$$= 66.5 \frac{mg}{liter}$$

The molecular weight of calcium sulfate is 136.14 gm/mole.

Tables 48 and 49 were constructed using the calculations presented in detail above. There is no consistent pattern of osmotic suction with depth, although some general statements can be made. In borings NB1-1, NB2-1, NB2-2, SB1-1, and SB1-3, the osmotic suction is nearly constant with depth. This indicates that there has not been much leaching of the salts by water permeating into the soil profile from the top or from the side.

Borings NB1-2, SB1-2, and SB2-1 all have a very high osmotic suction at some depth below the surface. The borings and the depths of the high osmotic suction measurement are listed below.

| Boring No. | Depth to the High Osmotic Suction, m |
|---|---|
| NB1-2 | 2.4 |
| SB1-2 | 0.8 |
| SB2-1 | 1.2 |

These high osmotic readings indicate the presence of large amounts of soluble salts in the soil. The high osmotic suction in boring NB1-2 roughly coincides with the depth at which seams of gypsum were found in that boring. High osmotic suction values near the surface, as in borings SB1-2 and SB2-1, may be due to salts that have been left behind when water was evaporated. Borings SB1-3, SB2-1, and SB2-2 have small values of osmotic suction near the surface which become larger with depth. This pattern clearly indicates leaching of the salts by water entering the soil profile from the surface and percolating downward.

Because the values of osmotic suction are found by subtracting the matric suction from the total suction, both measured by filter paper, and both subject to experimental error, it is prudent not to try to stretch the interpretation of the osmotic suction results too far. The interpretations of the osmotic suction profiles presented above are valid not simply because of the shape of the profile but also because they are corroborated by observations made at the time of sampling and of the sample appearance in the laboratory.

# CHAPTER 5
# CONCLUSIONS AND RECOMMENDATIONS

## RECOMMENDED REMEDIAL ACTION FOR SH 6 SITE

At the SH 6 site, the soil has a large amount of soluble sulfate, a high suction level, and a high osmotic suction level. Water is entering the soil profile from the surface due to water in the drainage ditches and median. The greatest heaves occur in the soil mass at those locations where the soil is most highly cracked, where water has more rapid access to greater depths, and where suction has changed more than elsewhere.

The moisture active zone at the SH 6 site varies between depths of 2.4 and 3.0 m, and the heaving takes place to a depth of 1.8 to 2.2 m. The heaving and pavement roughness will continue to appear for many years to come because the suction values in the soil profile are, in no instance except boring SB2-1, as wet as the soil can become (pF 2.5). The only way to arrest the heave is by identifying the source of the water and cutting it off. Because the water is entering beneath the pavements from the side ditches and medians, sealing these is the most practical way to stabilize these pavements against uncontrolled further movements. Because of the depth to which moisture penetrates below the ground surface, it is not considered possible to shut off all of the flow of moisture with a vertical moisture barrier.

Instead, sealing the entire median and the side ditches to a distance of 4.0 m beyond the flow line of the ditch will provide the necessary protection of the pavement. Because of the high levels of soluble sulfate in the soil, it would be unwise to use lime stabilization in any remedy used along the SH 6 site. As a less preferred alternative, a vertical moisture barrier can be installed at the edge of the paved shoulder to a depth of 2.4 m, both on the inside and outside of the pavement surface. As a hybrid alternative that is also less preferred, the median could be sealed *and* vertical barriers could be placed along the outside edge of the shoulders in each direction.

## RECOMMENDED REMEDIAL ACTION FOR SH 21 SITE

The SH 21 site is a highly variable stratified expansive soil about 2.0 m deep over a hard clay pan. All of the heave occurs in the top 2.0 m, and none occurs in the cemented clay pan

beneath it. Water that is carried in the roadside ditches and medians enters the soil profile and percolates downward until it reaches the clay pan. At that point, it stops and runs laterally on top of the clay pan and beneath the pavement where it causes highly variable heaves, reflecting the variability of the soil along the road. There is insignificant soluble sulfate in the soils along this road. The suction profiles along this road indicate that the water is being carried beneath the pavement along the slope of the clay pan and in the occasional granular layers that are interbedded with the clay.

Shutting off this flow of water is most conveniently done with a vertical barrier that is carried down to and tied into the intact clay pan at depths of 1.5 to 2.0 m. The barriers should be placed on the edge of the paved shoulders on both sides of each paved surface. Paving or sealing the medians and roadside drainage ditches will probably be a more costly solution at this site and less successful because of the horizontal flow on the surface of the hard clay pan.

## SITE INVESTIGATION PROCEDURE

For identifying soil profiles with the potential of causing pavement distortion, site investigation is a crucial step toward the selection of correct construction and rehabilitation techniques. Before pavement construction on or stabilization of expansive soils, detailed information on potential causes of roughness might provide feasible solutions at specific sites.

To begin the site investigation, existing information on the project areas should be reviewed. Geological survey maps and USDA county soil survey reports are valuable sources of information. Soil survey reports are rich in pedological data and provide basic geology of the particular area, detailed descriptions of the soil profiles, chemical and physical properties of soils, engineering classification, and index properties for the major layers of soils. Soil survey reports are an excellent source for estimating the applicability of ground penetrating radar (GPR). After reviewing the soil information, a site reconnaissance should be planned and conducted. Based on this field trip, the drainage condition of the area, slope condition, along with any cracking or undulating patterns of pavements should be observed and reported. If a planned site is suspected of having high salt concentrations, the soil should be tested using the electrical conductivity tool kit. This method was developed by Bredenkemp et al. (1993) to estimate salt contents in soils planned for stabilization. The electrical conductivity method

is very efficient when detailed investigations are necessary because a large area can be covered quickly. If high electrical conductivity values are encountered and the soil is to be stabilized with lime or cement, the soluble sulfate content of the soil should be measured. A certain level of sulfate (probably greater than 0.2%) in soils may induce a pavement heaving problem.

Before planning soil sampling, GPR can be very revealing. GPR shows where and how deep various soil layers are located. Successful GPR surveys can locate discontinuities such as lenses or seams in soils. A preliminary step for a GPR survey is to determine whether site conditions are suitable. Under certain conditions, interpretation of a GPR survey in deeper soil layers may be limited due to problems such as high clay content and high salt concentration of soils. In Texas, various amounts of dissolved salts are often found at the tops of certain soil layers.

Soil boring and sampling should be strategically planned based on the information obtained from a GPR survey or field trip. The location and depth of each boring should be strategically selected to identify the potential problem areas. To obtain undisturbed samples, Shelby thin-walled tube or equivalent samplers should be used. Undisturbed samples are used for determination of soil suctions, water contents, and in situ density in soils. Loss of moisture from field cores must be minimized. The following details should be reported on a boring log in the field:

- Location and boring number,
- Date of boring,
- Elevation of the ground surface,
- A detailed description of each stratum,
- The level at which boring was terminated, and
- Any unusual condition noted.

Soil suction tests using filter paper or the transistor psychrometer are essential for identifying the moisture activity in soils. A soil suction profile shows which direction soil water is migrating. A transistor psychrometer is capable of measuring the total suction in 1

hour. The filter paper method can measure both the total and the matric suction, but it takes 7 to 10 days. Equilibrium suction can also be estimated from Figure 11 using the Thornthwaite moisture index (Russam et al. 1961). Based on Figure 53, each suction profile can be interpreted using an equilibrium suction line. The equilibrium suction line reveals whether the soil condition is dry or wet when compared to measured suctions at a specific site. If high osmotic suction is found in the suction profile, sulfate contents should be measured.

To estimate the flow properties of the soil, the following laboratory tests are required:

- Atterberg limits (liquid limit and plastic limit),
- Water content,
- % finer than 75 μm, and
- % finer than 2 μm.

To determine the fine clay content, a particle size analyzer is recommended. It can more accurately determine the particle size distribution of fine-grained soils than the conventional hydrometer test, as discussed in Chapter 2. Using the relationship between the activity and cation exchange activity of soils, the suction compression index can be estimated. The diffusion coefficient and unsaturated permeability of soils should also be estimated. This is important to determine how deep and how wide to place a vertical moisture barrier or other drainage system.

Using the previously described site investigation information, determine the proper remedial actions.

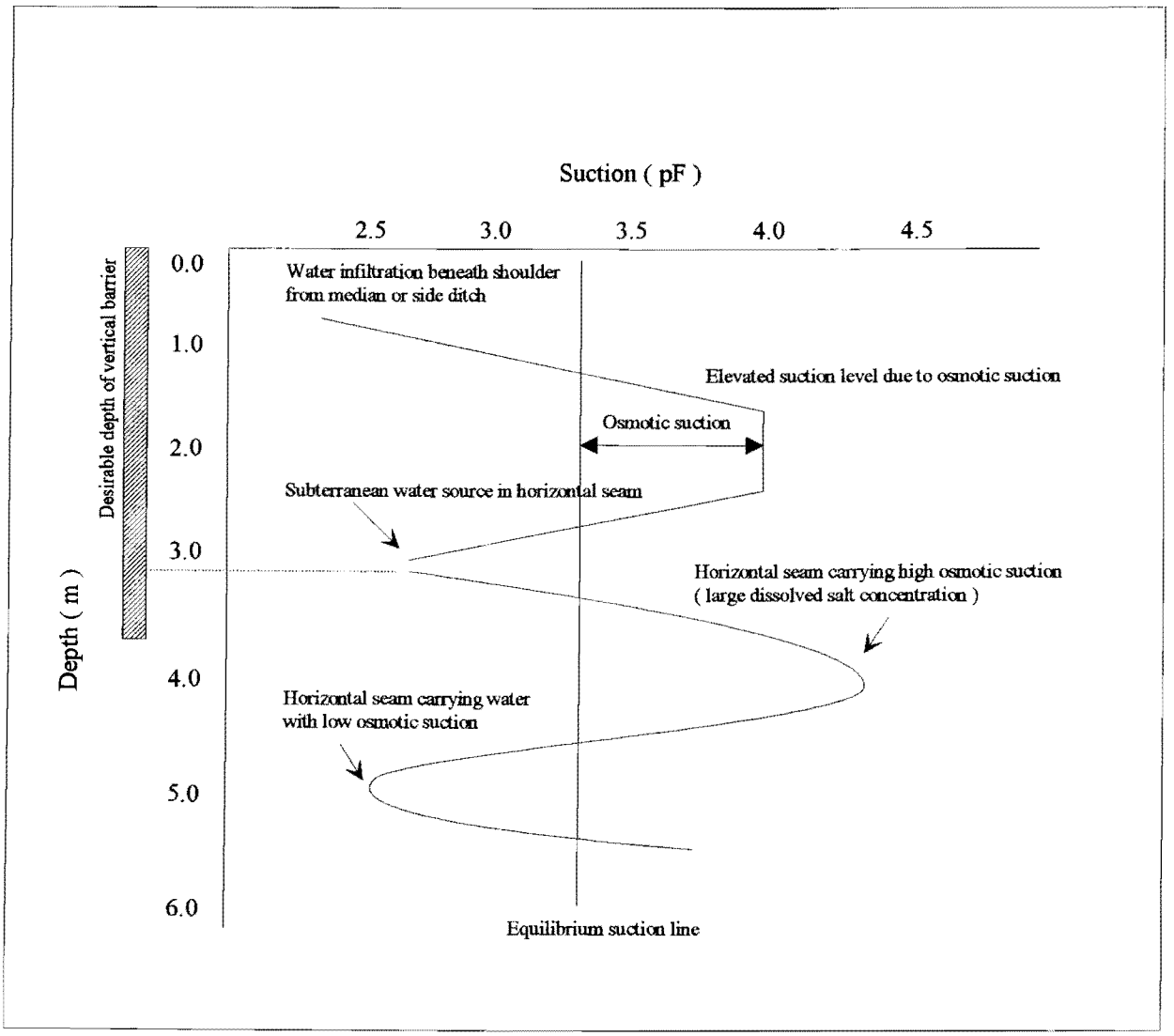


Figure 53. Interpretation of Total Suction Profile with Equilibrium Suction Line.

## STABILIZATION OF SULFATE BEARING SOILS

Currently, several approaches are available for reducing or controlling sulfate-induced swell of soils during lime or cement stabilization. The following suggestions are offered:

1. Double applications of lime - Soil with low sulfate contents may be stabilized by double applications of lime along with high water contents. The ettringite is formed after the first application of lime, and then the second application of lime provides strength and decreased swell potential of the soils. A total lime content of about 6% is suitable using 2 applications of 3% each with at least 21 days between. Sufficient water is required to solubilize the sulfate to permit reaction with the soluble aluminate from the clay and with the calcium from the lime to form ettringite during the delay period.
2. Prewetting and mellowing - A mixing water content about 3% to 5% above optimum and mellowing for a period of 7 days before compaction will reduce subsequent swell.
3. Low calcium stabilizers - Low calcium fly ash and other commercial products will minimize the amount of expansion of clay soils with relatively high sulfate contents.
4. Pretreatment with barium compounds - Pretreating soils with barium hydroxide and barium chloride reduces the amount of soluble sulfates by chemically changing them to insoluble minerals. Therefore, the formation of ettringite is diminished. Swells have been reduced over 20% using this pretreatment method.
5. Pretreatment with potassium-based chemicals - Pretreatment of sulfate bearing soils with potassium-based chemicals (potassium salt compounds) involves saturating the soil mass with potassium ions which form a permanent, irreversible chemical bond with the clay minerals. This chemical change in the clay mineral prevents water ions from migrating between the silica sheets and thus limits the expansion of clay soils when exposed to water.

# REFERENCES


1. Allen, T., Particle Size Measurement, 3rd Ed., Chapman and Hall, New York, NY, 1981.

2. Annan, A.P., Ground-Penetrating Radar Workshop Notes, Sensors and Software Inc., Ontario, Canada, 1992.

3. Ayhan, S.R., "Design and Development of a Laboratory Suction Measuring Device," Master's Thesis, Texas A&M University, College Station, TX, 1996.

4. Barr, G.L., "Application of Ground-Penetrating Radar Methods in Determining Hydrogeologic Conditions in a Karst Area, West-Central Florida," Water-Resources Investigations, Report 92-4141, U.S. Geological Survey, Tallahassee, FL, 1993.

5. Beres, M., Jr. and F.P. Haeni, "Application of Ground-Penetrating Radar Methods in Hydrogeologic Studies," Ground Water, Vol. 29, No. 3, 1991, pp. 375-386.

6. Black, K. and P. Kopac, "The Application of Ground-Penetrating Radar in Highway Engineering," Public Roads, 1992, pp. 96-103.

7. Bredenkamp, S. and R.L. Lytton, "Reduction of Sulfate Swell in Expansive Clay Subgrades in the Dallas District," TTI Report TX-94/1994-5, Texas Transportation Institute, Texas A&M University, College Station, TX, 1994.

8. Davis, J.L. and A.P. Annan, "Ground-Penetrating Radar for High Resolution Mapping of Soil and Rock Stratigraphy," Geophysical Prospecting, No. 37, 1989, pp. 531-551.

9. Daniel, J.J., "Fundamentals of Ground-Penetrating Radar," Proceedings of the Symposium on the Application of Geophysics to Engineering and Environmental Problems, The Society of Engineering & Mining Exploration Geophysicists, 1989.

10. Doolittle, J.A. and R.A. Rebertus, "Ground-Penetrating Radar as Means of Quality Control for Soil Surveys," Transportation Research Record, No. 1192, Transportation Research Board, National Research Council, Washington, D.C., 1988.

11. Environmental Protection Agency, "Methods for the Chemical Analysis of Water and Waste," EPA 600/A-79-020, 1979.

12. Ferris, G.A., J.L. Eades, G.H. McClellan, and R.E. Graves, "Improved Characteristics in Sulfate Soils Treated with Barium Compounds Before Lime Stabilization," Transportation Research Record, No. 1295, Transportation Research Board, National Research Council, Washington, D.C., 1991.

13. Fredlund, D.G. and H. Rahardjo, Soil Mechanics for Unsaturated Soils, John Wiley, New York, NY, 1993.

14. The Finnish Geotechnical Society, Ground Penetrating Radar: Geophysical Research Methods, The Finnish Building Center, Ltd., 1992.

15. Gardner, W. R., "Some Steady State Solutions of the Unsaturated Moisture Flow Equation with Application to Evaporation from a Water Table," Soil Science, 85, 1958, pp. 228-232.

16. Hayward Baker, Inc., Personal Communication, Ft. Worth, TX, 1996.

17. Holtz, R.D. and W.D. Kovac, An Introduction to Geotechnical Engineering, Prentice - Hall, Englewood Cliffs, NJ, 1981.

18. Hunter, D., "Lime-Induced Heave in Sulfate-Bearing Clay Soils," Journal of Geotechnical Engineering. Vol. 114, No. 2, 1988, pp. 150-167.

19. Jayatilaka, R., D.A. Gay, R.L. Lytton, and W.K. Wray, "Effectiveness of Controlling Pavement Roughness Due to Expansive Clays with Vertical Moisture Barriers," Texas Transportation Institute, Research Report No. FHWA/TX-92/1165-2F, Texas A&M University, College Station, TX, 1993.

20. O'Kane, M., "Soil Suction and Soil Water Content," University of Saskatchewan, Saskatoon, Canada, 1996.

21. Kutrubes, D.L ., "Dielectric Permittivity Measurement of Soils Saturated with Hazardous Fluids," M.S. Thesis, Colorado School of Mines, Golden, CO, 1986.

22. Lambe, T.W., Soil Testing for Engineers, BiTech Pub. , Vancouver, B.C., Canada, 1991.

23. Lee, H.C. and W.K. Wray, "Techniques to Evaluate Soil Suction - a Vital Unsaturated Soil Water Variable," Proceedings of the First International Conference on Unsaturated Soils, Paris, France, 1995, pp. 615-622.

24. Little, D.N., "GSM Calcium Sulfate as an Embankment Material," Texas Transportation Institute, Texas A&M University, College Station, TX, 1987.

25. Little, D.N. and T.M. Petry, "Recent Developments in Sulfate-Induced Heave in Treated Expansive Clays," Proceedings of the Second Interagency Symposium on Stabilization of Soils and Other Materials, 1992, pp. 5-18.

26. Lytton, R.L., "Foundations in Expansive Soils," Numerical Methods for Geotechnical Engineering, C.S. Desai and J.T. Christian, eds., McGraw-Hill Co., New York, NY, 1977.

27. Metha, P.K. and A. Klein, "Investigations on the Hydration Products in the System 4 $CaO \cdot 3Al_2O_3 \cdot SO_3 - Ca\,SO_4 - CaO - H_2O$," Special Report 90, Highway Research Board, National Research Council, Washington, D.C., 1966, pp. 328-352.

28. Michelson, R.C., Ground Penetration Radar Study, Georgia Tech. Research Institute, Atlanta, GA, 1985.

29. Mitchell, J.K., "Practical Problems from Surprising Soil Behavior," Journal of Geotechnical Engineering, Vol. 112, No. 3, 1986, pp. 259-289.

30. Mitchell, P.W., The Structural Analysis of Footings on Expansive Soil, Kenneth W.G. Smith & Associate, Research Report No. 1, Adelaide, Australia, 1980.

31. Mojekwu, E.C., "A Simplified Method for Identifying the Predominant Clay Mineral," M.S. Thesis, Texas Tech University, Lubbock, TX, 1979.

32. Nelson, J. D. and D. J. Miller, Expansive Soils: Problems and Practice in Foundation and Pavement Engineering, John Wiley, New York, NY, 1992.

33. Nyangaga, F.N., R.L. Lytton, and D.A. Gay, "Effect of Vertical Moisture Barriers on Roughness Development of Pavements on Expansive Soils," Proceedings of the First International Conference on Unsaturated Soils, Paris, France, 1995, pp. 991-998.

34. Petry, T.M. and D.N. Little, "Update on Sulfate-Induced Heave in Treated Clays: Problematic Sulfate Level," Transportation Research Record, No. 1362, Transportation Research Board, National Research Council, Washington, D.C., 1992, pp. 51-55.

35. Picornell, M., "The Development of Design Criteria to Select the Depths of a Vertical Barrier," Ph.D. Dissertation, Texas A & M University, College Station, TX, 1985.

36. Post-Tensioning Institute, Design and Construction of Post-Tensioning Slabs On - Ground, Phoenix, AZ, 1980.

37. Rhoades, J.D. and A.D. Halvorson, "Electrical Conductivity Methods for Detecting and Delineating Saline Seeps and Measuring Salinity in Northern Great Plains Soils," Agriculture Research Service W-42, United States Department of Agriculture, 1977.

38. Richards, L.A., L.E. Allison, L. Bernstein, C.A. Bower, and J.W. Brown, "Diagnosis and Improvement of Saline and Alkine Soils," Agriculture Handbook, No.60, United States Department of Agriculture, 1954.

39. Russam, K. and J.D. Coleman, "The Effect of Climate Factors on Subgrade Moisture Conditions," Geotechnique, Vol. 11, No. 1, 1961, pp. 22-28.

40. Saarenketo, T. and T. Scullion, "Ground Penetrating Radar Applications on Roads and Highways," Texas Transportation Institute, Research Report No. TX-95/1923-2F, Texas A&M University, College Station, TX , 1994.

41. Soil Survey of Brazos County, Texas, United States Department of Agriculture, Soil Conservation Service, 1981.

42. Soil Survey of Burleson County, Texas, United States Department of Agriculture, Soil Conservation Service, 1996.

43. Sutinen, R., "Glacial Deposits, Their Electrical Properties and Surveying by Image Interpretation and Ground Penetrating Radar," Geological Survey of Finland, Bulletin 359, 1992.

44. Texas Department of Transportation, "Laser Diffraction Particle Size Distribution Analyzer," TEX-238-F, Manual of Testing Procedures, Vol. 2, 1996.

45. Transportation Research Board, Advanced Technology Particle-Size Analyzer to Soil Sizing and Characterization, 1996.

46. Transportation Research Circular 180, State of the Art: Lime Stabilization, Transportation Research Board, National Research Council, Washington, D.C., 1976.

47. Ulriksen, C.P.F., "Application of Impulse Radar to Civil Engineering," Doctoral Thesis, Lund University of Technology, Department of Engineering Geology, 1982.

48. U.S. Geological Survey, "Geological Map of Brazos and Burleson Counties," United States Department of Interior.

49. Woodburn, J. , J. Holden, and P. Peter, "The Transistor Psychrometer: A New Instrument for Measuring Soil Suction," Unsaturated Soils , W.K. Wray and S.L. Houston, eds., American Society of Civil Engineers, New York, NY, 1993.

# APPENDIX A
# Locations of SH 6 and SH 21 Sites


SH 6 sites
BRYAN
COLLEGE STATION

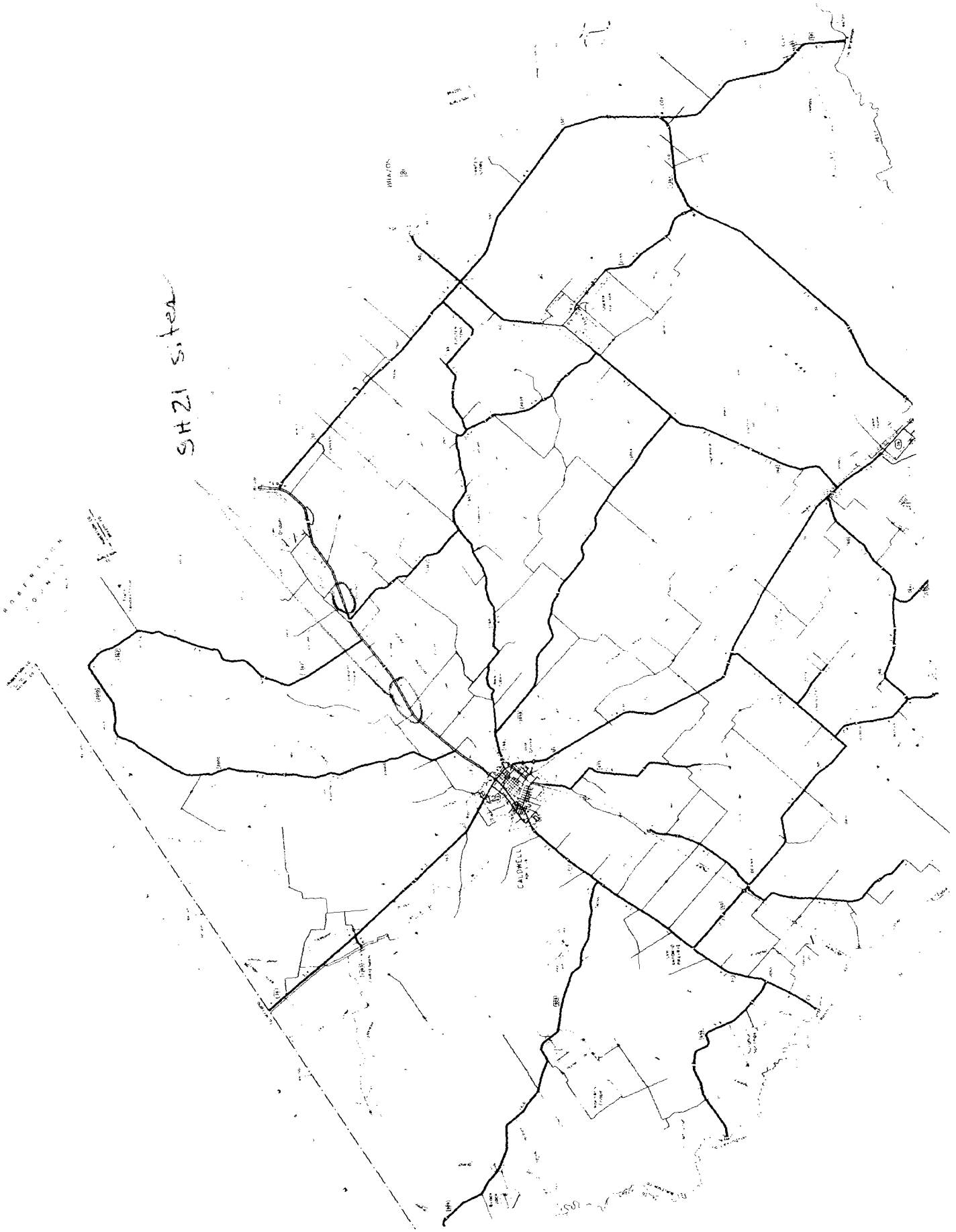
SH 21 site
CALDWELL

# APPENDIX B
# Borehole Log of SH 6 and SH 21 Sites

SH 21 Boring Number WB1 - 1

| Elevation 104.2 (m) | Stradum Depth (m) | Visual Soil Description | Sampling Depth (m) | Remarks |
|---|---|---|---|---|
| | | Tan clay (CL - CH) | 0.2 | |
| | 0.4 | Tan yellow clay (CH) | | |
| 103.6 | | | 0.6 | |
| | 0.6 | Brown clay (CH) | | |
| | | | 1.0 | |
| | 1.2 | | | |
| 102.7 | | Brown/gray clay (CH) | 1.4 | Notes: |
| | | | | Shelby thin - walled |
| | | | 1.8 | tube sampler |
| | 2.0 | Brown stiff clay (CH) | | (10.2 cm dia.) |
| | | | 2.2 | |
| 101.8 | | | | |
| | 2.4 | Boring terminated at 2.43 m | | |

Date drilled: March 11, 1996
Location: 1.77 km east from FM 1362 south

SH 21 Boring Number WB2 - 1

| Elevation 110.8 (m) | Stradum Depth (m) | Visual Soil Description | Sampling Depth (m) | Remarks |
|---|---|---|---|---|
| | | Tan brown clay (CH) | 0.1 | |
| | 0.2 | | | |
| 110.3 | | Brown/yellow clay (CH) | 0.3 | |
| | 0.6 | | | |
| | | Brown silty clay (CH) | 1.0 | |
| | 1.2 | | | |
| 109.4 | | Tan yellow clay with iron ore (CH) | 1.4 | Notes: Shelby thin - walled |
| | 1.55 | Sand seam | | tube sampler |
| | 1.62 | Brown silty clay (CH) | | (10.2 cm dia.) |
| | | | 1.8 | |
| | | | 2.3 | |
| 108.2 | | | 2.7 | |
| | 2.8 | Boring terminated at 2.83 m | | |

Date drilled: March 11, 1996
Location: 1.13 km west from FM 1362 north

SH 21 Boring Number WB2 - 2

| Elevation 110.1 (m) | Stradum Depth (m) | Visual Soil Description | Sampling Depth (m) | Remarks |
|---|---|---|---|---|
| | | Dark brown clay (CH) | 0.2 | |
| 109.4 | 0.4 | | | |
| | | | 0.6 | |
| | | Brown silty clay (CH) | | |
| | | | 1.0 | |
| 108.8 | | | | |
| | | | 1.4 | Notes: |
| | | | | Shelby thin - walled |
| | | | 1.8 | tube sampler |
| | | | | (10.2 cm dia.) |
| 107.9 | | | 2.2 | |
| | 2.4 | | | |
| | | Boring terminated at 2.43 m | | |

Date drilled: March 11, 1996
Location: 1.13 km west from FM 1362 north

SH 21 Boring Number EB1 - 1

| Elevation 128.6 (m) | Stradum Depth (m) | Visual Soil description | Sampling Depth (m) | Remarks |
|---|---|---|---|---|
| | | Brown stiff clay ( OL ) | 0.2 | |
| 128.0 | 0.4 | Tan clay ( CH ) | 0.6 | |
| | | | 1.0 | |
| | 1.2 | Tan brown clay ( CH ) | | |
| 127.1 | | | 1.4 | Notes: |
| | 1.6 | Dark gray clay ( CH ) | 1.8 | Shelby thin - walled tube sampler (10.2 cm dia.) |
| 126.5 | | | | |
| | | | 2.2 | Trace iron ore at 2.3 m |
| | 2.3 | Brown/gray clay ( CH ) | | |
| 125.9 | | | 2.7 | |
| | 2.7 | Brown clay ( CH ) | 3.0 | |
| 125.3 | | | | |
| | 3.3 | Boring terminated at 3.3 m | | |

Date drilled: March 6, 1996
Location: 5.31 km west from FM 1362 north

SH 21 Boring Number EB1 - 2

| Elevation 128.5 (m) | Stradum Depth (m) | Visual Soil Description | Sampling Depth (m) | Remarks |
|---|---|---|---|---|
| | | | 0.7 | |
| | | Black clay (CH) | 1.9 | |
| 127.7 | | | | |
| | | | 3.4 | |
| | | | 4.7 | |
| 126.8 | | | | |
| | | | 5.9 | |
| | 2.1 | | 7.3 | |
| 126.2 | | Brown/yellow clay (CH) | | Iron ore at 2.3 m |
| | | | 8.7 | |
| 125.6 | | | | |
| | | | 10.0 | |
| | | | | Notes: |
| 124.7 | 3.7 | | 11.3 | Shelby thin - walled tube sampler (10.2 cm dia.) |
| | | Boring terminated at 3.7 m | | |

Date drilled: March 7, 1996
Location: 5.31 km west from FM 1362 north

SH 21 Boring Number EB1 - 3

| Elevation 128.4 (m) | Stradum Depth (m) | Visual Soil Description | Sampling Depth (m) | Remarks |
|---|---|---|---|---|
| | | Tan brown clay (CL) | 0.2 | |
| | 0.4 | | | |
| 127.7 | | Dark brown clay (CL) | 0.6 | |
| | 1.0 | Tan brown/gray clay (CH) | 1.0 | |
| | | | 1.4 | |
| | 1.6 | Brown/gray clay (CH) | 1.8 | |
| 126.5 | 2.0 | Brown silty clay (CH) | | |
| | | | 2.2 | |
| | | | 2.7 | |
| 125.6 | | | | |
| | | | 3.0 | |
| | 3.2 | Brown/gray clay (CH) | | |
| 125.0 | | | 3.4 | Notes: Shelby thin - walled tube sampler (10.2 cm dia.) |
| | 3.7 | | | |
| | | Boring terminated at 3.7 m | | |

Date drilled: March 7, 1996
Location: 5.31 km west from FM 1362 north

SH 21 Boring Number EB1 - 4

| Elevation 128.0 (m) | Stradum Depth (m) | Visual Soil Description | Sampling Depth (m) | Remarks |
|---|---|---|---|---|
| | | | 0.2 | |
| 127.4 | | Tan gray clay (CL) | 0.6 | |
| | 0.9 | | | |
| | | Brown yellow clay (CH) | 1.0 | |
| 126.5 | | | 1.4 | |
| | 1.6 | Brown silty clay (CH) | | |
| | | | 1.8 | |
| 125.9 | 2.0 | Brown/yellow clay with gravel (CH) | 2.2 | |
| | 2.4 | Brown stiff clay with iron ore (CH) | | Notes: |
| 125.3 | | | 2.7 | Shelby thin - walled tube sampler (10.2 cm dia.) |
| | 2.8 | | | |
| | | Boring terminated at 2.8 m | | |

Date drilled: March 8, 1996
Location: 5.31 km west from FM 1362 north

SH 21 Boring Number EB1 - 5

| Elevation 127.4 (m) | Stradum Depth (m) | Visual Soil Description | Sampling Depth (m) | Remarks |
|---|---|---|---|---|
| | | | 0.2 | |
| | | Black clay (CL) | | |
| 126.8 | | | 0.6 | |
| | 0.8 | | | |
| | | Brown/yellow clay (CL) | 1.0 | |
| | | | | |
| | | | 1.4 | |
| 125.9 | 1.6 | | | |
| | | Brown silty clay (CH) | | |
| | | | 1.8 | |
| | | | | |
| | | | 2.2 | |
| 125.0 | | | | |
| | | | 2.7 | Notes: |
| | | | | Shelby thin - walled |
| | 3.3 | | | tube sampler |
| 124.1 | | Boring terminated at 3.3 m | | (10.2 cm dia.) |

Date drilled: March 8, 1996
Location: 5.31 km west from FM 1362 north

SH 6 Boring Number NB1 - 1

| Elevation 108.8 (m) | Stradum Depth (m) | Visual Soil Description | Sampling Depth (m) | Remarks |
|---|---|---|---|---|
| | | Black/brown silty clay (CL) | 0.2 | |
| | 0.4 | | | |
| 108.2 | | Tan gray silty clay (CL) | 0.6 | |
| | | | 1.0 | |
| | 1.1 | | | |
| 107.3 | | Brown/gray with sand (CH) | 1.4 | |
| | 1.6 | | | |
| | | Brown silty clay with sand (CH) | 1.8 | |
| | 2.0 | | | |
| 106.4 | | Brown/gray clay with sand (CH) | 2.2 | |
| | | | 2.7 | Notes: Shelby thin - walled |
| 105.8 | | | 3.0 | tube sampler (10.2 cm dia.) |
| | 3.3 | | | |
| | | Boring terminated at 3.3 m | | |

Date drilled: May 29, 1996
Location: 2.25 km north from FM 2818

SH 6 Boring Number NB1 - 2

| Elevation 108.3 (m) | Stradum Depth (m) | Visual Soil Description | Sampling Depth (m) | Remarks |
|---|---|---|---|---|
| | | | 0.2 | |
| | | Tan gray silty clay w/ sand (CL) | | |
| 107.6 | | | 0.6 | |
| | 1.0 | Brown silty clay (CL - CH) | | |
| | | | 1.0 | |
| | 1.2 | Tan brown silty clay with sand (CL - CH) | | |
| | | | 1.4 | |
| 106.7 | 1.6 | Tan gray silty clay (CH) | | |
| | | | 1.8 | |
| | 2.0 | | | |
| 106.1 | | Tan brown stiff clay with sand and gypsum (CH) | 2.2 | |
| | | | 2.7 | Notes: Shelby thin - walled |
| | | | 3.0 | tube sampler |
| 105.2 | 3.3 | Boring terminated at 3.3 m | | (10.2 cm dia.) |

Date drilled: May 29, 1996
Location: 2.25 km north from FM 2818

SH 6 Boring Number NB2 - 1

| Elevation 103.7 (m) | Stradum Depth (m) | Visual Soil Description | Sampling Depth (m) | Remarks |
|---|---|---|---|---|
| | | Brown silty clay w/ gypsum (CH) | 0.2 | |
| | 0.4 | | | |
| 103.0 | | Tan gray clay w/ gypsum (CH) | 0.6 | |
| | 0.8 | | | |
| | | Tan brown clay w/ gypsum (CH) | 1.0 | |
| 102.1 | | | 1.4 | |
| | | | 1.8 | |
| | 2.0 | Gray clay with sand (CH) | | |
| | 2.1 | | | |
| 101.5 | | Brown/gray clay w/ sand (CH) | 2.2 | |
| | 2.4 | | | |
| | | Tan brown clay (CH) | 2.7 | Notes: Shelby thin - walled |
| 100.6 | | | 3.0 | tube sampler (10.2 cm dia.) |
| | 3.7 | | | |
| | | Boring terminated at 3.7 m | | |

Date drilled: May 29, 1996
Location: 1.13 km south from OSR

SH 6 Boring Number NB2 - 2

| Elevation 103.2 (m) | Stradum Depth (m) | Visual Soil Description | Sampling Depth (m) | Remarks |
|---|---|---|---|---|
| | | | 0.2 | |
| | | Tan brown clay w/ gypsum (CH) | 0.6 | Notes: Shelby thin - walled |
| 102.4 | | | 1.0 | tube sampler (10.2 cm dia.) |
| | 1.2 | | | |
| 101.8 | | Tan gray clay (CH) | 1.4 | |
| | | | 1.8 | |
| 100.9 | | | | |
| | | | 2.2 | |
| | | | 2.7 | gypsum at 2.7 m |
| | | | 3.0 | |
| 100.0 | 3.3 | Boring terminated at 3.3 m | | |

Date drilled: May 29, 1996
Location: 1.13 km south from OSR

SH 6 Boring Number SB1 - 1

| Elevation 104.3 (m) | Stradum Depth (m) | Visual Soil Description | Sampling Depth (m) | Remarks |
|---|---|---|---|---|
| | | | 0.2 | |
| | | Gray stiff clay with melted gypsum (CH) | 0.6 | |
| 103.6 | 1.0 | | | |
| | | | 1.0 | |
| | | Tan brown clay with red clay seam (CH) | 1.4 | |
| 102.7 | | | | |
| | | | 1.8 | |
| | 2.0 | | | |
| 102.1 | | Brown/yellow clay (CH) | 2.2 | |
| | 2.5 | | | |
| | | Tan brown clay w/ gypsum (CH) | 2.7 | Notes: Shelby thin - walled |
| 101.2 | | | 3.0 | tube sampler (10.2 cm dia.) |
| | | | 3.4 | |
| | | | 3.9 | |
| 100.3 | 4.1 | | | |
| | | Boring terminated at 4.1 m | | |

Date drilled: May 30, 1996
Location: 1.13 km south from OSR

SH 6 Boring Number SB1 - 2

| Elevation 10.36 (m) | Stradum Depth (m) | Visual Soil Description | Sampling Depth (m) | Remarks |
|---|---|---|---|---|
| | | Gray clay with gypsum (CH) | 0.2 | |
| | 0.4 | | | |
| 103.2 | | | 0.6 | |
| | | Brown/gray clay with bulky gypsum (CH) | 1.0 | |
| | 1.2 | Tan gray silty clay with sand (CH) | | |
| 102.1 | | | 1.4 | |
| | 1.6 | | | |
| | | Brown gray clay w/ gypsum (CH) | 1.8 | |
| 101.2 | | | 2.2 | |
| | 2.4 | | | |
| | | Tan brown clay (CH) | 2.7 | Notes: Shelby thin - walled |
| 100.6 | | | 3.0 | tube sampler (10.2 cm dia.) |
| | 3.3 | | | |
| | | Boring terminated at 3.3 m | | |

Date drilled: May 30, 1996
Location: 1.13 km south from OSR

SH 6 Boring Number SB1 - 3

| Elevation 103.0 (m) | Stradum Depth (m) | Visual Soil Description | Sampling Depth (m) | Remarks |
|---|---|---|---|---|
| | | Brown/silty clay w/ gypsum (CH) | 0.2 | |
| | 0.3 | | | |
| 102.4 | | Tan brown/gray clay (CH) | 0.6 | |
| | | | 1.0 | |
| 101.5 | | | 1.4 | |
| | 1.6 | | | |
| | | Tan brown clay with gypsum (CH) | 1.8 | |
| | 1.8 | | | |
| 100.6 | | Tan gray clay (CH) | 2.2 | |
| | | | 2.7 | Notes: Shelby thin - walled |
| 100.0 | | | 3.0 | tube sampler (10.2 cm dia.) |
| | | | 3.3 | |
| | 3.7 | | | |
| | | Boring terminated at 3.7 m | | |

Date drilled: May 31, 1996
Location:1.13 km south from OSR

SH 6 Boring Number SB2 - 1

| Elevation 108.3 (m) | Stradum Depth (m) | Visual Soil Description | Sampling Depth (m) | Remarks |
|---|---|---|---|---|
| | | Tan gray clay with gypsum (CH | 0.2 | |
| | 0.4 | | | |
| 107.6 | | | 0.6 | |
| | | Dark brown clay with gypsum (CH) | 1.0 | |
| 106.7 | | | 1.4 | |
| | | | 1.8 | sand seam at 2.0 m |
| 105.6 | | | 2.2 | |
| | 2.4 | | | |
| | | Boring terminated at 2.4 m | | Notes: Shelby thin - walled (7.62 cm dia.) |

Date drilled: June 6, 1996
Location: 1.45 km south from OSR

SH 6 Boring Number SB2 - 2

| Elevation 108.8 (m) | Stradum Depth (m) | Visual Soil Description | Sampling Depth (m) | Remarks |
|---|---|---|---|---|
| | | Brown/gray clay with sand (CH) | 0.2 | |
| 108.2 | 0.8 | Tan brown clay with sand (CH) | 0.6 | |
| | | | 1.0 | |
| | | | 1.4 | |
| 107.0 | | | 1.8 | |
| | 2.0 | Tan brown silty clay with iron ore (CH) | | |
| | | | 2.2 | |
| | 2.4 | Tan brown clay with sand (CH) | | |
| | | | 2.7 | Notes: Shelby thin - walled tube sampler (7.62 cm dia.) |
| 105.8 | | | 3 | |
| | | | 3.4 | |
| | 3.6 | Brown silty clay with sand (CH) | | |
| | 3.7 | Tan brown clay with sand seam (CH) | | |
| 104.9 | | | 3.9 | |
| | 4.0 | Tan brown silty clay (CH) | | |
| | | | 4.3 | |
| | 4.4 | Brown/yellow silty clay with sand (CH) | | |
| 103.9 | | | 4.7 | |
| | 4.9 | Boring terminated at 4.9 m | | |

Date drilled: June 6, 1996
Location: 1.45 km south from OSR

# APPENDIX C
# Output from Radan for Windows (SH 6, NB-1)

NB1_LO.DZT  Mar, 07 1996, 11:18:52

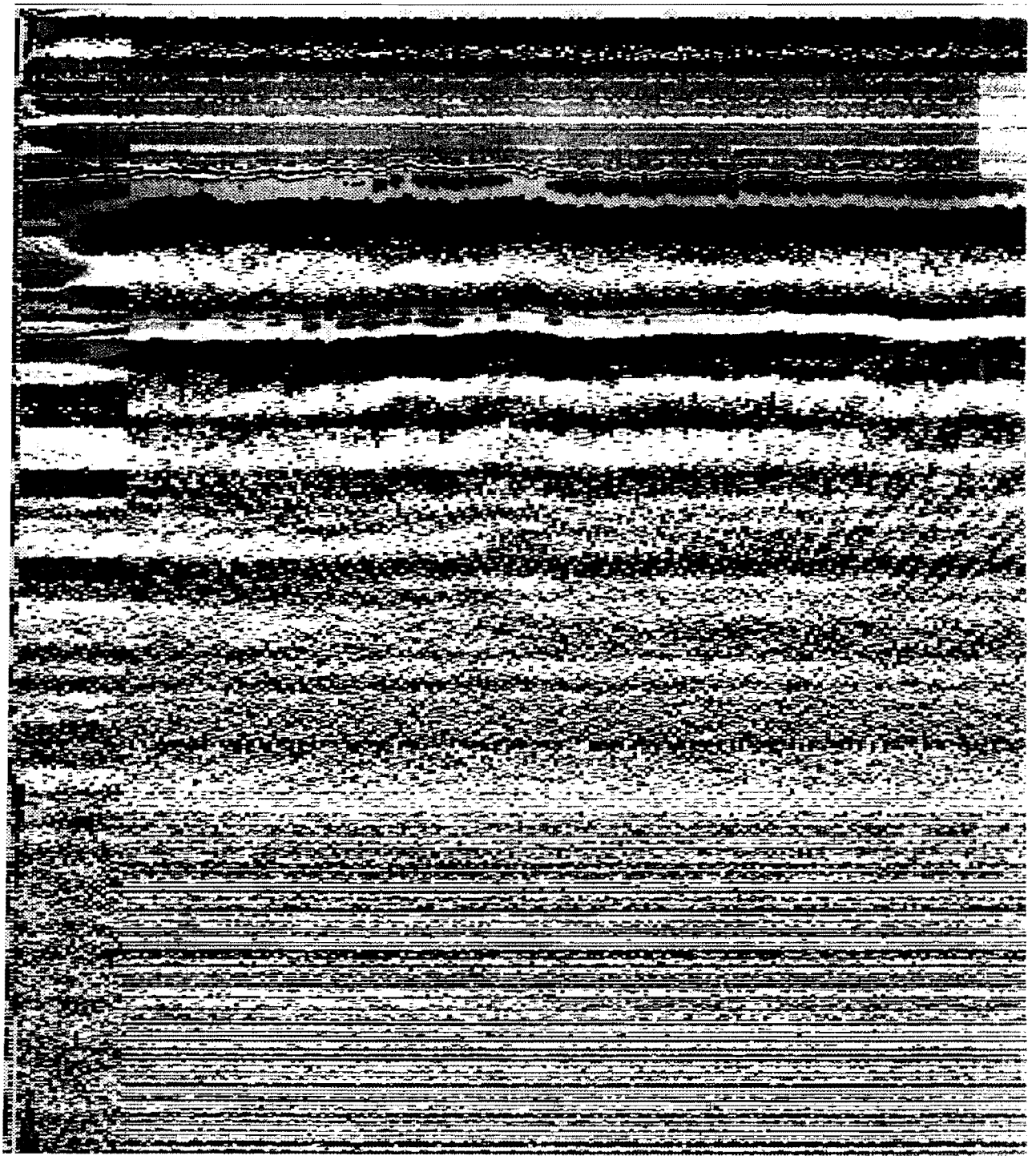

# APPENDIX D
# Output from Horiba LA 500 (SH 21, EB 1-3)

HORIBA LA-900
PARTICLE SIZE ANALYZER '96/06/05

SAMPLE : TTI
ID# : '96/06/05- -629
MODE : 1
SHAPE : 1
RF IND : 1.1
T % : 81.9%

## DISTRIBUTION GRAPH

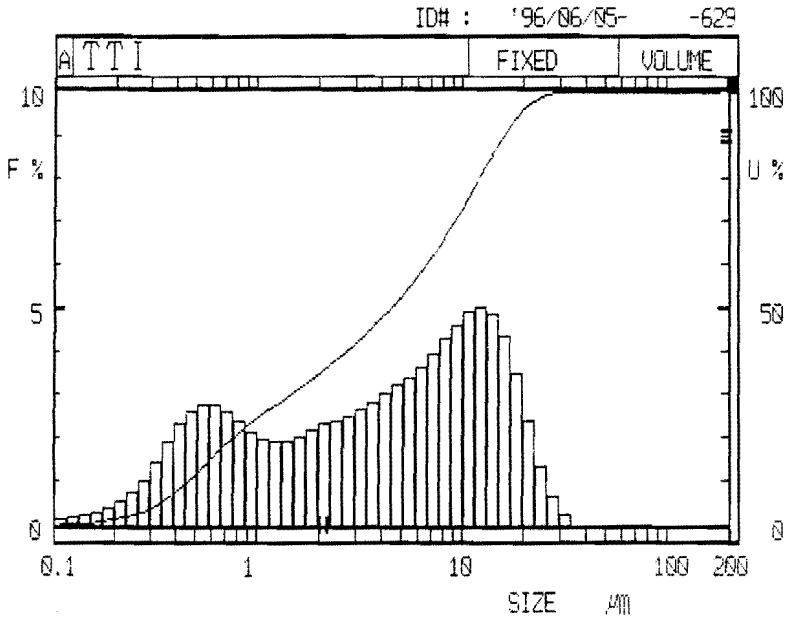


MEDIAN : 4.49 μm
SP.AREA : 44217 cm²/cm³
% on DIA : 2.1μm = 35.2 %
DIA on % : 90.0% = 16.31μm

## DISTRIBUTION TABLE

| SEG # | SIZE (microns) | INTVL % | UNDER SIZE% | SEG # | SIZE (microns) | INTVL % | UNDER SIZE% |
|---|---|---|---|---|---|---|---|
| (01) | 200.0 | 0.0 | 100.0 | (29) | 4.47 | 3.0 | 49.9 |
| (02) | 174.6 | 0.0 | 100.0 | (30) | 3.90 | 2.8 | 46.9 |
| (03) | 152.4 | 0.0 | 100.0 | (31) | 3.41 | 2.7 | 44.1 |
| (04) | 133.1 | 0.0 | 100.0 | (32) | 2.98 | 2.5 | 41.4 |
| (05) | 116.2 | 0.0 | 100.0 | (33) | 2.60 | 2.4 | 38.9 |
| (06) | 101.4 | 0.0 | 100.0 | (34) | 2.27 | 2.3 | 36.5 |
| (07) | 88.58 | 0.0 | 100.0 | (35) | 1.98 | 2.2 | 34.2 |
| (08) | 77.34 | 0.0 | 100.0 | (36) | 1.73 | 2.0 | 32.0 |
| (09) | 67.52 | 0.0 | 100.0 | (37) | 1.51 | 1.9 | 30.0 |
| (10) | 58.95 | 0.0 | 100.0 | (38) | 1.32 | 1.9 | 28.1 |
| (11) | 51.47 | 0.0 | 100.0 | (39) | 1.15 | 2.0 | 26.2 |
| (12) | 44.94 | 0.0 | 100.0 | (40) | 1.00 | 2.1 | 24.3 |
| (13) | 39.23 | 0.0 | 100.0 | (41) | 0.88 | 2.4 | 22.1 |
| (14) | 34.25 | 0.2 | 100.0 | (42) | 0.77 | 2.6 | 19.8 |
| (15) | 29.91 | 0.6 | 99.8 | (43) | 0.67 | 2.7 | 17.2 |
| (16) | 26.11 | 1.3 | 99.1 | (44) | 0.58 | 2.7 | 14.5 |
| (17) | 22.80 | 2.4 | 97.8 | (45) | 0.51 | 2.6 | 11.7 |
| (18) | 19.90 | 3.4 | 95.5 | (46) | 0.45 | 2.3 | 9.1 |
| (19) | 17.38 | 4.3 | 92.0 | (47) | 0.39 | 1.9 | 6.8 |
| (20) | 15.17 | 4.9 | 87.7 | (48) | 0.34 | 1.4 | 4.9 |
| (21) | 13.25 | 5.0 | 82.8 | (49) | 0.30 | 1.0 | 3.5 |
| (22) | 11.56 | 4.9 | 77.8 | (50) | 0.26 | 0.8 | 2.5 |
| (23) | 10.10 | 4.6 | 72.9 | (51) | 0.23 | 0.5 | 1.7 |
| (24) | 8.82 | 4.3 | 68.2 | (52) | 0.20 | 0.4 | 1.2 |
| (25) | 7.70 | 3.9 | 63.9 | (53) | 0.17 | 0.3 | 0.8 |
| (26) | 6.72 | 3.6 | 60.0 | (54) | 0.15 | 0.2 | 0.5 |
| (27) | 5.87 | 3.4 | 56.4 | (55) | 0.13 | 0.2 | 0.3 |
| (28) | 5.12 | 3.2 | 53.1 | (56) | 0.11 | 0.1 | 0.1 |

# APPENDIX E
# Calibration Suction Line of Transistor Psychrometer

Transistor Psychrometer Calibration

Trial #1
Temp = 23.2 C
Unit = Millivolts

| Suction | Probe # | | | | | | | |
|---|---|---|---|---|---|---|---|---|
| (pF) | 4 | 5 | 6 | 8 | 9 | 10 | 11 | 12 |
| 3.5 | 22 | 25 | 24 | 26 | 18 | 27 | 18 | 23 |
| 4.0 | 54 | 57 | 56 | 60 | 50 | 58 | 50 | 44 |
| 4.5 | 147 | 150 | 149 | 160 | 137 | 146 | 143 | 123 |
| 5.0 | 416 | 432 | 421 | 476 | 433 | 435 | 447 | 383 |

Trial #2
Temp = 23.2 C
Unit = Millivolts

| Suction | Probe # | | | | | | | |
|---|---|---|---|---|---|---|---|---|
| (pF) | 4 | 5 | 6 | 8 | 9 | 10 | 11 | 12 |
| 3.5 | 17 | 21 | 19 | 19 | 7 | 21 | 10 | 10 |
| 4.0 | 48 | 48 | 41 | 53 | 42 | 50 | 39 | 36 |
| 4.5 | 153 | 143 | 140 | 150 | 131 | 148 | 140 | 132 |
| 5.0 | 458 | 420 | 408 | 435 | 413 | 438 | 455 | 421 |

Trial #3
Temp = 23.5 C
Unit = Millivolts

| Suction | Probe # | | | | | | | |
|---|---|---|---|---|---|---|---|---|
| (pF) | 4 | 5 | 6 | 8 | 9 | 10 | 11 | 12 |
| 3.5 | 18 | 25 | 22 | 21 | 11 | 19 | 20 | 3 |
| 4.0 | 51 | 56 | 55 | 57 | 44 | 57 | 54 | 32 |
| 4.5 | 151 | 148 | 141 | 150 | 149 | 150 | 153 | 119 |
| 5.0 | 438 | 408 | 410 | 427 | 451 | 424 | 440 | 388 |

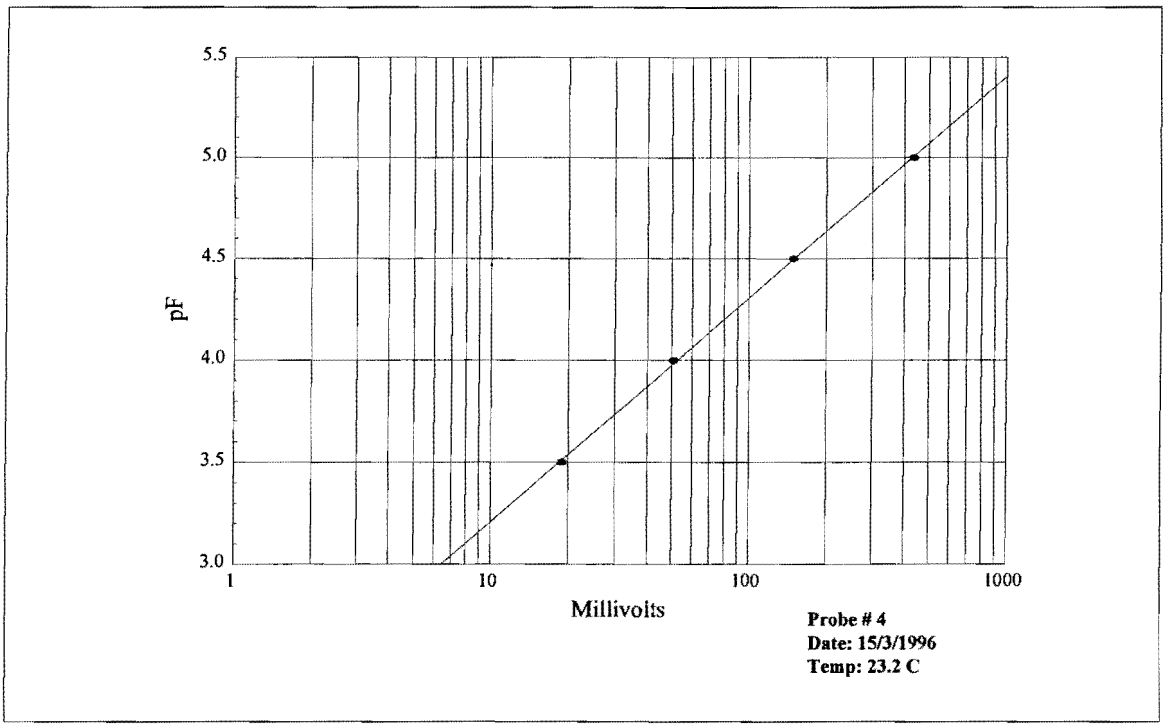
5.5
5.0
4.5
4.0
3.5
3.0
pF
1
10
100
1000
Millivolts
Probe # 4
Date: 15/3/1996
Temp: 23.2 C

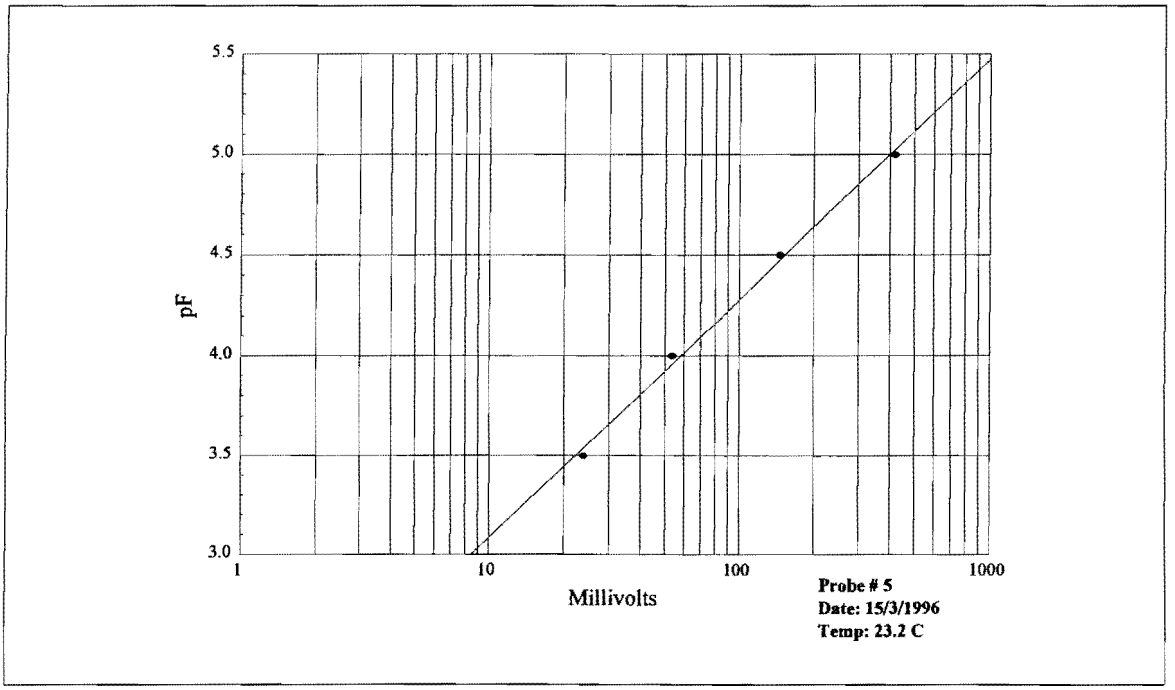
5.5
5.0
4.5
4.0
3.5
3.0
pF
1
10
100
1000
Millivolts
Probe # 5
Date: 15/3/1996
Temp: 23.2 C

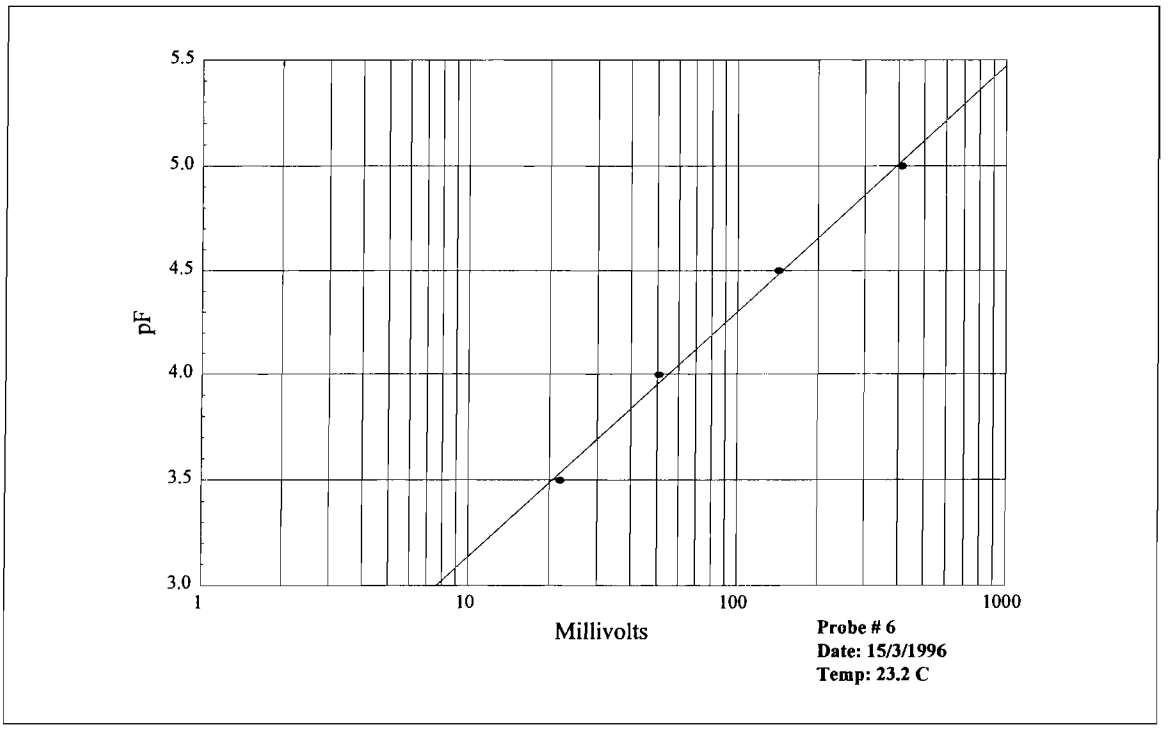
5.5
5.0
4.5
4.0
3.5
3.0
pF
1
10
100
1000
Millivolts
Probe # 6
Date: 15/3/1996
Temp: 23.2 C

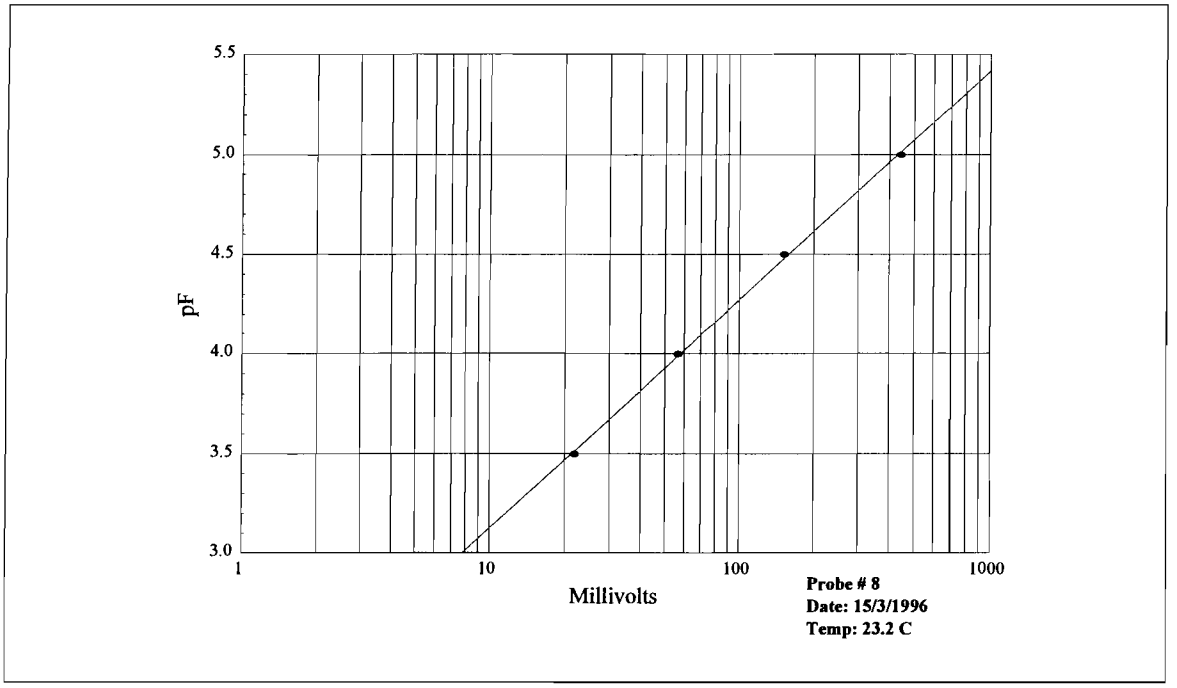
5.5
5.0
4.5
4.0
3.5
3.0
pF
1
10
100
1000
Millivolts
Probe # 8
Date: 15/3/1996
Temp: 23.2 C

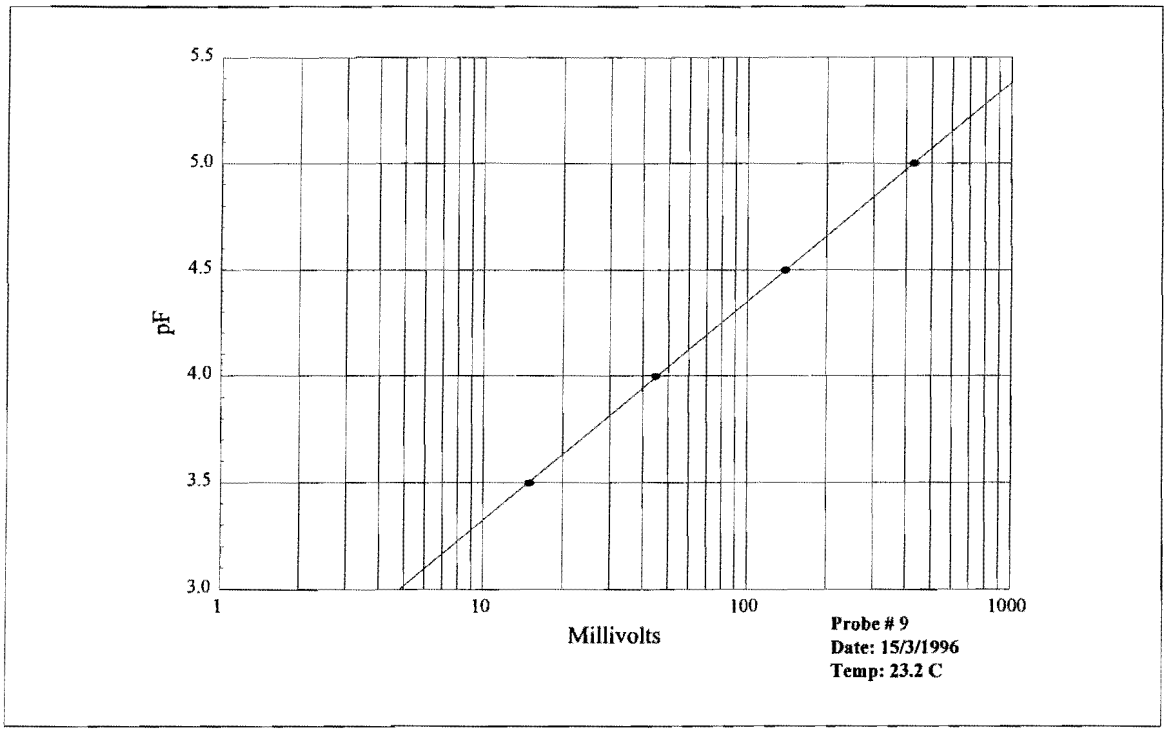
5.5
5.0
4.5
4.0
3.5
3.0
pF
1
10
100
1000
Millivolts
Probe # 9
Date: 15/3/1996
Temp: 23.2 C

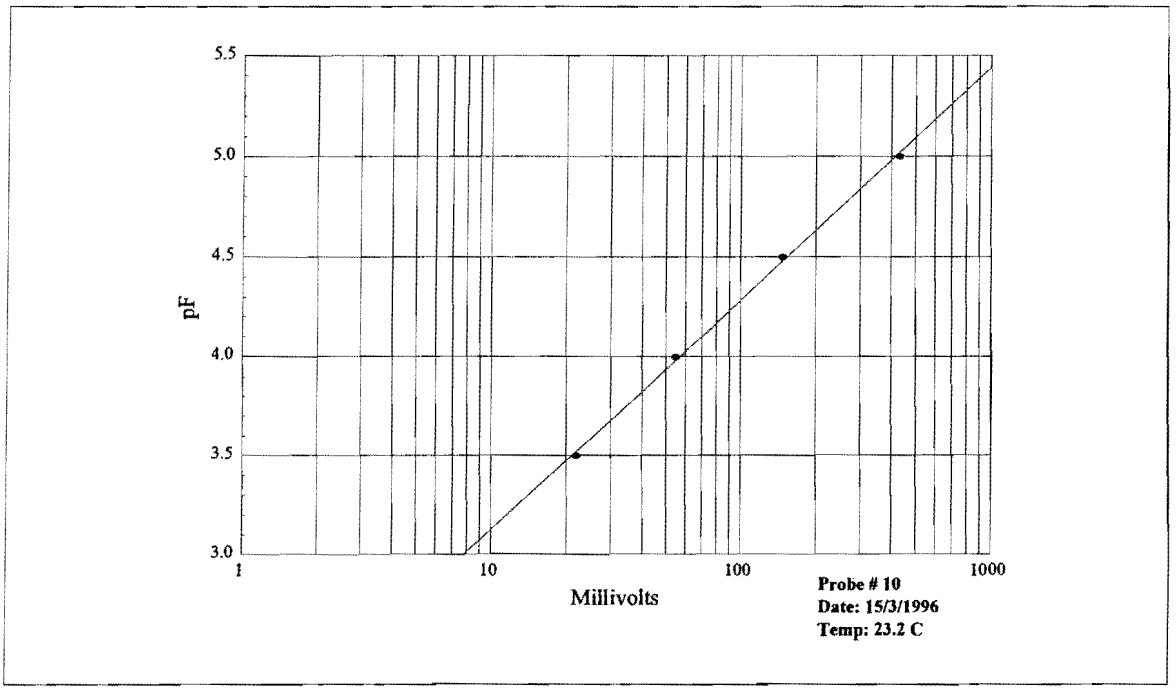
5.5
5.0
4.5
4.0
3.5
3.0
pF
1
10
100
1000
Millivolts
Probe # 10
Date: 15/3/1996
Temp: 23.2 C

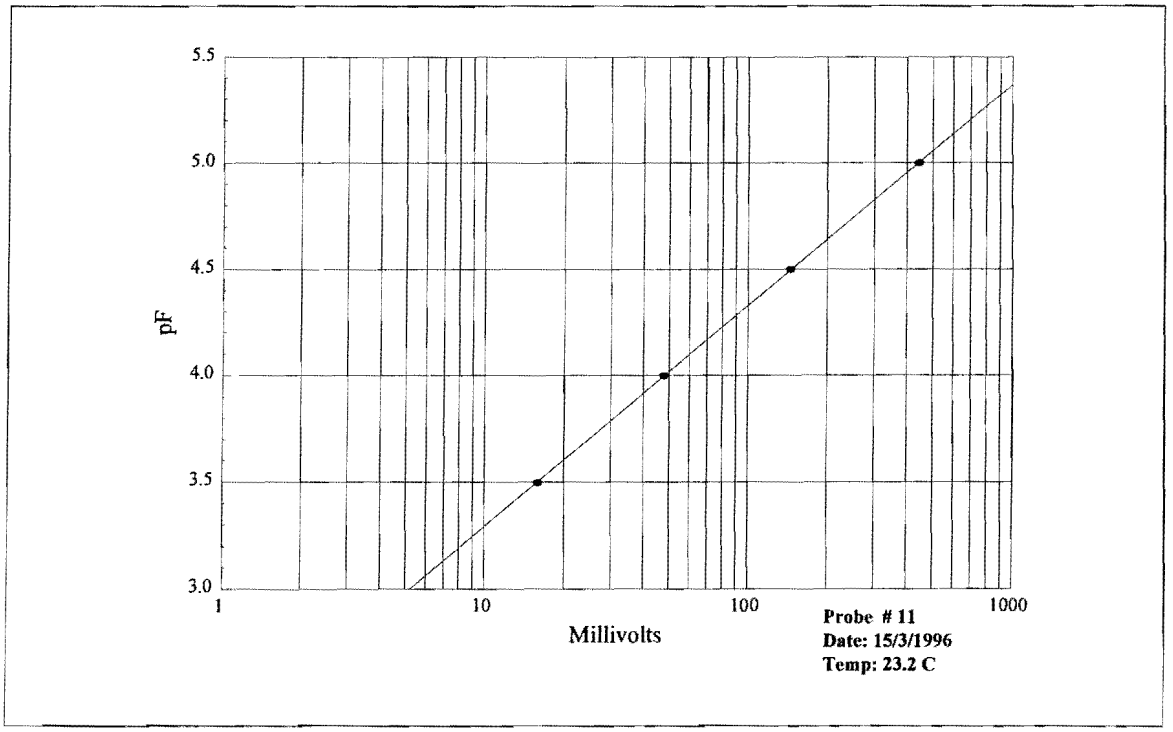
5.5
5.0
4.5
4.0
3.5
3.0
pF
1
10
100
1000
Millivolts
Probe # 11
Date: 15/3/1996
Temp: 23.2 C

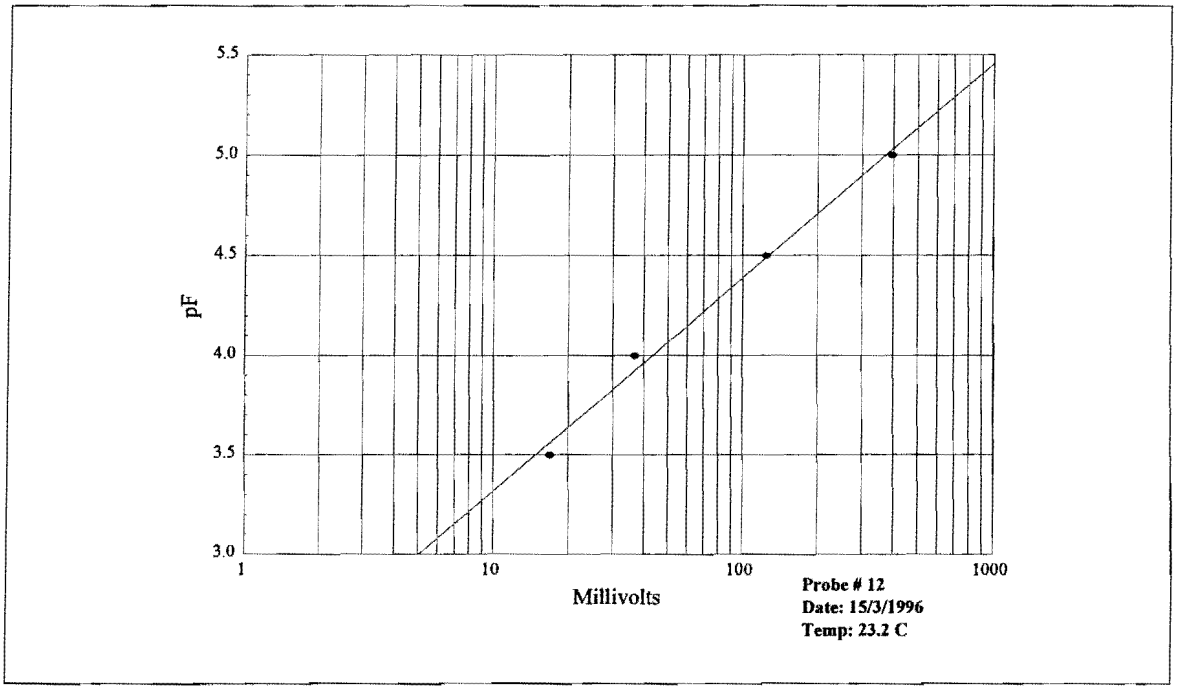
5.5
5.0
4.5
4.0
3.5
3.0
pF
1
10
100
1000
Millivolts
Probe # 12
Date: 15/3/1996
Temp: 23.2 C